Year 2023

East African Journal of Biophysical and Computational Sciences

Volume 4 No 1

Hawassa University
College of Natural & Computational Sciences

ISSN (Online): 2789-3618 **ISSN (Print): 2789-360X**

East African Journal of Biophysical and Computational Sciences (EAJBCS)

Editorial Board members

Editor-in-Chief

Editorial Manager

Associate Editors

Advisory Board members

Recognition to reviewers

Name	Affiliation	Email address
Dr. Fitsum Dullo	School of Veterinary Medicine, Wolaita Sodo University	dulofitsum@yahoo.com
Dr. Abebe Agonafir	Department of Animal Sciences, Debre Berhan University	dr.abuka@gmail.com
Dr. Tamene Hailu	Department of Physics, Dilla University	tamene05@gmail.com
Dr. Awoke Tadesse	Debre Birhan University	awoketaddesse@yahoo.com
Dr. Gashaw Tadesse	Bahir Dar Univerity	gashindian@gmail.com
Dr. Akewek Geremew	Addis Ababa University, College of Natural and Computational Sciences, Department of Zoological Sciences	khaliger@yahoo.com
Dr. Ibrahim Nasser	Addis Ababa Science and Technology University College of Applied Sciences Department of Industrial Chemistry	ibrahim.nasser@aastu.edu.et
Prof. Sissay Tadesse	Department of Chemistry, College of Natural and Computational Sciences, Hawassa University	sisaytad@gmail.com
Dr. Benyam Mebrate	Department of Mathematics, Wollo University	benyam134@gmail.com
Dr. Tsegaye Simon	Department of Mathematics, Kotebe Metropolitan University	tsegabitsue@gmail.com
Dr. Tolesa Hundesa	Department of Mathematics, Wolaita Sodo University	tolesa.hundesa@wsu.edu.et

Table of contents

ISSN (Online): 2789-3618 **ISSN (Print): 2789-360X**

East African Journal of Biophysical and Computational Sciences

Journal homepage : https://journals.hu.edu.et/hu-journals/index.php/eajbcs

Beef handling Practices at Abattoirs and Butcher Shops in Uganda: Implications for Meat Safety and Health of Consumers

Juliet Kyayesimira[1]* and Florence Muheirwe[2]

[1]*Department of Biological Sciences, Kyambogo University, P.O. Box 1, Kyambogo, Kampala, Uganda*
[2]*Valley University of Science and Technology, P. O Box 4, Bushenyi, Uganda.*

KEYWORDS:

Beef;

Handling practices;

Meat safety;

Consumer's health;

Uganda

Research article

ABSTRACT

Proper beef handling contributes to achieving sustainable development goals 3 (good health and well-being) and 12 (sustainable consumption and production patterns). This is because it ensures the safety of meat and consumers' health. However, the meat sector is still underdeveloped in most African countries. In addition, there is limited research addressing meat safety challenges. In Uganda particularly, in the recent past, there was whistle-blowing over contaminated beef on the market, indicating a loophole in food safety. Despite this, studies focusing on beef handling practices have remained scanty. Thus, this study aimed to examine beef handling practices at the abattoirs and butcher shops in Uganda's Central, Western and Eastern regions. A mixed-methods approach was employed to collect data through a survey, in-depth interviews and on-site observations. Findings revealed that beef handling practices were poor at abattoirs and butcher shops and that most facilities for safety measures were lacking or inadequate. Only 3% of the respondents had cold room storage facilities, and meat spoilage was relatively high (85.3%). Appropriate knowledge of meat safety among abattoir and butcher operators was inadequate, contributing to low compliance with food safety guidelines. Inappropriate handling practices and poor handling facilities may put consumers at a health risk. The study recommends that responsible authorities should ensure compliance mechanisms and sensitization initiatives are prioritized.

INTRODUCTION

Food safety ensures proper food handling, including beef and is crucial for ensuring the good health of consumers. Proper beef handling refers particularly to the practices that prevent microbial contamination and spoilage of beef at all points along the meat value chain, from the abattoir to the dining table (Niyonzima *et al*., 2013). It is noted that the unhygienic environment at both abattoirs and butcher shops (Bafanda *et al*., 2017) leads to unsafe meat due to microbial contamination. Poor handling of beef can result in the survival and multiplication of harmful microorganisms which grow on beef leading to beef spoilage (Rouger *et al*., 2017). Such meat is unsafe for consumption and may

*Corresponding author:
Email: Kyayejue@gmail.com

https://dx.doi.org/10.4314/eajbcs.v4i1.1S

lead to food poisoning (Haileselassie *et al*., 2013). This may contravene Sustainable Development Goal (SDG) number three, which focuses on good health and well-being of people. Additionally, suppose meat spoilage is high at butcher shops and abattoirs, fulfilment of the SDG 12 target of reduction of food waste at the retail and consumer levels to reduce food losses along production and supply chains may not be achieved (UNDP, 2015). Thus, appropriate handling of beef during and after slaughter is significant for fulfilling the SDGs. Poor food handling has been identified as one of the contributing factors to various ailments. For instance, poor food handling contributes to foodborne disease outbreaks (Gorman *et al*., 2002; Gilbert *et al*., 2007; PEH, 2008). Notably, microbial pathogens are responsible for most of the food borne disease burden in developing countries and cause 20%–40% of intestinal disorders (Grace, 2015). Food-borne illnesses manifest in ill health such as stomach upsets, diarrhoea, fever, vomiting, abdominal cramps, and dehydration to more severe illness and even death (Scallan *et al*., 2011; Thomas *et al*., 2013; Tegegne and Phyo, 2017; Yenealem *et al*., 2020). In pregnant women, foodborne illness may result in complications such as miscarriages, premature births, maternal and neonatal sepsis, and infant mortality (Tam *et al*., 2010). In this respect, promoting safe handling in the meat value chain contributes to food safety and is significant for the safe consumption of meat.

Meat safety requirements and standards in most poor countries are below the desired status. For instance, at the abattoirs, meat may be dressed on the floor (Fearon *et al*., 2014), and there are no basic facilities like stunning, bleeding, evisceration, and cooling rooms (Haileselassie *et al*., 2013). After slaughter, meat is transported in open trucks and poorly packaged without regard to safety measures (Fearon *et al*., 2014) when delivered to butcher shops. At most butcher shops, hand washing and water storage facilities may be lacking, inadequate, or inappropriate (Bogere and Baluka, 2014). In some premises, the meat is exposed to heat from the sun, which attracts dust and flies from the surrounding environment (Kyayesimira *et al*., 2019). Worse still, most people engaged in the meat production and processing value chain may not even be trained in hygienic procedures or meat technology (Akabanda *et al*., 2017). Therefore, such handlers may not implement measures they are unaware of or may not comprehend the significance of upholding the required standards.

A considerable amount of literature has been published on the meat sector. These include; studies on microbiological quality and meat safety (Koutsoumanis and Taoukis, 2005; Niyonzima *et al*., 2013; Obeng *et al*., 2013; Kebede *et al*., 2014; Santos *et al*., 2017) and meat handling practices (Birhanu *et al*., 2017; Pal *et al*., 2018). These studies above have been conducted in different contexts and are content specific. For instance, Santo and colleagues' study on butcher shops in Portugal cannot reflect the situation in developing countries because the food safety standards vary significantly. Although studies by; Kebede and colleagues in Ethiopia, Niyonzima in Kigali and Obeng in Ghana may represent the Sub-Saharan context, they do not holistically look at the practices in the meat value chain from slaughter houses to shops. Hence, studies on meat handling practices in Sub-Saharan Africa remain scanty.

Other scholars have studied meat hygiene and associated health hazards to consumers (Chepkemoi *et al*., 2015; Bafanda *et al*., 2017; Wambui *et al*., 2017) and knowledge and practices of meat safety (Sulleyman *et al*., 2018). Bafanda and colleagues (2017) focus on awareness among consumers, which may not change if meat handlers, who are the culprits, do not improve handling standards. Chepkemoi and colleagues (2015) focus on the sanitation of butcheries, while Wambui and colleagues focus on good hygiene in slaughterhouses. The two studies do not address the contamination that may occur both at slaughterhouses and butcher shops, putting consumers' health at risk.

In Uganda, studies on meat safety have also been conducted. Musoke *et al* (2016) examined meat inspection at slaughter to detect meat that may be unfit for home consumption for the prevention of zoonotic diseases. A study on the contamination of ready-to-eat meat in highway markets was also conducted (Bagumire and Karumuna, 2017). Compliance with post-harvest handling practices of beef along the Meat Value Chain has been studied (Kyayesimira *et al*., 2019). However, these studies do not focus on beef handling practices at abattoirs and butcher shops and meat safety for consumers' health, which is the focus of the present study.

In recent years, there has been an increasing amount of literature on meat, but few studies have been conducted in Uganda emphasising beef handling. Yet, in the year 2018, Uganda woke up to the news that meat in butcher shops had been contaminated with a chemical known as Formaldehyde, commonly found in hospitals to preserve dead bodies (Ssali, 2018). When sprayed over the meat, it was revealed that it keeps away the flies. Such premises attract customers who are lured into thinking that the butcher shop has high standards of hygienic conditions (Yiga, 2018). Such incidents revealed consumers' vulnerability to unsafe meat and meat products. Meat may appear appetizing or luring and may not be fit for human consumption. This may be due to contamination at either slaughterhouse before it reaches butcher shops. Improper meat handling practices contribute to making it unsafe for consumption. At any point of contamination, if such meat is consumed, it might contribute to health disorders of consumers. Therefore, the present study explored beef handling practices in the abattoirs and butcher shops in Uganda and implications for meat safety and consumers' health.

MATERIALS AND METHODS

Study sites

The research was conducted in the districts of Mbarara, Kampala, and Mbale, situated in the Western, Central, and Eastern regions of Uganda, respectively. The three (3) districts were selected because they are the biggest destinations for cattle market, with Kampala district housing the biggest abattoir in the country, which slaughters 500-700 cattle daily (Thorell, 2014).

Study design and data collection

A cross-sectional study design was employed. A survey, in-depth interviews, and observations were conducted using a mixed methods approach. The study units were slaughterhouses and abattoirs and butcher shops. A total of 460 respondents, comprising 105 respondents from

abattoirs and 355 from butcher shops, were selected from the three districts using simple random sampling. At each district, the department in charge of production provided the number of abattoirs and butcher shops. Respondents from abattoir and butcher shops were selected using the formula of Taro Yamane (1967), as indicated below

$$n = \frac{N}{1 + N(e)^2}$$

where n=the sample size, population size (30156 for butcher shops and 142 abattoirs), e= the acceptable sampling error at a 95% confidence interval.

This formula was chosen because proponents of this formula recommend that when one is studying a finite population, it is more appropriate (Adam, 2020; Singh *et al*, 2014). In this study, the finite population was respondents from abattoirs and butcher shops from the 3 study districts.

Respondents included abattoir operators, butchery owners, butchery operators, and butchers. Butchers are directly involved in slaughtering, transporting, and selling meat. They were selected to get views on the handling practices regarding the quality of meat, hygiene and safety measures and standards. Key informants (30) were purposively selected and distributed equally in all study districts. They included District Veterinary Officers (DVOs), meat inspectors, Uganda National Bureau of Standards (UNBS) staff and chairpersons of meat associations of butcher shops and abattoirs. These were interviewed to get perspectives on meat safety and compliance standards. The data was collected between June, 2018 to January, 2019.

Data collection methods

An interview guide enabled information collection on food safety guidelines and standards awareness. It also facilitated the collection of information on whether the meat processing industry and value chain actors understood the consequences of their actions on the health of families and the community. Participants were interviewed at workplaces and given priority to serve clients. The interviews were conducted in the mornings, afternoons, and evenings depending on customer flow at the butcher shops. The research team did not want to disrupt the attendants from serving customers but focused on gaining the respondents' undivided attention for more information. At the abattoir, interviews were conducted in the mornings when slaughtering was usually done. The research team wanted to observe the processes and practices of meat handling as it was slaughtered and distributed to customers. The time frame of the interview schedule varied from one place to another but took more than one hour to two on average. The time taken to conduct interviews was long because of the disruptions when clients showed up, and the researcher would pause the session to enable the respondent to attend to the client first. Interviews were conducted in the predominant local languages of the respective study areas which were Runyankore in Mbarara, Lumasaba in Mbale and Luganda in Kampala, to allow the respondents to express themselves freely.

Observation was also employed as a critical tool to establish the status of the butcher shops and abattoirs. In this exercise, the sense of smell and

vision were vital in establishing the hygiene of the business units operating as butcher shops and abattoirs. The researchers observed how customers were served the meat they had purchased. The processes of cutting meat, measuring and packaging for customers, chopping boards, the equipment used, the storage facilities, and the hygiene of the surroundings were observed.

Some relevant documents were also reviewed to understand and comprehend the meat handling practices and their implication for consumers. Reviewed documents included the Sustainable Development Goals, the UNBS standards, the National Environment Management Authority (NEMA) regulations and other policy documents, as well as, regulatory guidelines.

Data analysis

All quantitative data, mainly generated from the questionnaire, were processed and analyzed using the Statistical Package for Social Sciences (SPSS) version 20 (IBM Corp. Armonk, NY: Released 2011) and Sigma plot Version 14. Frequencies and percentages were computed for meaningful interpretation of results presented in the form of tables in the results and discussion section. Qualitative data were analyzed using the thematic approach, where common themes were categorized, coded, and interpreted for meaning. These were used to complement data from in-depth interviews and document reviews.

Research Ethical Considerations

Before data collection, approval was obtained from the National Council for Science and Technology in Uganda to implement this research under the RELOAD research project Uganda (RELOAD/A0401UNSCST2012). At the University, approval was acquired from the Mbarara University of Science and Technology Research Ethics Committee (MUST-REC). During data collection, participants were briefed about the aim of the research to seek consent and voluntary participation. This was done verbally, and a request to take pictures was made. Pictures taken and provided in this paper were taken from premises where respondents had consented verbally, and for those who were not willing, their concerns were respected. The pictures have been presented in blurred form to protect the participants' identities.

RESULTS AND DISCUSSION

Socio-demographic characteristics of respondents

This study was interested in the levels of education and gender of respondents. The study presumed that education should influence better meat handling practices. Previous studies reported high education level was related to safe food handling (Karabudak *et al*., 2008; Jianu and Goleț, 2014). Findings from the study (Table 1) revealed that most beef handlers at the abattoir and butcher shops had attained basic education. For instance, most abattoir operators had primary education (48.6%), while most butcher shop operators (46.2%) had acquired secondary education. Few of the respondents had no formal education. As this study reveals, there seems to be a basic literacy level among the meat industry operators. Similarly, in Malaysia, the majority of food handlers had primary and secondary level education (Rosnani *et al*., 2014). Contrary, in Ogun State of Nigeria, it was found that the majority of the handlers had low literacy levels of up to primary

education (Fasae and Bakare, 2016). These revelations suggest that the level of education of operators in the meat industry is low and could contribute to the unsafe handling of meat.

Gender was thought pertinent to this study because men and women may have different ways of conduct. This may determine varying meat handling practices. This study revealed that men dominated the meat sector, as indicated in Table 1. This could be attributed to the masculine nature of the work at the abattoirs and butcher shops. The findings of this study are similar to those of other scholars (Abdeirazig *et al*., 2017; Kikulwe *et al*., 2018) who found males dominating several food value chain nodes compared to their female counterparts. Notably, in Nigeria, 100% of beef handlers were male (Fasae and Bakare, 2016). Given the findings, men seem to dominate in sectors where activities may be strenuous.

Table- 1: Number of Respondents by Education and gender

Variable	Abattoir operators	Butcher shops operators
No formal Education	7 (6.7 %)	5 (1.4%)
Primary Education	51 (48.6%)	154 (43.4%)
Secondary Education	35 (33.3%)	164 (46.2%)
Tertiary Education	7 (6.7%)	16 (4.5%)
Graduate	5 (4.8%)	16 (4.5%)
Male	103 (98.1%)	352 (99.2%)
Female	2 (1.9%)	3 (0.8%)

Meat handling practices at slaughterhouses and butcher shops

Results from observations at abattoirs (slaughterhouses) showed that tools and carcasses were being handled unhygienically during and after the slaughter process, as shown in Plate 1.

Plate 1: Unhygienic slaughter process: on floor slaughter (left) and unhygienic meat handling practices at a slaughterhouse (right)

It was noted that workers wore dirty and torn protective wear, kept knives in gumboots, and carried meat over clothes. Also, flaying and dressing were done on the dirty floor. Most slaughterhouses did not separate stunning rooms from other processes. The slaughterhouses in all the study districts had substandard facilities and lacked design requirements per the standard for the design and construction of slaughter areas (UNBS, 2017). This seems not to have improved since an earlier study in Uganda also confirmed similar flaying practices and dressing on the floor (Bogere and Baluka, 2014). A similar study in Northern Nigeria reported that slaughterhouses lacked basic structures leading to unsafe meat (Bello *et al*., 2015).

In an interview with one of the officials from the meat inspection unit, it was further explained that, particularly in Mbarara and Mbale, the slaughterhouses were operating below the required standards, unlike in Kampala, where a few were complying. The official attributed this to the fact that the rate of compliance to standards in Kampala, a city, is higher than in urban areas in other regions. This study noted that in Mbale and Mbarara, there was one meat inspector per district, unlike in Kampala. This could probably explain the revelation from one of the key informants that there is slightly fair compliance to better meat handling practices in the city. However, from the observation in this study, there was no clear distinction in terms of compliance with proper meat handling in all the study areas. This seems to concur with the Ministry of Agriculture Animal Industry and Fisheries (MAAIF) report, which indicated that Uganda lacks better slaughter facilities that respect health, food safety, and environmental standards (MAAIF, 2020). In line with the current findings, a study in Abiia and the Immo states of Nigeria revealed low compliance of meat handlers to best practices (Iro *et al*., 2017). In Kenya, slaughterhouse meat handlers were not washing their hands, and equipment handling practices were inadequate (Wambui *et al*., 2017). These revelations suggest that Uganda is not the only country that does not meet the desired handling practices at slaughterhouses.

Regarding butchery structures (meat shops), findings revealed that most (96.6%) of beef sales in the study were made from kiosks with no cold rooms. Other beef sales were made in open structures, under the tree and a few butchers (3%) owned kiosks with cold rooms, as shown in Plate 2. .

Plate 2: The meat shops common in the study areas showing meat displayed along the dusty roads

Most of the butchery establishments (96.6%) lacked cooling facilities. It was observed that meat is displayed for sale, exposing it to dust and flies. When one of the respondents was probed about why meat was being displayed in the open, he had this to say,

'*…You may not attract potential clients if you do not display your meat. That is what everyone selling meat does in this area. When customers come, they move around as they check out the best and attractive meat before deciding to buy. If you do not display, nobody will know that you are selling meat, and they might think that your stock is finished….'*

This study indicates that meat retailers have been accustomed to displaying meat, and customers are used to buying meat on display. This could be attributed to the ignorance of both parties on proper meat handling and food safety standards. It is acknowledged that informal butcheries are widespread in Uganda (Agriterra, 2012). In this study, it was also observed that most butcheries lacked fly-proof windows or doors to prevent the entry of insects, and none had running water. A similar study in Kampala, Uganda, found that most butcheries lacked a standard fly screen and fly-proof window (Mirembe *et al*., 2015). This means the flies can transmit pathogens/microbes from one point of meat sale to another, leading to unhygienic situations. The close proximity of several butcheries and their practice of sharing weighing scales, stones, and cutting tools created a high risk of cross-contamination. If one piece of shared equipment became contaminated, it could potentially spread to all the participating businesses.

Storage facilities and transportation of beef

According to hygiene requirements for a butchery, a chilly environment for storage is a requirement for optimum meat safety. It was, therefore, significant for this study to examine storage facilities in the study area. Study findings revealed that slaughterhouses in Kampala had chillers but were lacking in the slaughterhouses in Mbarara and Mbale. Meat shops lacked cold storage facilities; daily meat for sale was stocked, but if all was not sold, it was left hanging in the facility. Butcheries lacked cold storage rooms because there was no power supply coupled with limited innovation on solar usage in refrigeration. In one of the discussions with the veterinary personnel, it was revealed that butcher operators in Mbarara and Mbale were reluctant to use cold storage rooms because the temperatures were not as high as in Kampala. This was also on the assumption that in places with cool temperatures, the spoilage rate and level of contamination may be below. In contrast, the contamination rates and levels are higher in the wet and rainy seasons (Bagumire and Karumuna, 2017). Another reason that was provided for not refrigerating meat was that customers consider refrigerated meat not to be fresh, as one respondent during the interviews noted:

'*You see most customers when they come, especially in the morning, they want to see the meat dripping with blood, and they even caution you that…please do not give me any meat that stayed overnight…some even check to confirm it is not chilled*.' *For that matter, I do not store meat in the chillers.*

In relation to this study, Agriterra (2012) reported that enormous roadside small-scaled butcheries in Kampala lacked refrigeration. The butchers preferred to buy meat in relatively small quantities that could be sold in one day. Agriterra further reveals that the butchery structures were not appropriate according to the Ugandan standard on hygienic requirements of butcheries (UNBS, 2007). In Kenya, Chepkemoi *et al*. (2015) noted that butcher shops in Nairobi and Isiolo counties stored meat by hanging it in

open spaces. Similarly, a study in South Sudan noted that many meat-selling structures were open shelters and kiosks that left meat hanging in the open air (Aburi, 2012). These revelations portray poor storage conditions, which can accelerate microbial growth and hence quicken meat contamination.

Transportation is another aspect that compromises the hygiene of meat and hence its safety. The conditions of transporting meat should provide adequate protection from contamination (Rani *et al*., 2017). This study aimed to understand how meat was transported, especially from slaughterhouses to butcheries. The results of the present study indicated that the majority (54%) of the carcass (beef) was transported by motorcycles, followed by bicycles (25%), and a few (1%) used wheel barrows or shoulder-to-shoulder logs. Motorcycles were not only popular in Uganda for transporting meat but also in Ghana, where the majority (93%) of the butcher men transport beef on bicycles, motorbikes, and motorized tricycles, popularly known as motor kings under very unhygienic conditions (Fearon *et al*., 2014). This study also observed that sometimes meat was carried in sacs or polythene bags and would drip blood, attracting dust and flies along the way. This is unlike Kenya, where meat is mostly transported in metallic containers (Chepkemoi *et al*., 2015). In this study, motorcycles were also loaded with wooden boxes where beef is placed and then covered during transportation, but some were left open. In Kenya, Chepkemoi *et al*. (2015) noted that metallic boxes in which meat is transported are mainly closed. Covering meat is important because in cases where the boxes are left open, and meat is not wrapped, it may expose it to dust, flies, and other sorts of contamination.

There are standards for transporting and handling meat at both the global and local levels. For instance, the code of hygienic practice for meat requires that it is handled, stored, and transported in a manner that will protect it from contamination and deterioration (CAC/RCP, 2005). The modes of transport of meat should maintain proper refrigeration temperatures at critical points such as loading and off-loading (Richardson *et al.,* 2009). However, refrigeration is unavailable in some abattoirs and during transportation in developing countries (Aburi, 2012; Agriterra, 2012; Chepkemoi *et al*., 2015; Rani *et al*., 2017). Poor modes of transport like shoulder-to-shoulder logs provide a conducive environment for contamination with and growth of some pathogenic and spoilage micro-organisms that would put consumers at risk.

Occurrences of beef spoilage at butcher shops

Beef spoilage could be common in facilities with poor storage and handling practices. Study results indicate that beef spoilage was common in butcheries. The kind of beef spoilage occurring at the slaughter included; bad odor, bruised meat, change of color, and rotting, among others, due to beef overstay at the point of sale. Over 85.3% of butchery operators reported beef spoilage, as in table 2.

Meat handling practices at slaughterhouses and butcher shops

Results from observations at abattoirs (slaughterhouses) showed that tools and carcasses were being handled unhygienically during and after the slaughter process, as shown in Plate 1.

Table 2: Frequency of beef spoilage occurrence at Butcher shops

		Mbarara	Kampala	Mbale	Average
% Occurrence of beef spoilage	Yes	102(85.2%)	100 (75.5%)	97 (95.1%)	85.3
	No	18 (14.8%)	33 (24.5%)	5(4.9%)	14.7
% Occurrence of beef spoilage	Daily	37 (27.9%)	41(34.4%)	37 (36.3%)	32.8
	Weekly	52 (39.3%)	28 (22.9%)	33 (32.4%)	31.5
	Biweekly	4 (3.3%)	1 (0.5%)	2 (2.0%)	1.9
	Monthly	18 (13.2%)	18 (15.1%)	17 (16.7%)	15.0
	Occasionally	2 (1.6%)	3 (2.1%)	8 (7.8%)	3.9
	Not applicable	20 (14.8%)	30 (25%)	5 (4.9%)	14.9
Type of spoilage incurred (%)	Bad odor	20 (14.8%)	1 (1.0%)	13(12.7%)	9.5
	Meat changes color	4 (3.4%)	8 (6.7%)	7 (6.9%)	5.6
	Rots after some days	22 (16.4%)	9 (7.8%)	12 (11.8%)	12.0
	Bruised meat	2 (1.6%)	3 (2.1%)	3 (2.9%)	2.2
	Drip loss	20 (14.8%)	19 (15.6%)	14 (13.7%)	14.7
	Beef wastes	48 (36.1%)	51 (42.7%)	48 (47.1%)	41.9
	Not applicable	17 (13.1%)	29 (24.0%)	5 (4.9%)	14.0
The fate of spoilt beef	Given to dog owners for free	22 (16.4%)	10 (8.3%)	39 (38.2%)	21.0
	Thrown away	89 (67.2%)	62 (51.6%)	9 (8.8%)	42.5
	Sells it to clients for dogs	20 (14.8%)	48 (40.1%)	33 (32.4%)	29.1
	Takes it home for consumption	2 (1.6%)	0 (0%)	21 (20.6%)	7.4

Daily, the average beef spoilage was reported at 32.8% in the study areas. The respondents at the butcher shops indicated that, at times, beef that remains at the end of the day is left hanging in the retail premises because of a limited refrigeration system. Similarly, butcher shops in Nairobi and Isiolo Counties, Kenya, also store meat by hanging it in open spaces (Chepkemoi *et al*., 2015). In this study, meat sales are made near dusty roadsides, and the meat is displayed for customers by hanging it on the veranda (close to the road). This exposes meat to contamination, accelerating the rate at which meat may get spoilt. A study in Uganda found that enormous roadside small-scaled butcheries in Kampala lacked refrigeration (Agriterra, 2012) and could accelerate beef spoilage. A previous pilot study in Uganda revealed that any balance of meat was either stored in the freezer or left hanging in the butchery. In contrast, the rest of the butcheries sold off the balance cheaply to avoid carry-over to another day (Kyayesimira *et al*., 2018). The beef left hanging in the butchery overnight is susceptible to microbial growth that quickens spoilage.

This study revealed that meat not sold off is carried on to the next day, mixed with fresh stock and sold to unsuspecting customers. One of the attendants of a butcher shop (key informant) confirmed this practice by saying:

'Normally the meat that stays is very little and so to avoid making losses when a customer comes, we cut fresh meat and as we measure the

amount requested by the customer, we add on the meat of the previous day'.

This practice is absurd since it lures consumers into thinking that the shops are selling fresh meat but instead, the meat is mixed with the previous stock, which may be spoilt. Mixing fresh stock with the previous one (unrefrigerated) may also contribute to the rate at which all stock may get spoilt.

This study observed that meat tending to spoilage attracted many fly populations. It was also revealed that when the environment of the meat-selling premises is not hygienic, it acts as fly breeding grounds that swim to butcher shops worsening the hygienic conditions of the premises and the meat. This situation could lead to a disease outbreak. As noted, in Thailand, there was a linkage between fly populations associated with disease outbreaks and cases of food-associated pathogens, for instance, *Vibrio fluvialis*, *E. coli*, *Vibrio cholera* and *Campylobacter spp* (Graczyk *et al*., 2001).

It was in the interest of this study to find out where the spoilt beef was taken. Findings revealed that the fate of beef after spoilage was to throw it away, as was reported by 42.5% of respondents, 29.1% reported that the spoilt meat was sold to clients, while 7.4% mentioned that they took it home for consumption. When probed about it, the respondents claimed that despite the unpleasant odour, it may not pose a danger to consumers' health if it is well cooked. The respondent's perspectives seem to concur with Bogere and Baluka (2014),who also noted that microorganisms might be destroyed if cooking is effectively conducted. However, in some households where raw meat is consumed, it could pose a health risk.

Other respondents explained that spoilt meat is roasted first to eliminate the unpleasant odour, a delicacy in some households. These revelations indicate that operators lack adequate knowledge regarding food safety and its health implications.

Meat inspection at slaughter and butcher shops

Meat inspection is crucial in the meat industry because it ensures meat safety and hygiene. During the study, it was observed that there were no meat inspections taking place at the slaughter slabs. Instead, the inspection was observed being conducted at the slaughterhouses. This may not conform to effective monitoring principles, where every stage in the slaughtering process is critical for meat safety. Abattoir operators informed the study that meat inspectors are supposed to inspect the meat that is slaughtered before it is distributed to clients. At butcher shops, respondents revealed that the team from the district does inspections. However, there seems to be concerns that meat inspection in Uganda has been inadequate. For instance, Bogere and Baluka (2014) noted that the inspection of abattoirs and butcher shops by both the veterinary and public health inspectors had been insufficient. Thus, the meat safety and hygiene standards have deteriorated (Bogere and Baluka, 2014). It should be noted that butcher's shops act as links between the inspected and approved safe meat for consumption, and therefore, inspection in the whole meat value chain is crucial for ensuring meat safety (Waldman *et al*., 2020).

At the slaughterhouses, it is a requirement to conduct ante mortem inspections. This study established that Kampala district had higher

compliance with conducting ante-mortem inspections than Mbarara and Mbale districts. Slaughter slabs (Plate 1) in the study area did not have inspectors to conduct antemortem inspections. It is noted that meat inspectors are in short supply in Uganda (Musaba, 2008). A study in western Kenya indicated that ante-mortem inspection was practiced at only 7% of slaughterhouses (Cook *et al*., 2017).

Ministry of Agriculture, Animal Industry and Fisheries (MAAIF) coordinates all meat inspection activities in the country and ensures that each district has meat inspectors (MAAIF, 2010). On the other hand, UNBS is mandated to plan an oversight role in monitoring the meat sector processes and activities for compliance (Muhwezi, 2018). In its Standardization Strategic plan (i.e. National) for the year 2019 to 2022, the bureau highlights the accountability of protecting the health, safety, welfare of people and the environment. In an interview with the official from UNBS, accordingly, no meat should be consumed by clients without inspection both at the abattoir and butcher shops. The official further informed the study that as a bureau, they may not be able to conduct routine inspections. However, at butcher shops, periodic investigations are carried out.

Knowledge of meat safety and hygiene by meat handlers

To adhere to proper handling practices, meat handlers must be knowledgeable about the consequences of their actions. This study sought to establish whether meat handlers were conversant with proper meat handling and safety. This study found that most beef handlers had limited meat handling and safety knowledge. In Kampala, respondents revealed that they had been receiving training occasionally from Kampala city council officials on meat handling practices, as well as, hygiene. One of the officials confirmed that strategies to sensitize butcher operators had been ongoing, especially in Kampala district, to ensure meat safety. It should be noted that UNBS and Kampala Butchers and Traders Association (KABUTA) signed a Memorandum of Understanding (MoU) in 2017, which was aimed at improving the quality of meat products and ensuring compliance (Kasirye, 2017). Accordingly, the MoU would enable UNBS to conduct sensitization awareness programs, among other activities. This was one of the strategies for fulfilling its mandate regarding the national standardization program that identified the animal sector as significant for protecting consumers from unsafe meat.

Respondents from Mbarara and Mbale revealed that they also received some knowledge on meat handling and safety through the district meat inspectors. It was explained that these trainings were on the spot, especially if the team found non-conforming practices. One of the respondents said;

'…we have never received organized training at this abattoir on handling meat to ensure meat safety. We normally induct each other into this business. However, when inspectors are passing around, and they find you doing something that is not proper, that is when they provide guidance and advice on how to do it better….'

As revealed by respondents, the kind of training received seemed to have been informal. These may not provide adequate knowledge meat handling and safety. Providing adequate knowledge to meat handlers is critical for

ensuring meat safety. Studies have found that most food handlers have limited basic knowledge of food safety, and this can lead to poor hygienic practices by food-handlers (Rosnani *et al*., 2014; Akabanda *et al*., 2017; Rani *et al*., 2017). Although respondents had not received adequate training in meat safety, they acknowledged that poor hygiene at the butchery and abattoir could contribute to disease-causing organisms and, consequently, disease outbreaks. This is contrary to the findings by Heilmann (2016), who concluded that butchers are unaware that poor handling standards and hygiene may contribute to infections.

Challenges of compliance with expected meat safety standards

Inappropriateness in handling meat and meat products at abattoirs and butcher shops reveals a lack of compliance with food safety procedures and guidelines. This study explored why business operators in the butcher shops and at abattoirs were not exhibiting adherence to compliance measures and standards. Three key factors emerged as crosscutting from the respondents. These included inadequate awareness of food safety and associated health consequences, ignorance of food safety guidelines and policies, as well as limited resources.

Revealing inadequate awareness of food safety and its implications, some butcher shop attendants were unaware that their beef handling practices were inappropriate. For instance, when probed why they were not putting on gloves, and yet they were handling money and putting meat on weighing scales, one of the respondents said:

'…here in Uganda, and especially in town, people consume cooked meat…. I am sure by the time meat gets ready, all parasites, bacteria or whatever you call it will not have survived… I have been in this business in this area for a long time, but I have not had any incidences where a customer came to confront me that I had sold them contaminated meat'.

The responses from the respondent were in line with also the affirmations from one official from UNBS, who explained that the bureau was aware of inadequate awareness regarding food safety practices. The official explained that this was one of the reasons that had led to the signing of the Memorandum of Understanding between UNBS and KABUTA in 2017. It was expected that this would raise awareness of stakeholders in the meat sector to promote safety handling practices and improve hygiene standards for meat destined for consumers. Quite related to inadequate awareness of food safety standards, and its implication was ignorance about food safety guidelines and policies. Interviews with respondents at abattoirs, especially in Kampala, revealed awareness of the existing laws regarding compliance standards at slaughterhouses. Although they were aware of the laws and witnessed daily inspection routines, some of the procedures were not being observed, such as using offal trays.

The third concern reported was limited resources. Respondents argued that complying with the set guidelines from UNBS, MAAIF and NEMA required resources to ensure that appropriate structures are established and facilities bought. However, this was seen as an expensive venture due to resource constraints where proprietors are focused on maximizing

resources. Whereas the views of respondents cannot be ignored, this excuse of limited resources was far from convincing since observations showed that even the basic utilities and work gear, such as gloves, were not being used. This could be attributed to inadequate awareness and sensitization strategies. Studies have shown that other challenges to meat safety could be ignorance of meat handlers about basic hygiene rules and personal hygiene (Birhanu *et al*., 2017; Andargie *et al*., 2008), as well as, the addition of dangerous food additives and chemical residues (Sofos, 2008).

CONCLUSION & RECOMMENDATIONS

This study notes that meat handling practices are still below the desired standard operation procedures in most slaughterhouses and butcher shops. The low compliance in meeting the requirements for butchery establishments and inappropriate storage facilities and other equipment for ensuring best practices does not guarantee meat safety. This may contribute to meat contamination and spoilage, putting consumers at a health risk. More so, ignorance of meat operators on food safety operating standards as per existing guiding documents inhibits compliance behaviours. Food safety programs and health education are thus crucial for ensuring meat safety standards and reducing meat spoilage. This may also contribute to achieving SDG 3 (the goal about promoting good health and well-being) and 12 (The goal about ensuring sustainable consumption and production patterns). Upholding meat safety is plausible by strengthening the existing food safety coordination mechanisms among stakeholders. Stringent measures should be established to halt the lack of adherence and compliance by abattoir and butcher operators. This may require the meat inspection team to conduct more on-site inspections at butcher shops, where most consumers are vulnerable to purchasing unsafe meat. This study recommends that further investigations exploring households' awareness of meat safety and health implications should be conducted.

Policy Implications on beef handling

This study has the following implications for policymakers;

- Meat policy should incorporate daily systematic monitoring of meat handlers and facilities against standard operating practices. The policies should empower consumers to make meat sellers accountable to expected handling standards. Consumers should be able to report to the local council administrative structures in cases where meat handling contravenes standards.
- Local council committees that already have members on village health committees and the environment should be mandated to intervene in the inspection of meat handling practices within their jurisdiction. This could be cost-effective instead of relying on the intervention from MAAIF, UNBS, and NEMA, which is never timely and is encumbered by logistical aspects. Meat handling facilities should be committed to providing safe and hygienic meat to consumers laid out and signed for the record by UNBS.
- Timely policies on meat safety should train all meat handlers in the entire value chain continuously to achieve an integrated and coordinated national meat safety system. Management of the

slaughterhouses and butcher shops should ensure meat safety rules and any other related information is displayed for the meat handlers to constantly increase knowledge awareness.

Acknowledgements

Authors thank the different actors at the abattoirs and butcher shops, District Veterinary Officers (DVOs), meat inspectors, Uganda National Bureau of Standards (UNBS) staff and chairpersons of meat associations. Special thanks to the field Assistants (Nicholas Twijukye, Kintu Davis, Orishaba Evalyne, Morris Mugumye and Buke Richard) for their contribution to data collection.

References

Abdeirazig A., Mustafa K. and Mohammed M. 2017. Hygienic Practices among Food Handlers in Restaurants of Al-Nohod Locality Market-west Kordofan-Sudan-2017. *Int. J. Pub Health Safety*, **2**(3): 2–5.

Aburi S. A. P. 2012. Assessment of Hygiene practices used by Small Butchers and Slaughter Slabs in beef value chain in Juba town-South Sudan. Master's Thesis, University of Applied Science

Adam A. M. 2020. Sample Size Determination in Survey Research. *J. Sci. Res. Rep.* **26**(5): 90–97. https://doi.org/10.9734/JSRR/2020/v26i530263

Agriterra. 2012. Identification of livestock investment opportunities in Uganda. www.agriterra.org

Akabanda F., Hlortsi H. E. and Owusu-Kwarteng J. 2017. Food safety knowledge, attitudes and practices of institutional food-handlers in Ghana. *BMC Public Health*, **17**(1): 1–9. https://doi.org/10.1186/s12889-016-3986-9

Andargie G., Kassu F., Moges F., Tiruneh M. and Huruy K. 2008. Prevalence of bacteria and intestinal parasites among food-handlers in Gondar Town, Northwest Ethiopia. *J. Health Popul. Nutr.* **26**(4): 451–455.

Bafanda R. A., Khandi S. A., Minhaj1 S. U. and Khateeb, A. M. 2017. Meat Hygiene and Associated Health Hazards Awareness among Consumers of Jammu District of Jammu and Kashmir Meat Hygiene and Associated Health Hazards Awareness among Consumers of Jammu District of Jammu and Kashmir. *Curr. Appl. Sci. Technol*. **23**(3): 1–11. https://doi.org/10.9734/CJAST/2017/36045

Bagumire A. and Karumuna R. 2017. Bacterial contamination of ready-to-eat meats vended in highway markets in Uganda. *Afr. J. Food Sci.* **11**: 160–170. https://doi.org/10.5897/AJFS2016.1550

Bello M., Lawan M. K., Aluwong T. and Sanusi M. 2013. Management of slaughterhouses in northern Nigeria and the safety of meat produced for human consumption. *Food Cont*. **49**: 34-39**,** https://doi.org/10.1016/j.foodcont.2013.09.007

Birhanu W., Weldegebriel S., Bassazin G., Mitku F., Birku L. and Tadesse M. 2017. Assessment of Microbiological Quality and Meat Handling Practices in Butcher Shops and Abattoir Found in Gondar Town , Ethiopia. *Intl. J. Microbiol. Res*. **8**(2): 59–68.

Bogere P. and Baluka A. S. 2014. Microbiological Quality of Meat at the Abattoir and Butchery Levels in Kampala City, Uganda. *Int. J. Food Saf*. **16**: 29–35.

CAC/RCP. 2005. Code of hygienic practice for meat (No. 58).

Chepkemoi S., Lamuka P. O., Abong G. O. and Matofari J. 2015. Sanitation and Hygiene Meat Handling Practices in Small and Medium Enterprise butcheries in Kenya -Case Study of Nairobi and Isiolo Counties. *Int. J. Food Saf*. **17**: 64–74.

Cook E., De Glanville W., Thomas L., Kariuki S., Bronsvoort B. and Fèvre E. 2017. Working conditions and public health risks in slaughterhouses in western Kenya. *BMC Public Health* **17**(1): 1–12. https://doi.org/10.1186/s12889-016-3923-y

Fasae O. A. and Bakare M. O. 2016. Cattle handling, hygiene and slaughtering techniques in selected cattle markets in Abeokuta and environs, Ogun state, Nigeria. *J. Agric. Sci. and Env*. **16**(2): 2315–7453.

Fearon J., Mensah S. and Boateng V. 2014. Abattoir operations, waste generation and management in the Tamale metropolis: Case study of the Tamale slaughterhouse. *J. Public Health Epidemiol.* **6**(1): 14–19. https://doi.org/10.5897/JPHE2013.0574

Gilbert S. E., Whyte R., Bayne G., Paulin S. M., Lake R. J. and Van der logt P. 2007. Survey of domestic food handling practices in New Zealand. *Int. J. of Food Microbiol*. **117**(3): 306–311. https://doi.org/10.1016/j.ijfoodmicro.2007.05.004

Gorman R., Bloomfield S. and Adley C. C. 2002. A study of cross-contamination of food-borne pathogens in the domestic kitchen in the Republic of Ireland. *Int. J. of Food Microbiol*., **76**(1–2): 143–150. https://doi.org/10.1016/S0168-1605(02)00028-4

Grace D. 2015. Food Safety in Low and Middle Income Countries. *Int. J. Environ. Res. Public Health* **12**:

10490–10507. https://doi.org/10.3390/ijerph120910490

Graczyk T. K., Knight R., Gilman R. H. and Cranfield M. R. 2001. The role of non-biting flies in the epidemiology of human infectious diseases. *Microbes Infect.***3**: 231–235.

Haileselassie M., Taddele H., Adhana K. and Kalayou S. 2013. Food safety knowledge and practices of abattoir and butchery shops and the microbial profile of meat in Mekelle City, Ethiopia. *Asian Pac J. Trop. Biomed*. **3**(5): 407–412. https://doi.org/10.1016/S2221-1691(13)60085-4

Heilmann M. 2016. Flies as vectors for Salmonella spp. and their control in pork butcheries in Kampala, Uganda- A contribution to improve public health. Freie Universität Berlin, Germany.

Iro O., Amadi C. O., Enebeli U. and Amadi A. N. 2017. Compliance Of Meat Handlers In Abia And Imo States Of Nigeria With HACCP – Based Standard Operating Procedures Checklist. *J. of Public Health* 3(7): 1-15.

Jianu C. and Goleţ I. 2014. Knowledge of food safety and hygiene and personal hygiene practices among meat handlers operating in western Romania. *Food Control* **42**: 214–219.

Karabudak E., Bas M. and Kiziltan G. 2008. Food safety in the home consumption of meat in Turkey. *J. Food Cont.* **19**, 320–327.

Kasirye A. 2017, September. Butchers to improve quality of meat products. New Vision. https://www.newvision.co.ug/news/1461553/butchers-improve-quality-meat-products

Kebede T., Afera B., Taddele H. and Bsrat A. 2014. Assessment of Bacteriological Quality of Sold Meat in the Butcher Shops of Adigrat, Tigray, Ethiopia Bureau of Agriculture and Rural Development. *Appl. J. Hyg.* **3**(3): 38–44. https://doi.org/10.5829/idosi.ajh.2014.3.3.8636

Kikulwe E. M., Okurut S., Ajambo S., Gotor E., Tendo R., Kubiriba J. and Karamura E. 2018. Does gender matter in effective management of plant disease epidemics ? Insights from a survey among rural banana farming households in Uganda. 10(March), 87–98. https://doi.org/10.5897/JDAE2017.0877

Koutsoumanis K. and Taoukis P. S. 2005. Meat safety, refrigerated storage and transport: Modeling and management. In Improving the Safety of Fresh Meat, pp.503-561 (Issue February 2018, pp. 1–89). https://doi.org/10.1533/9781845691028.2.503

Kyayesimira J., Kagoro-rugunda G., Lejju J. B., Matofari, J. W. and Nalwanga R. 2018. A pilot study on roles and operations of actors in the beef value chain in central and Western Uganda. *Int. J. Dev. Sustain*. **7**(7): 2063–2079.

Kyayesimira J., Rugunda G. K., Bunny L. J. and Matofari J. W. 2019. Compliance to Post-Harvest Handling Practices of Beef along the Beef Value Chain in Uganda. *J. Nutr. Weigh. Loss* **4**(16): 2–6.

MAAIF. 2010. Agriculture Sector Development Strategy and Investment Plan: 2010/11-2014/15: Agriculture for Food and Income Security, Entebbe, Uganda

MAAIF. 2020. Design of a movable slaughter facility for the ministry of agriculture, animal industry and fisheries.

Mirembe B., Ndejjo R. and Musoke D. 2015. Sanitation and Hygiene status of butcheries in Kampala, Uganda. *African J. Food, Agric. Nutr. Dev* **15** (3): 10153 - 10160.

Muhwezi G. 2018. UNBS is enforcing meat standards to protect consumers' health and safety, Monitor, https://www.monitor.co.ug/uganda/oped/commentary/unbs-is-enforcing-meat-standards-to-protect-consumers-health-and-safety-1737282

Musaba K. 2008, April. How safe is meat we buy from butcheries. New Vision, Uganda's Leading Daily. https://www.newvision.co.ug/new_vision/news/1190944/safe-meat-butcheries

Musoke D., Ndejjo R., Atusingwize E. and Halage A. A. 2016. The role of environmental health in One Health: A Uganda perspective. *One Health* **2**: 157–160. https://doi.org/10.1016/j.onehlt.2016.10.003

Niyonzima E., Bora D. and Ongol M. P. 2013. Assessment of beef meat microbial contamination during skinning, dressing, transportation and marketing at a commercial abattoir in Kigali city, Rwanda. *Pak. J. Food Sci*. **23**(3): 133–138.

Obeng A. K., Johnson F. S. and Appenteng S. O. 2013. Microbial Quality of Fresh Meat from Retail Outlets in Tolon and Kumbungu Districts of the Northern Region of Ghana.

Pal M., Ayele Y., Patel A. S. and Fitsum D. 2018. Microbiological and hygienic quality of Meat and Meat Products. *Beverage and Food World* **45**(5): 21–27.

PEH. 2008. Annual Summary of Outbreaks in New Zealand 2007 (Issue April). https://surv.esr.cri.nz/surveillance/annual_outbreak.php?we_objectID=4167

Rani Z., Hugo A., Hugo C., Vimiso P. and Muchenje V. 2017. Effect of post-slaughter handling during distribution on microbiological quality and safety of meat in the formal and informal sectors of South Africa: A review. *S. Afr. J. Anim. Sci*. **47**(3): 254-267.

Rosnani A. H., Son R., Mohhidin O., Toh P. and Chai L. 2014. Assessment of Knowledge, Attitude and Practices Concerning Food Safety among Restaurant Workers in Putrajaya, Malaysia. Food Science and Quality Management, 32. pp. 20-27 ISSN 2224–6088. www.iiste.org

Rouger A., Tresse O. and Zagorec M. 2017. Review: Bacterial Contaminants of Poultry Meat: Sources,

Species, and Dynamics. Microorganisms **5**(50): 1–16. https://doi.org/10.3390/microorganisms5030050

Santos A., Cardoso M. F., Correia da Costa J. M. and Gomes-Neves E. 2017. Meat Safety: An Evaluation of Portuguese Butcher Shops. *J. Food Prot.* **80**(7): 1159–1166. https://doi.org/10.4315/0362-028X.JFP-16-440

Scallan E., Hoekstra R. M., Angulo F. J., Tauxe R. V, Widdowson M., Roy S. L., Jones J. L. and Griffi P. M. 2011. Foodborne Illness Acquired in the United States - Major Pathogens. *Emerg. Infect. Dis.*, **17** (1): 7–15. https://doi.org/10.3201/eid1701.P11101

Singh, A. S. and Masuku M. B. 2014. Sampling Techniques and Determining Sample Size in Applied Statistics Research: an Overview. *Int. J. Economics, Commerce Manag.* **2**: 1–22.

Sofos J. N. 2008. Challenges to meat safety in the 21st century. *J. Meat Sci.* **78**(1–2): 3–13. https://doi.org/10.1016/j.meatsci.2007.07.027

Ssali G. 2018, January 6. More arrested in swoop on Kampala butcheries. The Independent. https://www.independent.co.ug/arrested-swoop-kampala-butcheries/

Sulleyman K. W., Adzitey F. and Boateng E. F. 2018. Knowledge and Practices of Meat Safety by Meat Sellers in the Accra Metropolis of Ghana. *Int. J. Vet. Sci.* **7**(3): 167–171.

Tam C., Erebara A. and Einarson A. 2010. Motherisk Update: Food-borne illnesses during pregnancy; Prevention and treatment. *Canadian Family Physician* **56**: 341–343.

Tegegne H. A. and Phyo H. W. W. 2017. Food safety knowledge, attitude and practices of meat handler in abattoir and retail meat shops of Jigjiga. *J. Prev. Med. Hyg.* **58**: 320–327.

Thomas M. K., Murray R., Flockhart L., Pintar K., Pollari F., Fazil A., Nesbitt A. and Marshall B. 2013. Estimates of the Burden of Foodborne Illness in Canada for 30 Specified Pathogens and Unspecified Agents, Circa 2006. *Foodborne Pathog. Dis.* **10**(7): 639-648. https://doi.org/10.1089/fpd.2012.1389

Thorell J. 2014. Cleaning Process of Abattoir Wastewater With Focus On Bacterial Pathogens (Thesis). Swedish University of Agricultural Sciences, Uppsala.

UNBS. 2007. Uganda standard: Hygienic requirements for butcheries. Uganda National Bureau of Standards.

UNBS. 2017. Design and operation of abattoirs and slaughterhouses - Requirements.

UNDP. 2015. Sustainable Development Goals (UNDP (ed.). UN.

Waldman L., Hrynick T. A., Benschop J., Cleaveland S., Crump J. A., Davis M. A., Boniface M., Mmbaga B. T., Niwael M.M., Gerard P., Sharp J., Swai E. S., Thomas K. M. and Zadoks R. N. 2020. Meat Safety in Northern Tanzania: Inspectors' and Slaughter Workers' Risk Perceptions and Management. *Front. Vet. Sci.* 7:**309**. https://doi.org/10.3389/fvets.2020.00309

Wambui J., Karuri E., Lamuka P. and Matofari J. 2017. Good Hygiene Practices among Meat Handlers in Small and Medium Enterprise Slaughterhouses in Kenya. *Food Control*, **5**(36). https://doi.org/10.1016/j.foodcont.2017.05.036

Yenealem D. G., Yallew W. W. and Abdulmajid S. 2020. Food Safety Practice and Associated Factors among Meat Handlers in Gondar Town : A Cross-Sectional Study. *J Environ Public Health* **2020**. https://doi.org/https://doi.org/10.1155/2020/7421745

Yiga F. 2018. Uganda-Meat contaminated by toxic chemicals. DW.COM. https://www.dw.com/en/uganda-meat-contaminated-by-toxic-chemicals/a-42110782

.

East African Journal of Biophysical and Computational Sciences

Journal homepage : https://journals.hu.edu.et/hu-journals/index.php/eajbcs

Study of Reaction Mechanisms in α + ^{69}Ga reaction at ≈10 – 50 MeV

F. K. Amanuel

[1]*Department of Applied Physics, Hawassa University, Hawassa, Ethiopia*

KEYWORDS:

Reaction cross-section;

COMPLETE code;

Reaction channel;

Excitation function

Research article

ABSTRACT

The excitation functions of ^{69}Ga(α, n)^{72}As, ^{69}Ga(α, 2n)^{71}As, ^{69}Ga(α, 3n)^{70}As, ^{69}Ga(α, x)^{69}Ge, ^{69}Ga(α, x)^{68}Ga and ^{69}Ga(α, x)^{67}Ga reactions formed in the interaction of α-projectile with ^{69}Ga-target were studied at ≈ 10-50 MeV. The produced nuclei were different isotopes of As, Ge, and Ga, some of which have important medical applications. The theoretical model predictions were based on the statistical code COMPLETE, and the predicted results were compared and discussed with existing experimental data. Good agreement between the theoretical predictions and experimental results were obtained. Pearson's relational statistics revealed moderate to strong positive associations between the theoretically predicted and experimentally measured reaction cross-sections. Furthermore, the present investigation revealed significant pre-compound contributions in the studied energy range. Therefore, it is important to consider the admixture of pre-equilibrium and equilibrium modes of reactions when predicting the reaction cross-sections.

INTRODUCTION

Advances in accelerator technology and cyclotrons have enabled the use of light- and heavy-charged nuclei as projectiles in nuclear reactions. This development has improved our understanding of the reaction mechanism and nuclear structure at various energies near and above the Coulomb barriers (Cavinato *et al*., 1995; Amorini *et al*., 1998; Gadioli *et al*., 1998). For example, at moderate excitation energies, reactions induced by nucleons and light-charged projectiles are found to proceed through the equilibrium (EQ) and pre-equilibrium (PE) mode reactions (Baure *et al*., 1995;Agrawal *et al*., 2001; Patronis *et al*., 2007; Johari and Saxena, 2015). To understand these reaction mechanisms, reaction cross-section data evaluation is essential. Accordingly, comparative studies based on experimental data and theoretical predictions are demanding. In this regard, nuclear reaction model-based computer codes can swiftly help to predict unknown reaction cross-sections and thus improve computer code predictions.

Studies of light-charged induced nuclear reactions help better understand the reaction mechanisms and test the validity of various available and newly evolving computer codes. Furthermore, in light-charged induced nuclear reactions, the processes of PE and EQ particle(s) emissions are vital in comprehending and characterizing the reaction mechanisms, attributable to the strong competition between

**Corresponding author:*
Email: rabirhanu@gmail.com,

https://dx.doi.org/10.4314/eajbcs.v4i1.2S

PE and EQ mode of reactions at moderate excitation energies.

Numerous studies have compared theoretically predicted and experimentally measured reaction cross sections for light-charged particle induced reactions, aiming to elucidate the underlying reaction mechanisms (Agarwal *et al*., 2002; Abhishek *et al*., 2008; Amanuel *et al*., 2011; Yigit and Tel, 2014; Asres *et al*., 2018; Asres *et al*., 2019; Amanuel, 2021). However, reasonable comparative reaction mechanisms studies between theory and experiment of ^{72}As, ^{71}As, ^{70}As, ^{69}Ge, ^{68}Ga, and ^{67}Ga reaction products produced in α-projectile induced reactions on ^{69}Ga-target at ≈10 – 60 MeV, have not been investigated efficiently; therefore, further investigations and scientific evidence are required (Ismail 1990; Rezvi *et al*., 1989; Didik *et al*., 1994). Furthermore, understanding the reaction mechanisms induced by a light-charged projectile, such as in α + ^{69}Ga reaction helps to investigate new works on producing pure and optimized ^{72}As and ^{68,} ^{67}Ga radionuclides that are useful in medical applications embracing the present and possible future needs.

The present work investigates the reaction mechanisms involved in the interaction of α-projectile with ^{69}Ga-target at ≈10 - 50 MeV. Excitation functions of ^{69}Ga(α, n)^{72}As, ^{69}Ga(α, 2n)^{71}As, ^{69}Ga(α, 3n)^{70}As, ^{69}Ga(α, x)^{69}Ge, ^{69}Ga(α, x)^{68}Ga and ^{69}Ga(α, x)^{67}Ga reactions were predicted using the statistical model code COMPLETE. The corresponding experimental data were collected from the EXFOR database (Levkovski, 1991). The COMPLETE computer code has proven effective in reaction mechanism studies, particularly for light- and medium-nuclei induced reactions (Agarwal *et al*., 2002; Asres *et al*., 2018; Asres *et al*., 2019).

THEORETICAL BACKGROUND

Several theoretical nuclear reaction model-based computer codes have been used to predict reaction cross-sections (Abhishek *et al*., 2008; Yigit and Tel, 2014; Amanuel, 2021). The nuclear reaction mechanisms change with light-charged projectile energies near and above the Coulomb barrier. The reaction mechanism is considered to proceed through EQ as well as PE emission of particles at moderate excitation energies (≈10- 60 MeV) (Baure *et al*., 1995; Agrawal *et al*., 2001; Pal *et al*., 2005; Johari *et al*. 2015; Asres *et al*., 2019). The EQ mode of reaction mechanism dominates in the low energy region (in general, below 20 MeV). Furthermore, this reaction mechanism occurs in a nuclear reaction time scale of about 10^{-16} to 10^{-18} s. In the EQ mode of reactions, the projectile is captured by the target nucleus, and its energy is shared and re-shared amongst the nucleons, losing their identity and forming a single excited complex system that eventually leads to a fully equilibrated compound nucleus (CN). The EQ emissions of nuclear reactions are usually treated using statistical models. For example, the Hauser-Feshbach (Hauser and Feshbach, 1952) formalism considers the angular momentum and the nuclear level structure to define the EQ emission spectrum. On the other hand, in the Weisskopf-Ewing (Weisskopf and Ewing, 1940) EQ emission formalism, angular momentum, and parity are not considered.

The PE mode of reaction mechanism becomes increasingly crucial at a relatively high energy region (above ≈20 MeV). Therefore, the PE emissions of nuclear reactions occur before the thermalization of a composite system and are usually treated using non-statistical models; and the popular models used for the description and calculations of the PE mode of the reaction mechanism are the exciton model (Griffin, 1966; Blann, 1975; Agassi *et al*., 1975), hybrid model (Blann, 1971), and geometry-dependent hybrid model (Blann and Vonach, 1983).

Various computer codes were developed for years based on different nuclear reaction models

that helped study nuclear structure and reaction mechanisms (Young *et al*., 1992; Uhl and Strohmaier, 1976; Strohmaier and Uhl, 1980). The ALICE-91 (Blann, 1991) analytic code developed by Blann was also vastly used over the years to predict reaction cross-sections in the intermediate energy regions. The computer code COMPLETE (Ernst, 1997) is an advanced modified version of the ALICE-91 code family and has been successfully applied to the calculation of EQ and PE reaction cross-sections (Aydin *et al*., 2010; Asres *et al*., 2018; Asres *et al*., 2019; Amanuel, 2021).

COMPLETE code

The computer code COMPLETE with new corrections and capabilities has successfully predicted nuclear reaction cross-sections, especially for reaction mechanisms studies (Asres *et al*., 2018; Asres *et al*., 2019; Amanuel *et al*., 2011). This code employs the Weisskopf-Ewing formalism (Weisskopf and Ewing, 1940) for the EQ reaction component and Hybrid (H) model (Blann, 1971) as well as the Geometric Dependent Hybrid (GDH) model of Blann (Blann and Vonach, 1983) for the PE reaction component. According to the Weisskopf-Ewing model, and based on Bohr's independence hypothesis, the nuclear reaction cross-section for a reaction with entrance channel α and exit channel β can be expressed as

$$\sigma_{\alpha\beta} = \sigma_{CN}(\alpha)\frac{\Gamma_\beta}{\Gamma} \qquad (1)$$

Where $\sigma_{CN}(\alpha)$ is the cross-section for the formation of the CN and Γ_β, Γ, respectively, represent the energy average width for the decay of the CN in channel β, and the energy averaged total width. In Eq. (1) Γ_β can be given as:

$$\Gamma_\beta = \frac{2S_\beta + 1}{\pi\hbar^2}\mu_\beta \int d\varepsilon \sigma_\beta^{inv}(\varepsilon)\varepsilon\frac{\omega_1(U)}{\omega_1(E)}$$

Where μ_β and D_β represent the ejectile's reduced mass and spin, respectively, the quantity $\sigma_\beta^{inv}(\varepsilon)$ represents the inverse reaction cross-section, and U the excitation energy of the residual nucleus. $\omega_1(E)$ corresponds to the total single-particle level density at excitation energy, E.

The H model formulation of Blann and Vonach (Blann and Vonach, 1983) for PE reaction differential cross-section is given by:

$$\frac{d\sigma_\nu(\varepsilon)}{d\varepsilon} = \sigma_R P_\nu(\varepsilon) \qquad (2)$$

$$P_\nu(\varepsilon)d\varepsilon = \sum_{\Delta n=+2}^{\bar{n}_{n=n_o}} \left[\frac{x_\upsilon N_n(\varepsilon,U)}{N_n(\varepsilon)}\right] g_\nu d\varepsilon \left[\frac{\lambda_c(\varepsilon)}{\lambda_c(\varepsilon)+\lambda_+(\varepsilon)}\right] D_n, \qquad (3)$$

Here,$\sigma_R$represents the reaction cross-section, and $P_{\nu(\varepsilon)d\varepsilon}$ represents the number of particles of the type ν emitted into the unbounded continuum with channel energy between ε and ε+dε. The quantity in the first set of the square bracket of Eq. (3) represents the number of particles to be found (per MeV) at a given energy "ε" with respect to the continuum for all scattering processes leading to an "n" excition configuration. The nucleon-nucleon scattering energy partition function, $N_n(\varepsilon, U)$ represents the number of combinations with which n exciton may share the excitation energy, E_{ex} and x_ν represent the exciton number of ν type nucleon for a given total exciton state n.g_ν corresponds to the single-particle level density for nucleon of the “ν" type. The second set of a square bracket in Eq. (3) represents the fraction of the ν type particles at energy ε, which should undergo emission into a continuum rather than making an inter-nuclear transition. The D_n represents the average fraction of the initial

population surviving the treated exciton number. The quantity $\lambda_c(\varepsilon)$ represents the continuum emission rate for particles with "ε" channel energy, and $\lambda_+(\varepsilon)$ represents the intranuclear transition rate. The quantities U and E represent the residual nucleus and composite system excitation energies, respectively.

The GDH hybrid model has successfully reproduced a wide range of nuclear reaction data (Blann, 1972; Blann and Vonach, 1983; Harp *et al*., 1966). The GDH model is a modified version of the H model in which the nuclear geometry effects are considered. In addition, the GDH model oonsiders the reduced matter density, hence the shallow potential. Accordingly, the PE decay formalism incorporated the diffused surface properties sampled by higher impact parameters.

The differential cross-section for PE emission in the GDH model is formulated as follows:

$$\frac{d\sigma_v(\varepsilon)}{d\varepsilon} = \pi\lambda^2 \sum_{l=0}^{\infty}(2l+1)T_l P_v(l,\varepsilon) \qquad (4)$$

The quantity T_l represents the transmission coefficient for the l^{th} partial wave, and $P_l(l,\varepsilon)$ represents decay probability at channel energy "ε" and orbital angular momentum "l". λ is the reduced de-Broglie wavelength.

Pearson's correlation coefficient

The prediction quality of our optimization in fitting COMPLETE code using essential input parameters for the experimental reaction cross sections available in the literature was evaluated using the statistical Pearson's coefficient, R(Sedgwick, 2012; Wang, 2012; Patrick, 2018). In addition, the present work used Pearson's correlation coefficient to provide information on the linear relational strength between the COMPLETE projected and experimentally measured reaction cross-sections.

Pearson's correlation coefficient, R, is given by:

$$R = \frac{N\left(\sum_{i=1}^{N} X_{T_i} X_{E_i}\right) - \left(\sum_{i=1}^{N} X_{T_i}\right)\left(\sum_{i=1}^{N} X_{E_i}\right)}{\sqrt{\left[N\sum_{i=1}^{N} X_{E_i}^2 - \left(\sum_{i=1}^{N} X_{E_i}\right)^2\right]\left[N\sum_{i=1}^{N} X_{T_i}^2 - \left(\sum_{i=1}^{N} X_{T_i}\right)^2\right]}} \qquad (5)$$

Where N is the number of the theoretical and experimental data points, X_{T_i} and X_{E_i} are the theoretical and experimental cross-section of the i^{th} value, respectively. Eq. (5) returns unitless values for R between -l and +l, where +l represents a strong positive relationship, -l indicates a strong negative relationship; and 0 indicates no relationship. If $0 < R < 0.3$, the correlation is weak and positive, if $0.3 \leq R < 0.7$ the correlation is moderate and positive; and if $0.7 \leq R < l$ the correlation is strong and positive.

RESULTS AND DISCUSSION

Excitation functions of ^{69}Ga(α, n)^{72}As, ^{69}Ga(α, 2n)^{71}As, ^{69}Ga(α, 3n)^{70}As, ^{69}Ga(α, x)^{69}Ge, ^{69}Ga(α, x)^{68}Ga and ^{69}Ga(α, x)^{67}Ga reactions produced via EQ and PE processes were considered at ≈ 10-50 MeV. The experimentally quantified excitation functions were compared with the theoretical model code COMPLETE predictions, which account for both EQ and PE processes. In this code, the level density parameter a, which predominantly affects the EQ components of a cross-section, is calculated from the expression a = A/K MeV^{-1}, where A is the nucleon number of a CN and K is an adjustable constant. K may vary to match the experimenta1 data. The initial exciton number n_o (n_o= n+p+h, which is described by the number of neutrons (n), the number of protons (p) in excited states, and the number of holes (h) after the first collision) that governs the PE component, represents the initial configuration

of the number of particles in the excited states and the number of holes after the first collision.

In the present work, to match the experimental data, the values of important input parameters K(K=8, 10, 12) and n_o (n_o=4, 5, 6) were varied for a representative ^{69}Ga(α, n)^{72}As Reaction. Figure 1 displays the experimentally measured excitation functions and theoretical predictions using different K and n_o values for ^{69}Ga(α, n)^{72}As Reaction.

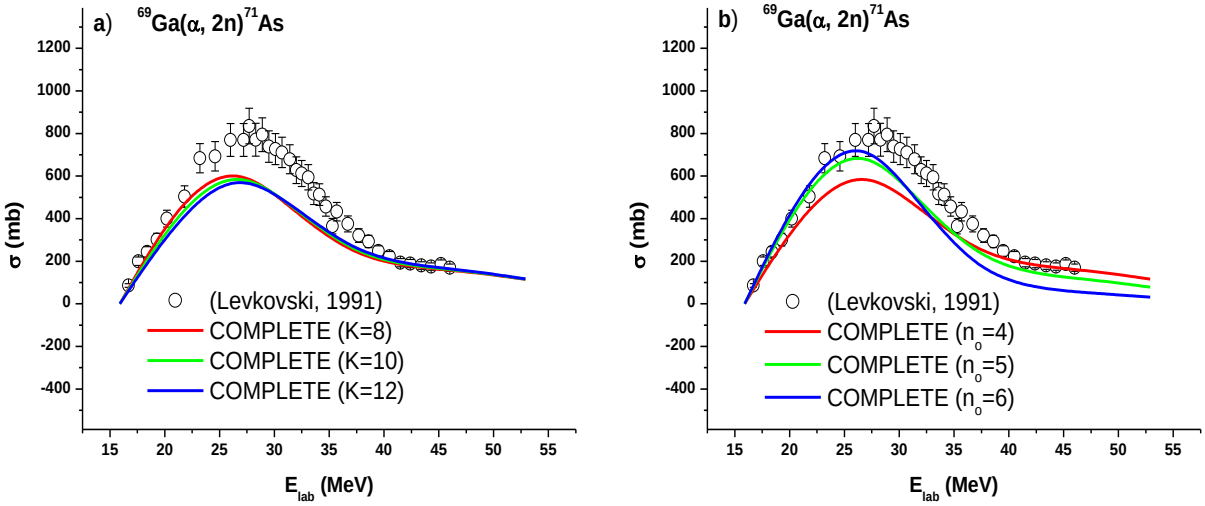

Figure 1: Experimentally measured and theoretically calculated excitation functions for ^{71}As residue.

The curves represent the theoretical predictions (admixture PE and EQ) for different values of K (K = 8, l0, and l2) in panel (a) and n_o (n_o = 4, 5, and 6) in panel (b). The open circles represent the experimental cross-sections.

As this figure indicates, the measured excitation function is well reproduced by COMPLETE code for values of K=8 and n_o=5. It may be observed from Fig 1(a) that the predicted excitation functions for different K values are related; if they differ, the alterations are minimal. For other reaction channels populated in the interaction of α-projectile with ^{69}Ga-target, a combination of K=8 and n_o=5 has been consistently used to predict the reaction cross-sections.

A) ^{9}Ga(α, n)^{72}As Reaction

When α-projectile bombarded ^{69}Ga-target, a composite [^{73}As]* nucleus is produced in excited states. The excited [^{73}As]* nucleus then emits a neutron leaving the ^{72}As nucleus as a residue, i.e., α + ^{69}Ga ⟶ [^{73}As]* ⟶ n + ^{72}As

Figure 2(a) displays the experimentally measured excitation function and the COMPLETE code predictions for ^{69}Ga (α, n)^{72}As reaction. As shown in Figure 2(b), the experimentally quantified excitation function is comparatively higher than the theoretically predicted excitation functions (with and without PE contribution), though the shapes of the two excitation functions showed a similar trend. The observed enhancement on the measured cross-section may be attributable to impurity contributions from the heavier residue(s). In addition, Pearson's correlation coefficient

between theoretically predicted and experimentally measured production cross-sections has a value of R=0.96. Hence, the theoretical results indicated a strong and positive correlation with the experimental.

B) ^{69}Ga(α, 2n)^{71}As Reaction

In the case of ^{69}Ga(α, 2n)^{71}As reaction, the residue ^{71}As may be produced following the emission of two neutrons from an excited composite nucleus, [^{73}As]*, i.e.,

$$\alpha + {}^{69}\mathrm{Ga} \longrightarrow [{}^{73}\mathrm{As}]^* \longrightarrow 2n + {}^{71}\mathrm{As}$$

Fig. 2(b) shows the theoretically predicted excitation functions (with and without the contribution of PE reaction) along with the experimentally measured excitation function for ^{69}Ga(α, 2n)^{71}As Reaction. As shown in this figure, the predictions of the COMPLETE code, after incorporating the PE reaction, agree with the measured excitation function. Furthermore, Pearson's correlation coefficient value ($R \approx 0.94$) indicated a strong and positive correlation between theoretically predicted and experimentally measured production cross-sections.

C) ^{69}Ga(α, 3n)^{70}As reaction

The measured excitation function and theoretical predictions obtained from COMPLETE code for ^{70}As residue populated via (α, 3n) channel are shown in Figure 2(c).

Note that in the ^{69}Ga(α, 3n)^{70}As reaction, the residue ^{70}As may be formed through the reaction:

$$\alpha + {}^{69}\mathrm{Ga} \longrightarrow [{}^{73}\mathrm{As}]^* \longrightarrow 3n + {}^{70}\mathrm{As}$$

It may be observed from Figure 2(c) that up to 40 MeV (up to the peak portion), the predicted excitation function after incorporating PE contribution, in general, reproduced the measured excitation function satisfactorily. However, above 40 MeV (in the tail portion of the excitation function), the predicted values are higher than the experimental data. Moreover, Pearson's correlation coefficient between theoretically predicted and experimentally measured reaction cross-sections has a value of R=0.86. Hence, the theoretical results indicated a strong and positive correlation with the experimental.

D) ^{9}Ga(α, x)^{69}Ge reaction

In ^{69}Ga(α, x)^{69}Ge reaction, ^{69}Ge residue may be formed through the emissions of unidentified particles, x from the composite nucleus, [^{73}As]* via (α, x) complex channel. As seen in Figure 2(d), the predicted excitation functions with the inclusion of PE contribution is in good agreement with the measured excitation function.

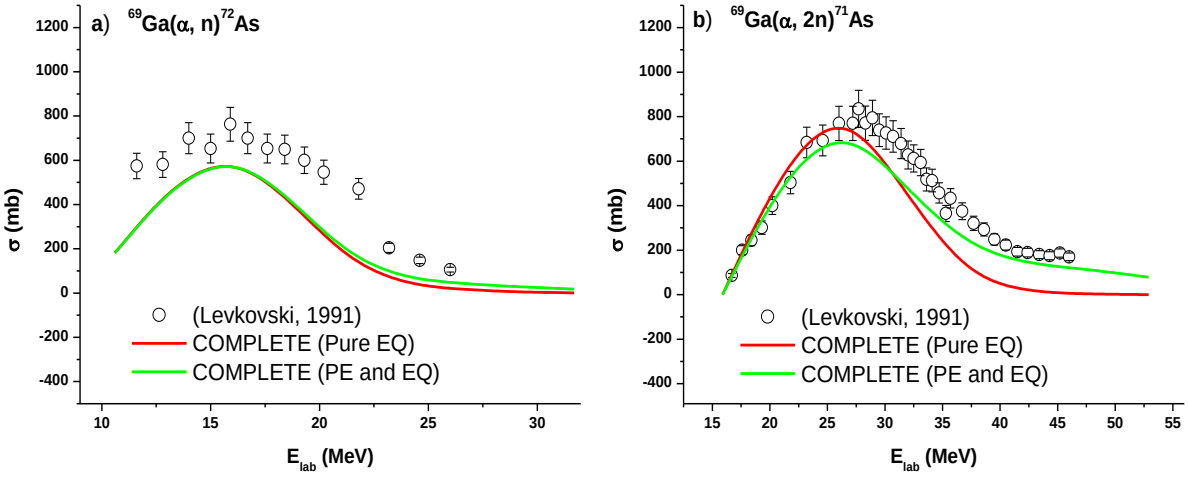

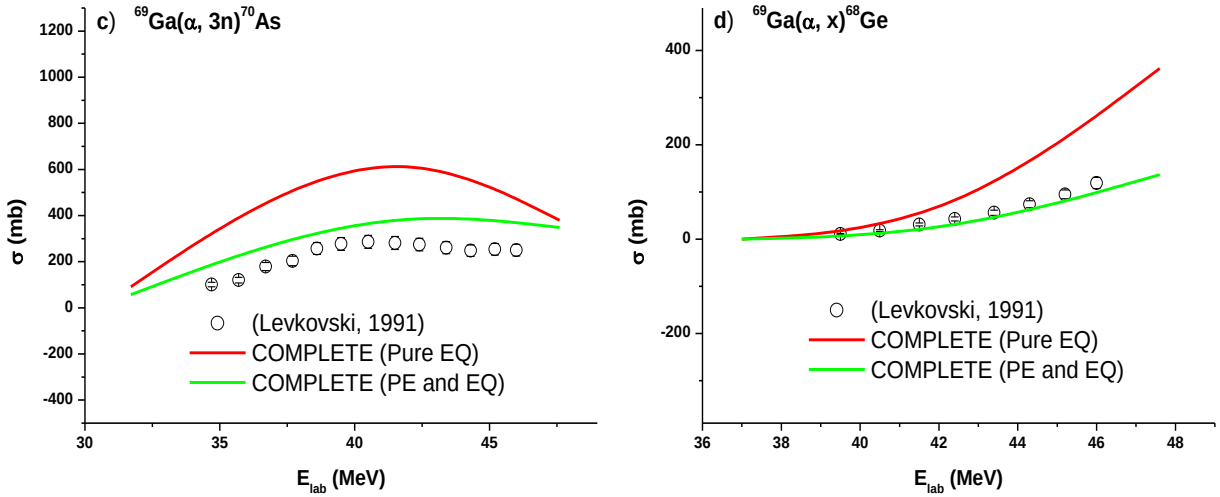

Figure 2. Experimentally quantified and theoretically predicted excitation functions for 72As, 71As, 70As, and 69Ge residues.

The curve represents the theoretical prediction, and the symbols represent the experimental cross-sections.

Pearson's correlation coefficient between theoretically predicted and experimentally measured production cross-sections is R ≈ 0.99. This result indicated a strong positive association between the predicted and measured production cross-sections.

A) ^{9}Ga(α, x)^{68}Ga reaction

^{68}Ga residue is produced when unidentified particles (x) are emitted from an excited composite nucleus [^{73}As]* via ^{69}Ga(α, x)^{68}Ga complex reaction channel. Figure 3(a) shows the theoretically predicted excitation and experimentally measured excitation functions.

It may be observed from Figure 3(a) that the predicted (pure EQ) excitation function is in good agreement with the measured one. Furthermore, Pearson's correlation coefficient between the predicted (pure EQ) and measured cross-sections have a value of R ≈ 0.5, indicating a moderate and positive correlation between the measured and the predicted excitation functions.

B) ^{69}Ga(α, x)^{67}Ga reaction

The measured excitation[6] functions, along with the theoretical predictions (with and without the contribution of PE reaction) for ^{69}Ga(α, x)^{67}Ga complex reaction channel, are shown in Figure 3(b). Note that ^{67}Ga residue is produced when unidentified particles (x) are emitted from an excited composite nucleus [^{73}As]* via ^{69}Ga(α, x)^{67}Ga complex reaction channel.

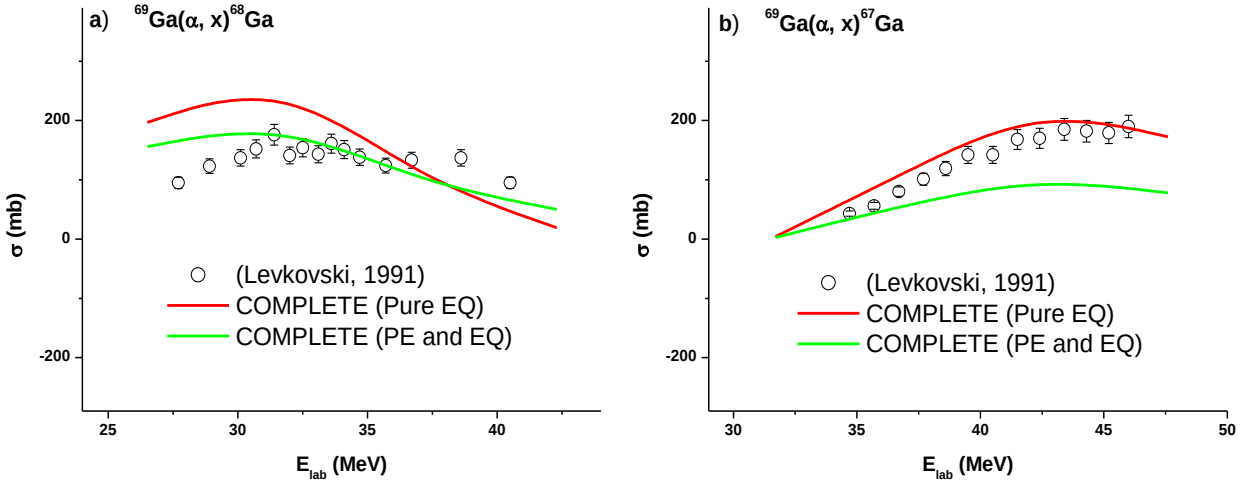

Figure 3. Experimentally measured and theoretically calculated excitation functions for ^{68}Ga and ^{69}Ga residues.

The curve represents the theoretical prediction, and the symbols represent the experimental cross-sections.

Figure 3(b) shows that the pure EQ-predicted excitation function agrees with the experimentally measured excitation function. Furthermore, Pearson's correlation coefficient value (R≈0.98) indicated a strong and positive correlation between theoretically predicted and experimentally measured reaction cross-sections.

CONCLUSION

Excitation functions of ^{69}Ga(α, n)^{72}As, ^{69}Ga(α, 2n)^{71}As, ^{69}Ga(α, 3n)^{70}As, ^{69}Ga(α, x)^{69}Ge, ^{69}Ga(α, x)^{68}Ga and ^{69}Ga(α, x)^{67}Ga reactions populated in the interaction of α-projectile with ^{69}Ga-target were studied at ≈10 -50 MeV. Except for ^{69}Ga(α, x)^{68}Ga reaction, the theoretically predicted (admixture of PE and EQ reactions) reaction cross-sections using the statistical model code COMPLETE with the K=8 and n_o=5, in general, were found to be in good agreement with the experimentally measured excitation functions.

Furthermore, Pearson's correlation coefficients r moderate to strong positive correlations between the theoretically predicted and experimentally measured excitation functions for investigated reaction channels. The present results also disclosed a significant contribution from a pre-equilibrium reaction, particularly in the tail sections of the excitation functions. Thus, the admixtures of pre-equilibrium and equilibrium modes of reactions must be considered when predicting total reaction cross-sections.

Acknowledgment

The author gratefully acknowledges Webshet Beharu and Anabel T. Abosse for their valuable scientific discussions that contributed to this work. The author remains solely responsible for all opinions and any errors.

References

Abhishek Y., Singh P. P., Sharma M. K., Singh D. P., Singh B.P., Prasad R., Musthafa M.M. and Calicut U. 2008. Large pre-equilibrium contribution in α + natNi interactions at ≈8− 40 MeV. *Phys. Rev. C* **78**, 044606.

Agrawal A., Bhardwaj K. M., Rizvi A. I. and Chaubey A.K. 2001. Equilibrium and pre-equilibrium studies

in some alpha induced reactions on rhodium. *J. Phys. Soc. Jpn*. 702003–8.

Agarwal A., Rizvi I. A. and Chaubey A. K. 2002. Excitation function studies of alpha induced reactions for niobium and pre-equilibrium effects. *Physical Review Part C, Nuclear Physics* **65**, 034605.

Amorini F., Cabibbo M., Cardella G., Pietro A. Di., Figuera, A. Musumarra, M. Papa, G. Pappalardo, F. Rizzo and S. Tudisco, S. 1998. Pre-equilibrium γ ray emission in complete and incomplete fusion reactions in the collision $^{12}C+^{64}Ni$ at 8 MeV/nucleon. *Phys. Rev. C* **58:** 987-995.

Amanuel F. K., Zelalem B., Chaubey A. K., Avinash A. and Rizvi I. A. 2011. Significant amount of pre-equilibrium contribution in the alpha+ 93Nb system at energies ~18-40 MeV. *Chinese J. Phys.* **49**, 884-892.

Amanuel F. K. 2021. Nuclear model prediction for production of medical 22Na, 51Cr, 60Co, 61Cu, 64Cu, 65Zn, 67, 68Ga, 88Y and 99Mo radionuclides: Comparison of experimental and theoretical data. *Appl. Radiat. Isot.* **172**: 1096746.

Asres H. Y., Mathuthu M. and Birhane, D. M. 2018. Analysis of reaction cross-section production in neutron induced fission reactions on uranium isotope using computer code COMPLET. *Appl. Radiat. Isot.*13981–5.

Asres H. Y., Manny M. and Yinager A. F. 2019. Investigation of nuclear reaction mechanisms of Nickel isotopes at various energies induced by alpha particles. *J. Phys. Comm*. **3**, 115018.

Agassi D., Weidenm¨uller H. A. and Mantzouranis G. 1975. Equilibrium and nonequilibrium formalisms made unified. *Phys. Rep*. **22**, 145.

Aydin A., Tel E., Kaplan A. and Büyükuslu H. 2010. Pre-equilibrium cross section calculations in alpha induced reactions on 65Cu and 209Bi. *Ann. Nucl. Energy*, 37 (10): 1316-1320.

Bauer W. and Botvina A. 1995. Pre-equilibrium particle emission and critical exponent Analysis. *Phys. Rev. C* **52**: 1760 - 1763.

Blann M. 1971. Hybrid model for pre-equilibrium decay in nuclear reactions: *Phys. Rev. Lett*. **27**: 337–340.

Blann M. 1972. Importance of the nuclear density distribution on pre-equilibrium decay. *Phys. Rev. Lett*. **28**: 757.

Blann M. 1975. Preequilibrium Decay. *Annu. Rev. Nucl. Sci*. **25**: 123 – 166.

Blann M. and Vonach H.K. 1983. Global test of modified pre-compound decay models. *Phys. Rev. C* **28**: 1475–1492.

Blann M. 1991. NEA Data Bank, Report No.PSR-146, Gif-sur-Yvette, France.

Cavinato M., Fabrici E., Gadioli E., Vergani P., Crippa M., Colombo G., Redall I. and Ripamonti M. 1995. Study of the reactions occurring in the fusion of 12C and 16O with heavy nuclei at incident energies below 10 MeV/nucleon: *Phys. Rev. C* **52**: 2577.

Didik V. A., Malkovich R. Sh., Skoryatina E. A. and Kozlovskii V. V. 1994. Experimental determination of the cross sections of nuclear reactions by the method of analysis of the concentration profiles of transmutation nuclides: *Atomnaya Energiya* **77**(1): 570–572.

Ernst, J. 1997. Nstitut Fuer Strahlen- Und Kernphysik, Nussallee 14-16, Bonn F.R. Germany. Email: ernst@servax.iskp.uni-bonn.de

Gadioli E., Brattari C., Cavinato M., Fabrici E., Gadioli E., Allori V., Cerutti F., Di Fillippo A., Vailati S., Stevens T. G., Connell S. H., Sellschop J. P. F., Nortier F. M., Steyn G. F. and Marchetta C. 1998. Angular Distributions and Forward Recoil Range Distributions of Residues Created in the interaction of 12C and 16O with 103Rh. *Nucl Phys. A* **641**: 271-296.

Griffin J. J. 1966. Statistical Model of Intermediate Structure. *Phys. Rev. Lett*. **17**: 478.

Harp G. D., Miller J. M. and Berne B. J. 1968. Attainment of Statistical Equilibrium in Excited Nuclei. *Phys. Rev*. **165**: 1166.

Hauser W. and Feshbach H. 1952. The inelastic scattering of neutrons. *Phys. Rev. C* **87**: 366–373.

Ismail M. 1990. Measurement and analysis of the excitation function for alpha-induced reactions on Ga and Sb isotopes. *Phys. Rev. C* **41:** 87.

Johari A. and Saxena K. A. 2015. Study of alpha-induced nuclear Reaction in the energy range up to 60 MeV on ^{54}Fe. *Adv. Appl. Sci. Res.* **6**: 69–74

Levkovski V. N. 1991. Cross sections of medium mass nuclide activation A=40-100) by medium energy protons and alpha-particles (E=10-50 MeV): Act. Cs. By Protons and Alphas, Moscow.

Patronis N., Papadopoulos C. T., Galanopoulos S., Kokkoris M., Perdikakis G., Vlastou R., Lagoyannis A., and Harissopulos S. 2007. Activation cross section and isomeric cross-section ratio for the (n, 2n) reaction on 191Ir. *Phys Rev. C* **75**: 034607.

Pal J., Saha C. C., Pal J., Saha S., Dey C. C., Banerjee P., Bose S., Sinha B. K., Chatterjee M. B., and Basu S. K. 2005. Pre-equilibrium and equilibrium emission of neutrons in 114Cd(α, xn) reactions. *Phys. Rev. C* **71**. 034605.

Patrick S. 2018. Correlation Coefficients: Appropriate Use and Interpretation. *Anesth. Analg.* **126**(5): 1763-1768.

Rizvi I. A., Bhardwaj M. K., Ansari M. A., Chaubey A. K. 1989. Nonequilibrium effects in α- particle induced reactions on gallium isotopes. *Can. J. Phys.* **67**(9). *https://doi.org/10.1139/p89-150*

Sedgwick P. 2012. Pearson's Correlation Coefficient: *Br. Med. J.* 345, e4448. *Doi: https://Doi.org/10.1136/bmj.e4483*

Strohmaier B. and Uhl M. 1980. International Atomic Energy Agency Report: IAEA-SMR-43, p. 313.

Uhl M. and Strohmaier B. 1976. Computer Code for Particle Induced Activation Cross Section and Related Quantities: Report 76/01, Vienna.

Wang J. 2012. On the Relationship between Pearson correlation Coefficient and Kendall's Tau under Bivariate Homogeneous Shock Model: International Scholarly Research Network: ISRN Probability and Statistics, Volume 2012, Article ID 717839. *Doi: https://doi.org/10.5402/2012/717839*

Weisskopf V. F. and Ewing D. H. 1940. On the yield of nuclear reactions with heavy Elements. *Phys. Rev*., 57: 472–485.

Yigit M. and Tel E. 2014. Nuclear model calculation for production of 18F, 22Na, 44,46Sc, 54Mn, 64Cu, 68Ga, 76Br and 90Y radioniclides used in medical applications. *Ann. Nucl. Energy* **69**: 44–50.

Young P. G., Arthur E. D. and Chadwick M. B. 1992. International Center for Theortical Physics Workshop on Computation and Analysis of Nuclear Data Relevant to Nuclear Energy and Safety: H4.SMR614/1 (Italy).

.

East African Journal of Biophysical and Computational Sciences

Journal homepage : https://journals.hu.edu.et/hu-journals/index.php/eajbcs

Population Dynamics and Yield Estimation of Common Carp (*Cyprinus carpio*, Linnaeus, 1758) in Ayalew Reservoir, Gamo Zone, Southern Ethiopia

Buchale Shishitu Shija*, and Atnafu W/yohans Firew

Fisheries and Aquaculture, Southern Agricultural Research Institute (SARI), Arba Minch Agricultural Research Center, P.O.Box 2228, Arba Minch, Ethiopia

KEYWORDS:

Ayalew reservoir;

Cohort analysis;

Condition factor;

Cyprinus carpio;

Length-weight relationship;

Population dynamics parameters

Research article

ABSTRACT

Common carp (*Cyprinus carpio*) is an imported fish species in Ayalew reservoir. The study was intended at estimating important population dynamics parameters and production potential in the reservoir. Total length (TL) and total weight (TW) data were collected from a total of 276 fish samples (141 females and 135 males). The obtained data were analyzed using FiSAT II software. The population and production potential were assessed by using Jones length based cohort analysis model and length-based Thompson and Bell yield prediction models. The average total length was 26 cm and the dominant length groups ranged from 17 to 33 cm were 87%. The length-weight relationship parameters were ($TW = 0.0565TL^{2.53}$, R^2 = 0.95) and the condition factor K = 1.29. The parameters of von Vertalanffy growth curve were $L\infty$ = 41 cm, k = 0.52, t_o = -0.29, θ = 2.9 and A0.95 = 5.5 years. The assessed values of the total, natural and fishing mortalities were Z = 1.23, M = 0.55 and F = 0.68, respectively. The current exploitation rate, 0.55, indicates slightly overexploitation. The estimated fish population and the annual fish yield were 59,304 and 1.5 tons, respectively. However, investigation on reproductive biology, limnolocal aspects and stock enhancements should be required for the sustainability of these resources.

INTRODUCTION

Common carp (*Cyprinus carpio*) is considered to be a very important aquaculture species in many Asian and some European countries. It is widely distributed and frequently considered a nuisance species outside its native range (Penne and Pierce, 2008; Mohammad, 2015). The Common carp is one of the most common freshwater fish invaders worldwide, creating adverse effects on water quality and impacting ecosystem structure and function (Letvin *et al*., 2017). It is highly adaptable to new environments and can alter the biotic and abiotic integrity of aquatic ecosystems (Bajer *et al*., 2012).

*Corresponding author:
Email: buchale.shishitu@yahoo.com

https://dx.doi.org/10.4314/eajbcs.v4i1.3S

In Ethiopia, *Cyprinus carpio* was first introduced to Aba Samuel Dam (Awash River basin) in 1940 from Italy (Getahun, 2017). Later, it has been introduced in Lake Ziway in the late 1980s (FAO, 1997; Abera *et al.*, 2015). For food security purpose, *C. carpio* was introduced in highland lakes such as Ashengie, Ardibo, and Maybar and the introduction was successful (Golubtsov and Darkov, 2008).

Ayalew reservoir is one of the highland water bodies in Gamo Zone Chencha woreda. According to gathered information from Chencha woreda, *C. carpio* was introduced in Ayalew reservoir in the late 1980s by National Fishery and Aquatic Life Research Center. After some years later, the fish was adapted and has been observed by the local community in the reservoir. Since then, there was no any documented information about the population dynamics of *C. carpio* in Ayalew reservoir. For sustainable management and utilization, information on the population dynamics and production potential is very important for this species. Therefore, the objective this study was to estimate the population dynamics and production potential of *C. carpio* in the reservoir.

MATERIALS AND METHODS

Description of the study area

Ayalew reservoir is found in Chencha woreda in Gamo Zone. It is situated at the coordinates of 06°25′068″N latitude and 037°57′368″E longitude with an elevation of 2861 meters above sea level. The area of the reservoir is about 4.37 ha or 0.0437 km^2 with a maximum depth of 5.3 meters.

.

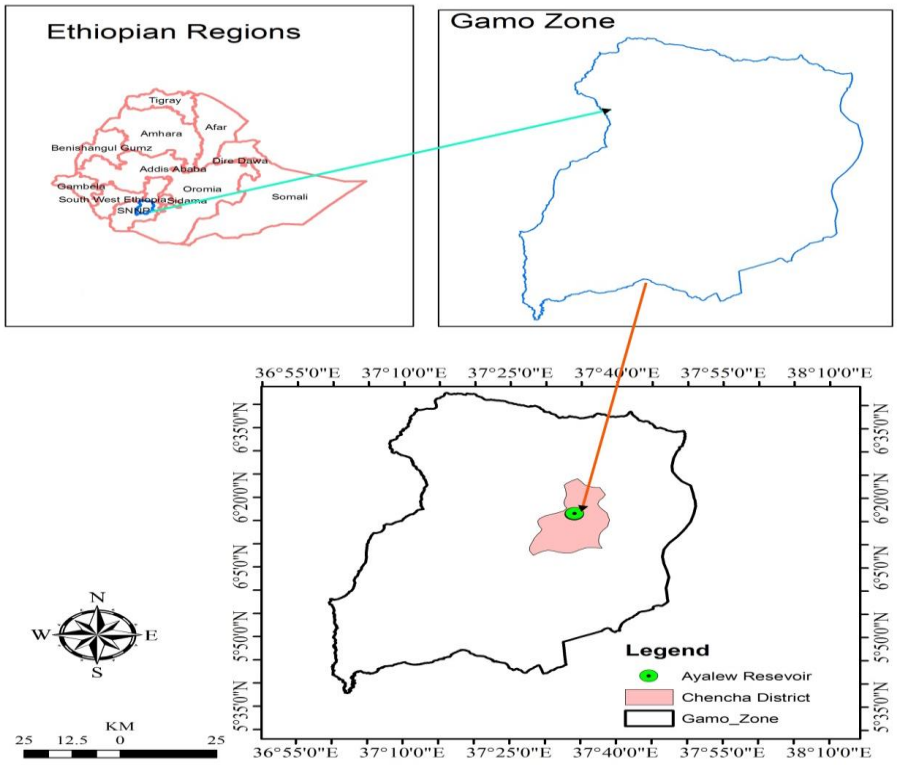

Figure 1. Location of Ayalew reservoir in Chencha woreda, Gamo zone, Southern Ethiopia

Methods of sampling and data collection

Ten youths were trained about fish catching and data recording systems. For the trained youths a boat and four monofilament gill nets with 3.5 mesh sizes were delivered for the research activities. Two data collectors were selected based on their skill and involved in data collecting process. The gillnets were deployed with plastic bottles as floats across the reservoir at 5:00 PM and collected at 7:00 AM the next morning. Immediately following capture, the total length (TL) and weight (TW) of the fish were measured, using a measuring board and sensitive balance, to the nearest 0.1 cm and 1 g, respectively. Data were collected weekly for eight months, from October 2021 to May 2022.

Length-weight relationship and condition factor

Length-weight relationship was calculated using power function (Le Cren, 1951).

$TW = aTL^b$ ---------- [1]

Where,

TW = total weight (g), a = the intercept, TL = total length (cm), b = the slope of length-weight regression

The Fulton's condition factor (*K*) is often used to reflect the nutritional status or well-being of an individual fish. It was calculated by using the formula described by Fulton (1904) which indicated below.

$K = \frac{TW}{TL^3} * 100$ ---------- [2]

Where,

K = Fulton's condition factor

TW = total weight of fish in gram (g)

TL = total length of fish in centimeter (cm)

Data summarization and analysis

Catch data were compiled and summarized in a format suitable for the Jones length-based cohort analysis and the length-based Thompson and Bell yield prediction models. Microsoft Office Excel (2010) was employed for both data summarization and subsequent analysis.

Estimating growth parameters

The K-scan technique available in the ELEFAN I module of the FiSAT II software was utilized to estimate asymptotic length (L∞) and growth rate (k) from the length-frequency data. Pauly's empirical formula (1979) was then applied to calculate the theoretical age at length zero (t_0)

Log (–*to*) = –0.392 – 0.275*log L∞–1.038*log k ----------[3]

Where,

t_o = is the theoretical age at which fish would have at zero length.

L∞ = asymptotic length, k = von Bertalanffy growth rate constant

Growth performance indexes were calculated as Munro and Pauly (1983):

$\theta = \log(k) + 2 \times \log(L\infty)$ ---------- [4]

Where, θ = growth performance index

The length at first maturity (L_{50}) was computed as Froese and Binohlan's (2000) equation:

$\log(L_{50}) = 0.8979 \times \log(L\infty) - 0.0782$ ---------- [5]

Estimating mortality parameters based on length composition data

For the estimation of total mortality rates, linearized length converted catch curve method was applied and the mortality parameters were calculated based on the following formula (Pauly, 1984).

$$\Delta t = 1/k*Ln[(L\infty - L_1)/[(L\infty - L_2)] \text{ ----------[6]}$$

$$t\ (L_1+L_2)/2 = -1/k\{Ln[(1-(L_1+L_2)/2/(L\infty)] \text{ --------[7]}$$

$$Ln\{[C(L_1, L_2)]/[\Delta t(L_1, L_2)]\} = a- Z*t(L_1+L_2)/2 \text{ ---[8]}$$

Where: Δt = is age interval between L_1 and L_2 or the time taken by fish of length L_1 to reach length L_2

$t(L_1+L_2)/2$ = age of the average consecutive length groups (X variable)

$Ln\{[C(L_1,L_2)]/[\Delta t(L_1, L_2)]\}$ = Y variable

The natural mortality coefficient (M) was estimated using Taylor's method (1958) as follows:

$$M = -ln(1-0.95)/A0.95 \text{ ---------- [9]}$$

Where, A0.95 = longevity, the age at which 99% of the cohort would be dead as a result of natural means (Spare and Venema, 1997).

$$A0.95 = t_o+2.996/k \text{ ---------- [10]}$$

Where, t_o = is the theoretical age at which fish would have at zero length;

k = von Bertalanffy growth rate constant

To obtain total mortality, regression analysis was conducted between X and Y variables as described in formula 7 and 8, respectively.

Total mortality (Z) = fishing mortality (F) + natural mortality (M) ---------- [11]

Then, the fishing mortality rate (F) was obtained by subtracting *M* from *Z*.

Estimating population sizes and fishing mortalities by length group (Jones, 1984)

Jones length-based cohort analysis model was used to estimate the population size and fishing mortality coefficient of *C. carpio* by length groups. This was done in the following three steps:

i) Population number estimate of the largest length group in the catch.

N(largest L) = C(Largest L)*(Z Largest L/F Largest L) ---------- [12]

Where, N (largest L) = the population of the largest length group in the catch;

C(largest L) = the catch of the largest length group;

Z(largest L) = the total mortality rate of the largest length group in the catch;

F(largest L) = the fishing mortality rate of the largest length group in the catch;

$C(L_1, L_2)$ = the catch of the length groups of $N(L_1)$

ii) Population numbers estimate of consecutively younger length groups in the catch.

$$N(L_1) = [N(L_2) * H(L_1, L_2) + C(L_1, L_2)] * H(L_1, L_2) \text{ ---------- [13]}$$

Where, $N(L_1)$ = The population number of L_1 (younger) fish

$N(L_2)$ = The population number of L_2 (older) fish

$H(L_1, L_2)$ = the fraction of $N(L_1)$ fish that survived natural death as it grows from length L_1 to L_2 and computed as the following equation (Jones, 1984).

$$H(L_1, L_2) = [(L\infty - L_1)/ (L\infty - L^2)] (M/2k) \text{ ------- [14]}$$

Where, $L\infty$ = the asymptotic length (cm) of *C. carpio* attained at mature size;

L_1 and L_2 = consecutive length groups of fish (cm) that contributed to the fishery;
K = von Bertalanffy growth rate constant (yr^{-1});
M = the rate of natural mortality coefficient

iii**)** Fishing mortality rate estimate of the respective length groups.

Fishing mortality values for each length group was estimated using the equation as follows:

$$F(L_1, L_2) = (1/\Delta t) * \ln[N(L_1)/N(L_2)] - M \text{ -------- [15]}$$

Where, $F(L_1, L_2)$ = Fishing mortality coefficient pertaining to the respective length group;
$N(L_1)$, $N(L_2)$ and *M* are as defined above.

To know the status of the stock, the exploitation rate (*E*) was estimated from mortality parameters as: $E = F/Z$. The exploitation rate (*E*) equal to 0.5 is considered as optimum level of exploitation; whereas less than 0.5 refers to under exploitation and greater than 0.5 refers to overexploitation (Gulland, 1971).

Thompson and Bell (1934) yield prediction procedure

Step 1) Estimating the total annual yield obtained under the current level of fishing

i) Estimating the yield obtained per year from each length group

Yield from each length group obtained per year ($Y(L_1, L_2)$ - is catch in number per length group per year ($C(L_1, L_2)$ multiplied by the average weight of each length group i.e.,

$$Y(L_1, L_2) = C(L_1, L_2) * W(L_1, L_2) \text{ ---------- [16]}$$

Where, $Y(L_1, L_2)$ = the yield (weight) of fish obtained per year from respective length group;
$C(L_1, L_2)$ = total annual catch of fish obtained from respective length group;
$W(L_1, L_2)$ = the mean weight of each length group estimated using equation

$$W(g) = a* L^b \text{ ---------- [17]}$$

Where,
W(g) = the average weight of each length group,
L = the average length (cm) of each length group i.e., $L = (L_1+L_2)/2$ in which L_1 and L_2 are the length intervals of consecutive length groups. '*a*' and '*b*' are values of the regression coefficients.

ii. Estimated yield was obtained from all length groups per year by adding up the contribution of each length group.

RESULTS AND DISCUSSION

Length-weight relationship and Fulton's condition factor

The values of the regression coefficient "*b*" for females (n =141), males (n =135) and combined sexes (n =276) obtained from the length-weight relationship by using the best-fit regression of power function gave 2.51, 2.47 and 2.53, respectively (Fig. 2). Analysis of variance (one-way ANOVA) showed the significant differences between the regression coefficient "*b*" and the cubic value of "*b"* (3) ($P < 0.05$).

As indicated in Table 1, the t-test also revealed that the presence of significant difference between the regression coefficient "*b*" in female, male and combined sexes ($P < 0.05$).

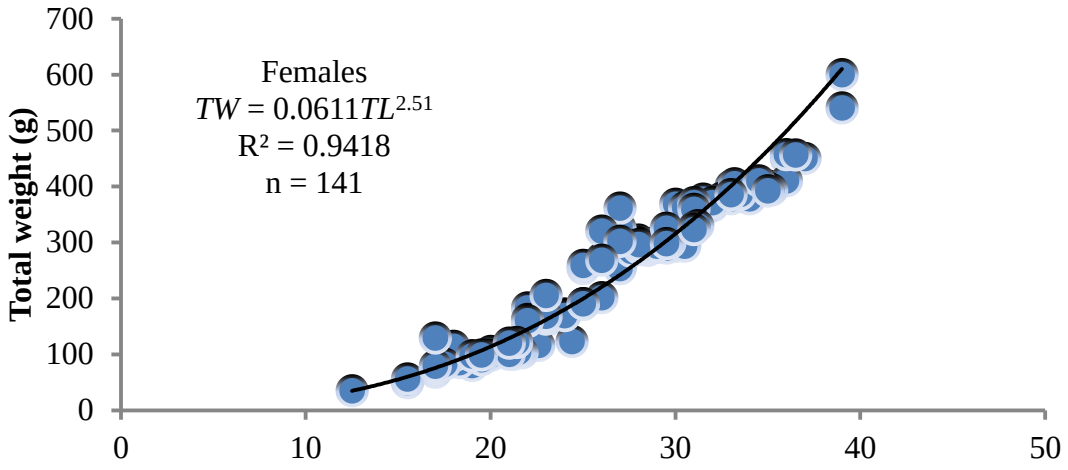

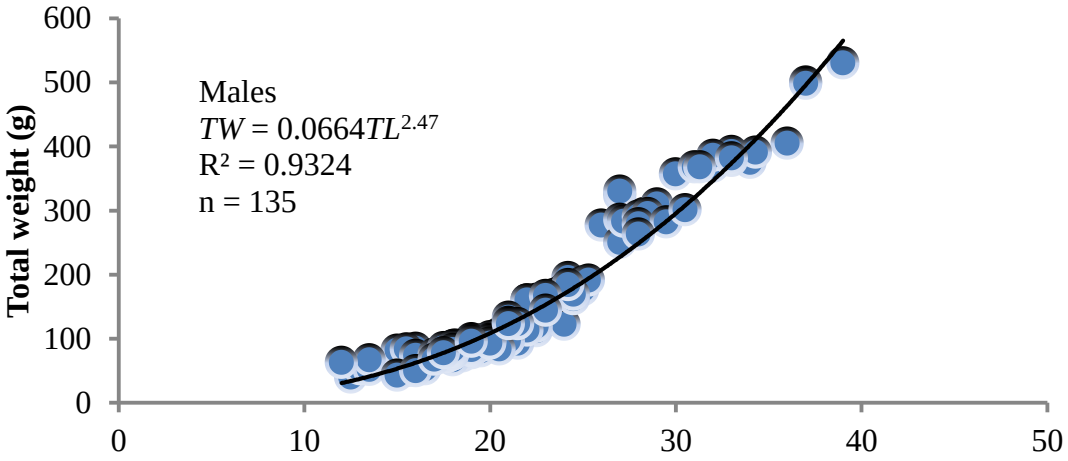

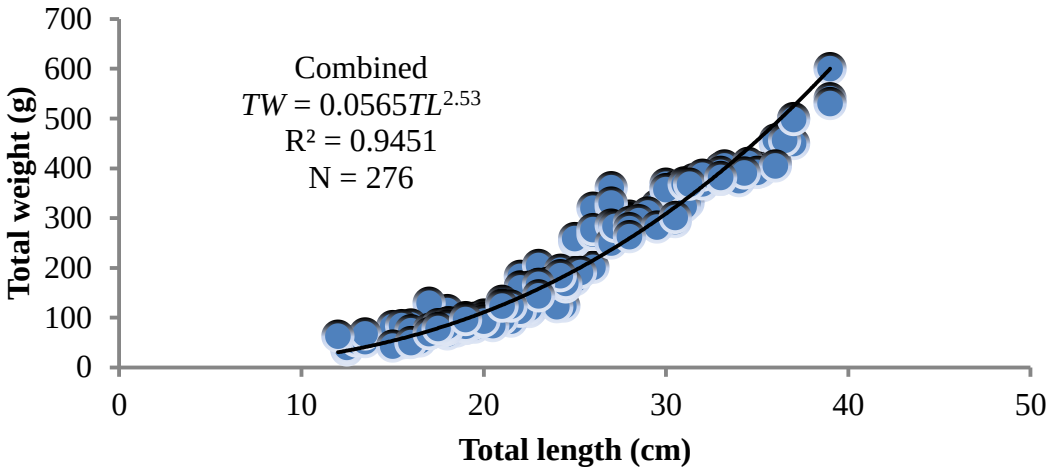

Figure 2. Length-weight relationship of *C. carpio* from Ayalew reservoir

In this study, the length-weight relationship showed that *C. carpio* showed a negative allometric growth. Values of *b* equal to 3 indicate that the fish grows isometrically; values other than 3 indicate allometric growth (Tesch, 1971). The *b* value is often 3.0 and generally between 2.5 and 3.5 (Froese, 2006). The *b* values in fish is species specific and therefore varies with sex, age, seasons, physiological conditions, growth increment and nutritional status of fish (Ricker, 1975; Bagenal and Tesch, 1978). Mert and Bulut (2014), Saylar and Semra (2014), Yilmaz *et al*. (2012), Ünver and Yildirim (2011), and Richard *et al*. (2018) also reported negative allometric growth for *C. carpio* in different water bodies worldwide, and their *b* values were 2.9, 2.8, 2.83, 2.89 and 2.75, respectively.

However, positive allometric growth values for this species were documented by (Karataş *et al*., 2007; Kirankaya and Ekmekçi, 2004), who reported b values of 3.21 and 3.022, respectively. The difference in the results of the current and previous publication might possibly be associated with reasons related to ecosystem and biological phenomena such as seasons, feeding behavior, competition for food, and maturity stages.

Table 1. Regression static parameters of *C. carpio*.

Parameters	Female	Male	Combined
a value	0.0611	0.0664	0.0565
b value	2.5135	2.4698	2.5303
Std. Error (S_b)	28.61	30.05	29.58
R^2	0.9418	0.9324	0.9451
t-calculated	48.62	42.55	69.26
t-critical (5%)	1.97	1.97	1.97
No of observation	141	135	276
Significance	0.000	0.000	0.000

Monthly mean Fulton's condition factor (*K*) ranged from 1.15 to 1.39 for females, 1.16 to 1.44 for males and 1.23 to 1.38 for combined sexes (Table 2). The average *K* value for females, males and combined sexes were 1.28, 1.30 and 1.29, respectively. Females exhibited their lowest condition factor (1.15) in February and their highest (1.39) in May. In contrast, the lowest value for males (1.16) was recorded in November, and the peak value (1.44) occurred in April. For combined sexes, the minimum value (1.23) was recorded in November and the highest (1.38) in April and May. Fulton's Condition factor indices have been widely used as indicators of relative health and depend on the environmental conditions and food availability. April and May are highly rainy season in the study area and might be the reason for the variation in monthly condition factor. The results indicated that there was no significant difference between sexes as well as month's interaction in mean condition factor of *C. carpio* ($P > 0.05$).

Table 2.The mean monthly Fulton's condition factor of female, male and combined C. *carpio* in Ayalew reservoir.

Moths	Female	Male	Combined
October	1.28	1.21	1.25
November	1.33	1.16	1.23
December	1.23	1.30	1.26
January	1.28	1.38	1.33
February	1.15	1.32	1.25
March	1.22	1.25	1.24
April	1.32	1.44	1.38
May	1.39	1.36	1.38
Average	**1.28**	**1.30**	**1.29**

Morton and Routledge (2006) divided the *K* values into five categories as very bad (0.8–1.0), bad (1.0–1.2), balance (1.2–1.4), good (1.4–1.6) and very good (> 1.6). On the other hand, Ayoade (2011) suggests that the Fulton's condition factor higher than one is a good fish health condition. Based on the five categories above, the condition factor in the present study was not in the range of 1.4-1.6 and *C. carpio* in the reservoir was not in a good health condition. This might be due to anthropogenic factor that affects the limnological aspects of the reservoir.

The length composition of sampled catch and estimated annual catch of *C. carpio*

The mean total length catch composition and yield contribution of *C. carpio* are indicated in Fig. 3. The compositions were ranged from 13 to 39 cm with an average length of 26cm. The mean length ranged from 17 cm to 33 cm were about 87% of the total catch and had a high contribution in fish yield.

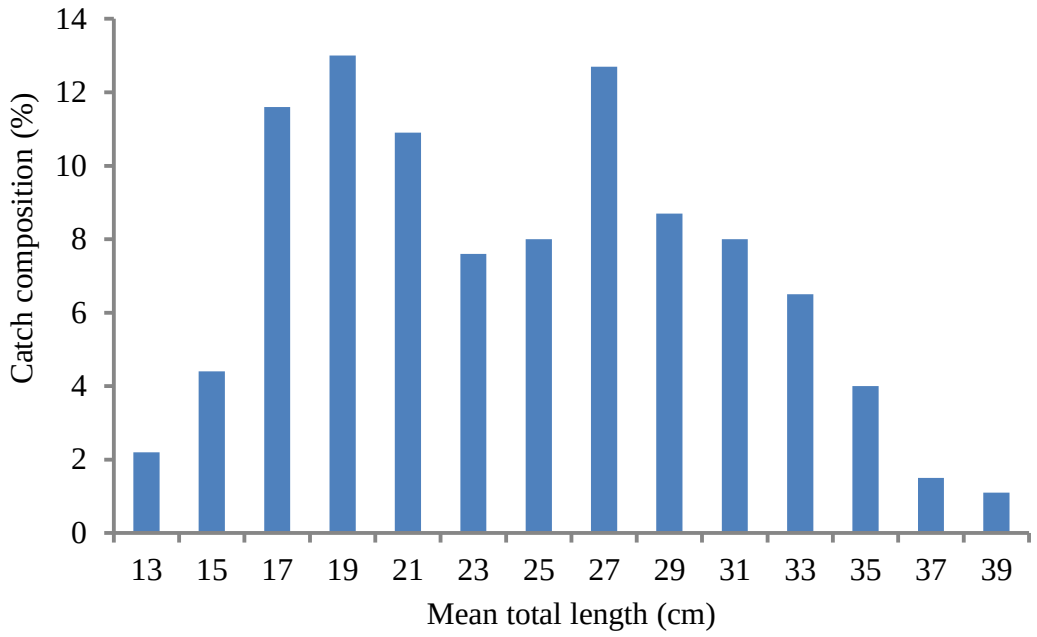

Figure 3. Size structure of *C. carpio* harvested from Ayalew reservoir

Estimation of growth and mortality parameters

The estimated asymptote length (L∞) and the length at first maturity (L_{50}) were 41 cm and 23.44 cm, respectively. The annual growth constant (k) and the growth performance index Phi (θ) were 0.52 yr^{-1} and 2.9, respectively (Fig. 4). The theoretical age at which fish would have at zero length (t_o) was -0.29 and the Longevity (A0.95), the age at which 99% of the cohort would be dead as a result of natural means was 5.5 years.

The fish species with a growth constant (k) value greater than or equal to one (1) is a fast growing fish species (Gulland, 1983; Sparre and Venema, 1998). Besides the genetic makeup which determines the growth potential of the fish species, food availability, environmental conditions and fishing effects could affect the growth performance index of a particular fish species (Getabu, 1992). According to Sambo and Haruna (2012), the growth performance index is a function of L∞ in which increase in L∞ leads to an increase in the growth performance index. The growth constant (k) value ranges from 0.06 to 0.48, 0.12 to 0.75 and 0.11 to 0.69 for *C. carpio* species that live naturally in rivers, lakes and reservoirs, respectively (Fish Base, 2011).

The growth constant (k) of *C. carpio* in Ayalew reservoir was 0.52 $yr^{-1}$and laid into the range of 0.11-0.69 for the *C. carpio* fish populations that live naturally in water of reservoirs.

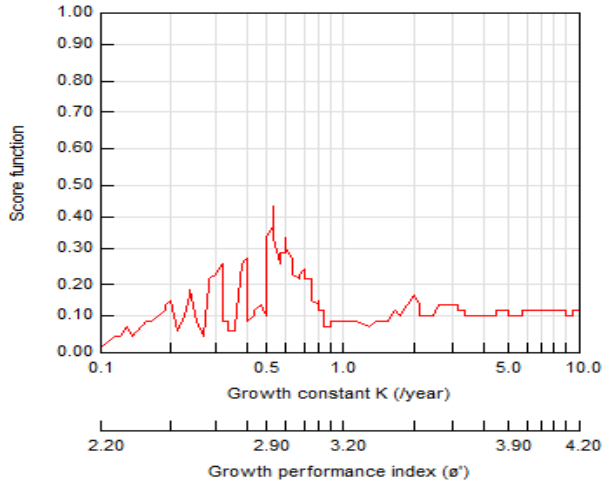

Figure 4. ELEFAN I K- scan routine FiSAT II output for *C. carpio* from Ayalew reservoir.

A length composition data prepared for a linear regression analysis was established between X and Y variables for estimation of total mortality (Table 3).

Table 3. Parameters for length-based catch curve analysis

Length group (cm)	Annual Catch C(L1,L2)					**X**	**Y**
		k	L∞ (cm)	Δt (L1,L2)	(L1+L2)/2	t(L1+L2)/2	Ln(C(L1,L2)/Δt)
16-18	859	0.52	41	0.16	17	1.03	8.59
18-20	967	0.52	41	0.17	19	1.20	8.62
20-22	859	0.52	41	0.19	21	1.38	8.40
22-24	564	0.52	41	0.21	23	1.58	7.88
24-26	591	0.52	41	0.24	25	1.81	7.81
26-28	967	0.52	41	0.28	27	2.07	8.16
28-30	644	0.52	41	0.32	29	2.36	7.60
30-32	591	0.52	41	0.39	31	2.71	7.33
32-34	483	0.52	41	0.48	33	3.14	6.91
34-36	349	0.52	41	0.65	35	3.70	6.29
36-38	107	0.52	41	0.98	37	4.48	4.69
38-40	81	0.52	41	2.11	39	5.81	3.64

Based on the linearized length-based catch curve analysis, the mortality parameters were estimated. As indicated in figure 5, the slope of the regression line (b) is -1.23 and hence, the estimated total mortality rate (*Z*) was 1.23 yr^{-1}. Out of the total mortality, natural mortality rate (*M*) and fishing mortality rate (*F*) were 0.55 yr^{-1} and 0.68 yr^{-1}, respectively. Using these mortality estimates, the exploitation rate (*E*) was computed as 0.55 and indicates that the *C. carpio* is slightly overexploited.

Based on the computed exploitation rate (*E*), the *C. carpio* in Ayalew reservoir was overexploited and the fish population was not abundant enough to utilize the resource sustainably. The exploitation rate (*E*) of a fish stock is at its maximum level and sustainable if the value of *F* was equivalent with or same with the value of *M* or the rate of exploitation (*E*) had value of 0.5 (Gulland, 1983).

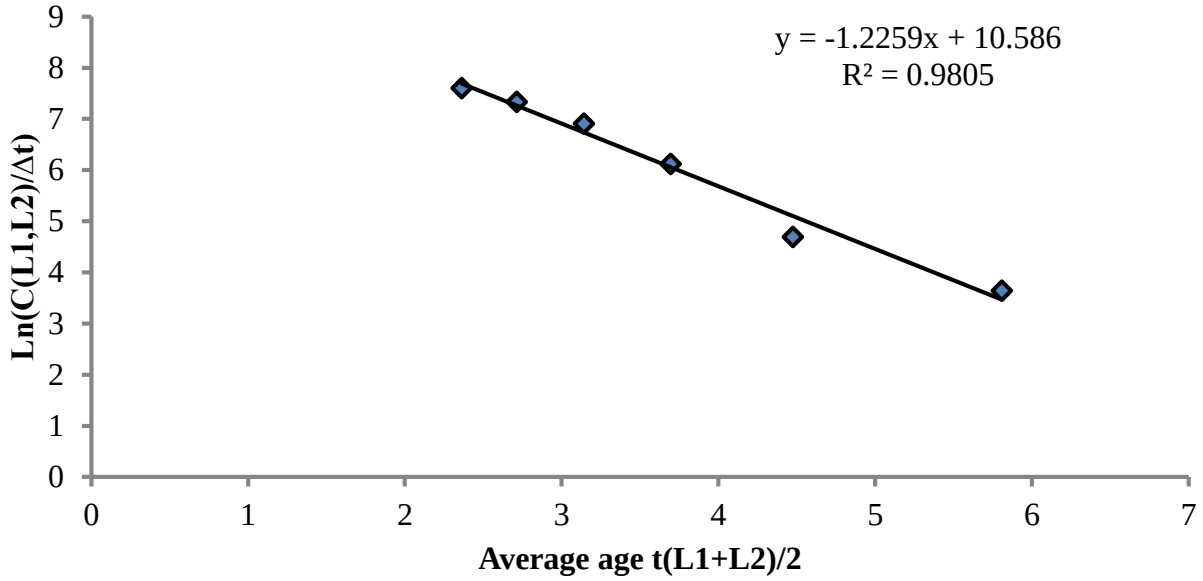

Figure 5. Linearized length-based catch curve of *C. carpio* from Ayalew reservoir

Estimated population sizes and current yield by length group

The estimated population number and annual yield of *C. carpio* in the study area were about 59, 304 and 1.5 tons, respectively (Table 4). The recruitment pattern of the fish was year-round with two peak recruitment period in the year. The peak recruitment takes place twice a year, in April and July to August for this particular fish species (Figure 6). The projected annual recruitment of *C. carpio* in the reservoir was about 9,118 as indicated in Table 4 (column 8; row 3). Based on the estimated population, it is possible to obtain about 7.4 tons of fish biomass and 1.5 tons of fish yield per year.

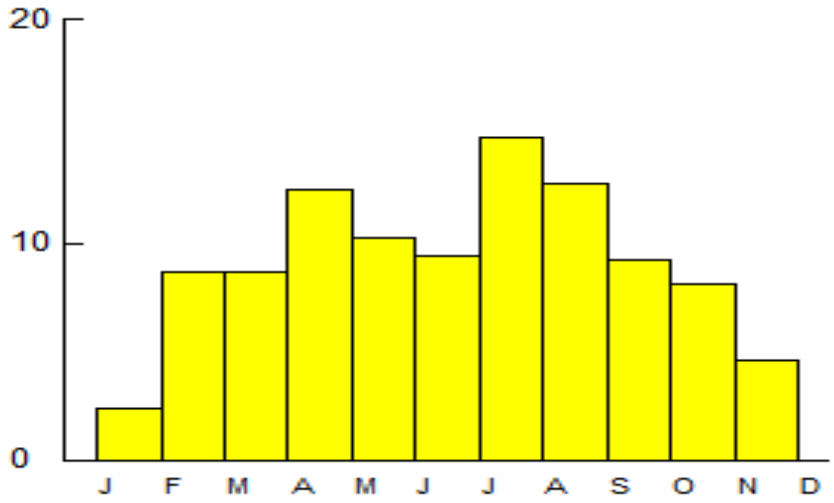

Figure 6. Recruitment pattern output from FiSAT II for *C. carpio* in Ayalew reservoir

Table 4. Estimated population, current yield and other parameters of *C. carpio* by length group

Length group (cm)	Annual catch			**x**	**y**			
		Δt (L_1,L_2)	$(L_1+L_2)/2$	$t(L_1+L_2)/2$	$Ln(C(L_1,L_2)/\Delta t)$	H	$N(L_1,L_2)$	Current yield
12-14	161	0.14	13	0.73	7.07	1.01	9118	6
14-16	322	0.15	15	0.88	7.69	1.01	8774	18
16-18	859	0.16	17	1.03	8.59	1.01	8264	64
18-20	967	0.17	19	1.20	8.62	1.01	7220	95
20-22	805	0.19	21	1.38	8.34	1.01	6081	102
22-24	564	0.21	23	1.58	7.88	1.02	5115	89
24-26	591	0.24	25	1.81	7.81	1.02	4400	115
26-28	940	0.28	27	2.07	8.14	1.02	3665	222
28-30	644	0.32	29	2.36	7.60	1.02	2597	182
30-32	591	0.39	31	2.71	7.33	1.03	1847	197
32-34	483	0.48	33	3.14	6.91	1.04	1170	189
34-36	295	0.65	35	3.70	6.12	1.05	623	134
36-38	107	0.98	37	4.48	4.69	1.08	284	56
38-40	81	2.11	39	5.81	3.64	1.17	146	48
Total	**7,410**						**59,304**	**1,517**

CONCLUSIONS & RECOMMENDATIONS

The growth pattern of *C. carpio* was negative allometric which implied that the fish became thinner as its body length increases. The wellbeing of the fish was not in a good health condition. The mean length groups ranged from 17 cm to 33 cm was about 87% of the total catch and had a high contribution in fish yield. The *C. carpio* in Ayalew reservoir can grow up to the maximum length (L∞) 41 cm with growing speed (k) of 0.52 per year. The long lifespan (A0.95) of the cohort and the length at first maturity were 5.5 years and 23.44 cm, respectively. The production potential of the fish was about 7.4 tons of fish biomass and 1.5 tons of yields per year. However, investigation on reproductive biology, limnological aspects and stock enhancement are required in the reservoir.

Acknowledgements

The authors would like to highly acknowledge the Southern Agricultural Research Institute (SARI) for the financial support, Arba Minch Agricultural Research Center for allowing access to the necessary facilities and Arba Minch Agricultural Research Center staff members for their valuable assistance during the execution of the experiment.

Conflicts of interest

The authors declare that there is no conflict of interest in publishing the manuscript in this journal.

References

Abera L., Getahun A. and Lemma B. 2015. Some aspects of reproductive biology of the common carp (*Cyprinus carpio* Linnaeus, 1758) in Lake Ziway, Ethiopia. *Glob. J. Agric. Agric. Sci.* **3(3)**: 151–157.

Ayoade A.A. 2011. Length-weight relationship and diet of African Carp Labeoogunensis (Boulenger, 1910) in Asejire Lake Southwestern Nigeria. *J Fish Aquat Sci.* **6**: 472-478.

Bagenal T.B. and Tesch F.W. 1978. Age and growth. In: Bagenal TB (ed) Methods for assessment of fish production in fresh waters. Blackwell Science Publications, Oxford, pp 101-136.

Bajer P.G., Chizinski C.J., Sillbernagel J.J. and Sorensen P.W. 2012. Variation in native micro-predator abundance explains recruitment of mobile invasive fish, the Common Carp, in a naturally unstable environment. *Biol. Invasions*. **14(9)**:1919–1929.

Fish Base 2011.Growth parameters for *Cyprinuscarpio* http://www.fishbase.org.

Froese R 2006. Cube law, condition factor, and weight-length relationships: History, meta- analysis, and recommendations. *J Appl. Ichthyol* **22**:241–253.

Froese R. and Binohlan C. 2000. Empirical relationships to estimate asymptotic length, length at first maturity and length at maximum yield per recruit in fishes, with a simple method to evaluate length frequency data. *J. Fish Biol.* **56**: 758–773. doi: 10.1111/j.1095-8649.2000.tb00870.x

Fulton T.W. 1904. The rate of growth on fishes. Twenty-second Annual Report, Part III. Fisheries Board of Scotland, Edinburgh.pp.141-241.

Getabu A. 1992. Growth Parameters and total Mortality in *Oreochromis niloticus* (Linnaeus)from Nyanza Gulf, Lake Victoria. *Hydrobiologia* **232**: 91-97.

Getahun A. 2017. The freshwater fishes of Ethiopia, diversity, and utilization. Addis Ababa: View Graphics and Printing Plc. Pp. 349.

Golubtsov A.S. and Darkov A.A. 2008. A review of fish diversity in the main drainage systems of Ethiopia based on the data obtained by 2008, Ecological and faunistic studies in Ethiopia, Pavlov D.S. et al. (Eds.), Moscow: KMK Sci.Press, pp. 69–102.

Gulland J.A 1983. Fish stock assessment. *A Manual of Basic Methods* (Chicester: John Willey and Sons) p 233.

Gulland J.A. 1971. The fish resources of the Ocean. Fishing News (Books), West Byfleet, pp 255.

Jones R. 1984. Assessing the effects of changes in exploitation patterns using length composition data

(with notes on VPA and Cohort analysis). FAO Fisheries Technical Paper, 256:118.

Karataş M., Çiçek E., Başusta A. and Başusta N. 2007. Age, growth and mortality of common carp (Cyprinus carpio Linneaus, 1758) population in Almus Dam Lake (Tokat-Turkey). *J. Appl. Biol. Sci*. 1:81–85.

Kirankaya Ş.G. and Ekmekçi F.G. 2004. Growth properties of mirror carp (Cyprinus carpio L., 1758) introduced into Gelingüllü Dam Lake, (in Turkish). *Turk. J. Vet. Anim. Sci.* **28**:1057–1064.

Le Cren E.D. 1951. The length-weight relationship and seasonal cycle in gonad weight and condition in the perch (Percafluviatilis). *J. Anim. Ecol.* **20**(**2**): 201-209.

Letvin A.P., Brown M. L., Bertrand K. N. and Weber M. J. 2017. Effects of Common Carp on Trophic Dynamics of Sport Fishes in Shallow South Dakota Water Bodies. T*rans. Am. Fish. Soc.***146**: 331-340,DOI: 10.1080/00028487.2016.1269022.

Mert R. and Bulut S. 2014. Some biological properties of carp (Cyprinus Carpio L., 1758) Introduced into Damsa Dam Lake Cappadocia Region. Turkey. *Pakistan J Zool* **46**:337-334.

Mohammad M. 2015. Role of common carp (*Cyprinuscarpio*) in aquaculture production systems. *Front. Life Sci.* **8** (**4**): 399–410, http://dx.doi.org/10.1080/21553769.2015.1045629.

Morton A. and Routledge R.D. 2006. Fulton's condition factor: is it a valid measure of sea lice impact on juvenile salmon? *North American Journal of Fisheries Management*. 26: 56–62.

Munro, J.L and Pauly D. 1983. A simple method for comparing the growth of fishes and invertebrates. Fishbyte 1: 5–6.

Pauly D. 1984. Length-converted catch curves. A powerful tool for fisheries research in the tropics (Part II). ICLARM Fishbyte, 2(1): 17-19.

Pauly D.G. 1979. Estimation of mortality and growth parameters from the length frequency of a catch. Rapp. P. –V. Reun. CIEM, 175: 167-169.

Penne C.R. and Pierce C.L. 2008. Seasonal distribution, aggregation, and habitat selection of Common Carp in Clear Lake, Iowa. *Transactions of the American Fisheries Society*. 137:1050–1062.

Richard K., Chunxia G., Xiaojie D. Siquan T. and Feng W. 2018. Population Dynamic Parameters for Cyprinus carpio in Dianshan lake, Shanghai Ocean University, Shanghai, China. An *International Journal of Marine Sciences*. https://doi.org/10.1007/s41208-017-0062-x.

Ricker W.E. 1975. Computation and interpretation of biological statistics of fish populations. Bulletin of the fisheries research board of Canada. Bulletin 191, Ottawa.http://www.dfo mpo.gc.ca/Library/ 1485.pdf.

Sambo F. and Haruna M. 2012. Some Aspects of the Growth Parameters of the Fishes of Ibrahim Adamu Lake, Kazaure Jigawa State, Nigeria. *Bayero Journal of Pure and Applied Sciences*, **5**(**1**): 175 – 181.

Saylar Ö. and Semra B. 2014. Age and Growth Characteristics of Carp (Cyprinuscarpio L., 1758) in Mogan Lake, Ankara, Turkey. *Pakistan J. Zool.* **46**(**5**):1447–1453.

Sparre P. and Venema S.C 1997. Introduction to tropical fish stock assessment. Part 1. Manual. FAO Fisheries Technical Paper, v. 2, n. 306.1, p. 1-420.

Sparre P. and Venema S.C. 1998. Introduction to tropical fish stock assessment, Part 1-Manual FAO Fish Tech. Pap.306-1 rev. 2.385 p.

Taylor C.C. 1958. Cod growth and temperature. *Journal du Conseil International pour l`Exploration de la Mer*. **23**: 366-370.

Tesch F.W. 1971. Age and Growth. In: Ricker W.E. (ed) Methods for Assessment of Fish Production in Fresh Waters. Blackwell Scientific Publications, Oxford, pp 98–103.

Thopson W.F and Bell F.H. 1934. Biological statistics of the pacific halibut fishery. Effects of changes in intensity upon total yield and yield per unit of gear. Report of the international fisheries (pacific halibut) commission, (8):49p.

Ünver B. and Yildirim M. 2011. Population characteristics of carp from Tödürge Lake in 583 Sivas, Turkey. *Int. J. Agric. Biol*. **13**:935–940.

Yilmaz S., Yazicioğlu O. and Polat N. 2012. Age and Growth Properties of Common Carp (*Cyprinus carpio* L., 1758) from Bafra Fish Lakes (Samsun, Turkey). *Black Sea J Sci*. 2:1–12.

East African Journal of Biophysical and Computational Sciences

Journal homepage : https://journals.hu.edu.et/hu-journals/index.php/eajbcs

Synthesis, Characterization and Antibacterial activity of Benzimidazole Derivatives and their Cu (ii), Ni (ii) and Co (ii) complexes

Haftom Welderufael*, Dagne Addisu Kure, Endalkachew Asefa Moges, Lelisa File, Salah Hamza Sherif

Department of Chemistry, Hawassa University, Hawassa, Ethiopia

KEYWORDS:

Antibacterial;
Benzimidazole;
Metal complex;
Schiff base

Research article

ABSTRACT

Benzimidazole is one of the privileged nitrogen-containing heterocyclic compounds, which is found in many bioactive compounds, benzimidazole and its derivatives have evolved as an important heterocyclic system due to their potency in a wide range of biologically active compounds like anthelmintic, antibacterial, antifungals, anti-inflammatory, antiviral, and so on. Derivatives of 1-arylsulfonylbenzimidazole and their respective Cu (II), Ni (II) and Co (II) complexes were successfully synthesized. The structures of all the synthesized ligands were confirmed by using IR, UV-Visible, ^{1}H NMR, and ^{13}C NMR spectroscopy. The Cu (II), Ni (II) and Co (II) complexes were confirmed by using IR and VU-Visible spectra. The IR spectra of ligands and its metal complexes imply that the benzimidazol derivative ligands behave as basic bidentate ligands coordination through the azomethine nitrogen and oxygen atom. *In-vitro* antibacterial activity of all the synthesized ligands and their metal complexes were evaluated by using disc diffusion method against *K. pneumoniae, E. coli,* and *S. aureus* bacterial species .The tested compounds and metal complexes exhibited from good to excellent activity (zone of inhibition (ZI) ranged 10 mm to 23 mm). Compound BIL1 exhibited better activity than the standard drug against *E. coli* (ZI of 15 mm) and *K. pneumoniae* (ZI of 5 mm) compared with gentamycin ((ZI of 15mm). Complex CoC exhibited better activity against *S. aureus* (ZI of 23 mm) compared with *gentamicine* (ZI value of 21 mm). This compound is a good starting point to develop new drug for treating pathogenic diseases. Therefore, synthesis of more analogue were recommended for further discovery of a new drug candidate.

INTRODUCTION

Microbial resistance is one of the critical public health issues and the greatest challenges of the twenty-first century (Marinescu, 2021) especially as increasing numbers of strains are becoming resistant to multiple antimicrobial agents, with some bacteria now being resistant to all available antibiotics, there is an pressing need to develop new drugs with novel mechanisms of action (Fatmah *et al.*, 2015). Nitrogen-heterocycles play a vital role in medicinal chemistry and they have been intensively used as scaffolds for drug development, among nitrogen containing heterocyclic compounds, benzimidazole is continuously drawing the interest of many researchers for the

*Corresponding author:
Email: haftish1@gmail.com, 251 926046602

https://dx.doi.org/10.4314/eajbcs.v4i1.4S

development of newer drug moiety (Majumder *et al*., 2013).

Benzimidazole derivatives are known to possess varied biological activities, substituted benzimidazole derivatives have been reported to possess antimicrobial (Ansari *et al*., 2009; Özkay *et al*., 2010; Shaharyar *et al*., 2017), anti-inflammatory (Mariappan *et al*., 2015; Achar *et al*., 2017), and antiviral (Zou *et al*., 1996; S. Hirashima *et al*., 2006; Bhagdev, K. and Sarkar, 2021), anticancer (Błaszczak-S´ *et al*., 2014; Sharma *et al*., 2017; Ting-Ting *et al*, 2018) activities. The structural similarity of the benzimidazole moiety to naturally occurring nucleotides makes it a valuable drug scaffold in medicinal chemistry. The strong link between the benzimidazole core and a wide range of biological activities is well-documented and established in the literature. Benzimidazole derivatives have also been used as good ligands for transition metal ions due to the large conjugated pi-system and the azomethine nitrogen which can positively affect the structures of the complexes (Galal *et al*., 2010).

Due to their potent biological activity, metal complexes with aromatic Schiff base ligands, particularly those based on imidazoles, have gained considerable interest in recent years (Kumaravel *et al*., 2017). The biological activities of several metal complexes with benzimidazole ligands have been created and investigated (Horacio *et al*., 2008; Kopel *et al*., 2015; Ashraf *et al*., 2016; Kumaravel and Raman 2017).

In this paper, the synthesis and antibacterial activity investigations of benzimidazole derivatives and their metal complex against *K. pneumonia, E. coli*, and *S. aureus* bacterial strains were presented. These bacteria were selected on the basis that E. coli known to cause Urinary tract infections, *K. pneumoniae* know to be the causative agent of pneumonia and *S. aureus* is multi drug resistant (Abioye *et al*., 2013). Therefore, the objective of this study was to compare the activity of the ligands with their metal complexes.

MATERIALS AND METHODS

All reagents and solvents were of analytical grade and used as received. Reaction mixtures were monitored via thin-layer chromatography (TLC) on silica gel plates. Column chromatography employing silica gel (100–200 mesh) was primarily used for purification of the intended products. Melting points were determined using open capillary tubes and are reported uncorrected. Infrared (IR) spectra were collected on an FT-IR Bruker Alpha spectrometer. Nuclear magnetic resonance (NMR) spectra were acquired using a Bruker Advance NMR spectrometer operating at 400 MHz, with tetramethylsilane (TMS) as the internal standard.

Chemistry

The benzimidazole derivatives was prepared as outlined in scheme 1, the intermediate, 2-substituted benzimidazole was prepared by refluxing o-phenylendiamine with appropriately substituted benzaldehyde in Dimethyl formamide (DMF) in the occurrence of $NaHSO_4$ as a catalyst, the benzene sulphonyl substituted compounds were prepared by stirring 2-substituted benzimidazole derivatives with benzene sulphonyl chloride at room temperature in acetone in the presence of sodium carbonate.

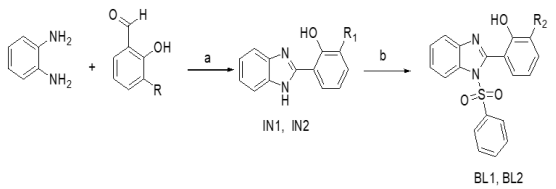

IN1, R_1 = OCH_3, IN_2, R_1= H; BIL1, R_2 = OCH_3, BIL2, R_2 = H

SCHEME 1: reagent and condition: a) $NaHSO_3$, DMF, reflux 90-100^oC; b) K_2CO_3 acetone, RT

Synthesis

Synthesis of 2-(1H-benzo[d]imidazol-2-yl)-6-methoxyphenol(IN1)

A mixture of o-phenylendiamine (1.09g, 10mmol) and (1.248g, 10mmol) sodium hydrogen sulphite were dissolved in 15 mL dimethyl formamide (DMF) stirred at room temperature for 30min, to this solution (1.52g, 10mmol) 2-o-vanillin were added, the mixture was refluxed for about 6hr at 90^{o}C-100^{o}C, the development of the reaction was regulated by TLC. At the end of the reaction, the reaction mixture was cooled and extracted with ethyl acetate. The organic layer was separated, dried over anhydrous Na_2SO_4, and concentrated under reduced pressure. The resulting material was purified by column chromatography using a 9:1 mixture of hexane and ethyl acetate.

Synthesis of 2-(1H-benzo[d]imidazol-2-yl) phenol (IN2)

A mixture of *o*-phenylendiamine (0.54g, 5mmol) and (0.624g, 5mmol) of sodium hydrogen sulphite were dissolved in 15 mL dimethyl formamide (DMF) stirred at room temperature for 30min, to this mixture (0.605g, 5mmol) salisaldehyde were added and the mixture was refluxed for about 6hrs. at 90^{o}C-100^{o}C,the progress of the reaction was regulated by TLC. At the end of the reaction, the reaction mixture was cooled and extracted with ethyl acetate. The organic phase was harvested and dried over anhydrous Na_2SO_4; the solvent used was removed under reduced pressure recrystallized from methanol.

Synthesis of N-benzenesulfonyl-2-(1H-benzo[d]imidazol-2-yl)-6-methoxyphenol (BIL1)

2-(1H-benzo[d]imidazol-2-yl)-6-methoxy phenol (IN1) (0.38g, 1.77mmol) were dissolved in 10 mL acetone and (0.614g, 4.429mmol) K_2CO_3 were added and stirred at room temperature for 30min, then 0.3 mL of benzene sulfonyl chloride was added drop wise to the mixture and refluxed for 6 hours, The reaction's progress was followed by thin-layer chromatography (TLC). Once complete, the reaction mixture was partitioned between water and ethyl acetate. The organic phase was collected, dried over anhydrous sodium sulfate (Na_2SO_4), and concentrated in vacuo. The resulting product was then subjected to column chromatography, using a 9:1 mixture of hexane and ethyl acetate as the mobile phase.

Synthesis of N-benzenesulfonyl-2-(1H-benzo[d]imidazol-2-yl) phenol (BIL2)

2-(1H-benzo[d]imidazol-2-yl)phenol(IN2) (1.15g, 5.4 mmol) was dissolved in 10 mL of acetone,K_2CO_3(1.8g, 13.5mmol) were added

and stirred at room temperature for 30min, 0.8 mL of benzene sulfonyl chloride were added to the mixture drop wise and refluxed for 6 hours, The progress of the reaction was monitored by TLC. At the end of the reaction, the reaction mixture was cooled and extracted with ethyl acetate. The organic phase was collected and dried on anhydrous Na_2SO_4 and crystallized under abridged pressure. The product was then further purified by column chromatography.

Synthesis and Characterization of metal complexes of BIL1

A methanolic solution of ligand BIL1 (0.38 g, 0.5 mmol, in 10 mL) was combined with a separate methanolic solution (5 mL) of either $Cu(CH_3COO)_2 \cdot H_2O$, $Ni(CH_3COO)_2 \cdot 4H_2O$, or $CuCl_2 \cdot 6H_2O$ (1 mmol each). The combined solutions were refluxed for 8 hours, with the reaction being monitored by thin layer chromatography (TLC). After allowing the mixture to cool in an ice bath, the precipitate was collected by filtration and washed with dichloromethane. The solid was dried under vacuum overnight, and then recrystallized from methanol.

Antibacterial activities

Culture media and disk preparation

Nutrient agar, Muller Hinton agar and Nutrient broth were prepared according to the manufacturer instruction in which the prepared media was autoclaved at 121^{o}C for 15 minutes. Then the prepared culture media was checked for the sterility for 24 hours at 37 ^{o}C. For quality control, strains of *Staphylococcus aureus* (*S. aureus*), *Escherichia coli* (*E. coli*) and *Klebsiella pneumonia* (*K. pneumonia*), which were obtained from the College of medicine and health science of Hawassa University, known American type culture collection committee (ATCC) were used to perform the antibacterial activities of the agents. Whatman filter paper 41 is used to prepare a disk of 5mm diameter using manual paper punching.

Preparation of chemical solution and media for the antibacterial activity

By using analytical balance, a 0.005g of each chemical powder was added to 15µl dimethyl sulphoxide (DMSO) and mixed to form a homogenous solution. A 5µl of the solution was added to the sterile disk prepared before using sterile micropipette. The aforementioned bacterial strains (meant for quality control) were inoculated on sterile nutrient agar plates using sterile loop. The streaked plates were incubated for 24 hours at 37^{o}C. A 3 to 5 colonies were picked with sterile loop and suspended in 5 mL nutrient broth to form standards. The culture suspension was then inoculated on sterile Muller Hinton agar plate using sterile cotton swab in three directions to get uniform inoculum. The antibiograms profiles of the test organisms to the control antibiotic were checked. Then an autoclaved disks with a control gentamicin and solution impregnated disks were carefully positioned on the plate and incubated for 24 hours at 37^{o}C. The unique ID number of each disk was mentioned with permanent marker on the back of the Petri dishes. After incubation the diameter of the zone of inhibition was measured using ruler. The result was given in (table 1)

RESULT AND DISCUSSION

Characterization

Characterization of 2-(1H-benzo[d]imidazol-2-yl)-6-methoxyphenol (IN1)

Light red solid; Yield:76.1%;Mp:195-197 ^{o}C; IR(KBr, Cm^{-1}): 3394(-NH), 3240(-OH), 3047(C-H, aromatic), 2854(C-H, methyl), 1593(C=N); ^{1}H-NMR (DMSO-d_6,400MHz): δ_H 13.12(s, 1H,-OH), 7.91-789(m, 2H, Ar-H), 7.73-763(m, 2H, Ar-H), 7.42-7.37(m, 2H, Ar-H), 7.26-7.25(m, 1H, Ar-H), 5.00(s,1H,-NH), 3.7(s,3H,OCH_3); ^{13}C-NMR (DMSO-d_6, 100MHz): δ_C 149.2, 147.1, 142.6, 137.0, 123.5, 122.8, 121.1, 120.1, 114.3, 111.0, 42.7

Electronic spectra of compound IN1

The UV-Vis spectrum of the IN1 compound was recorded in DMSO. The electronic absorption spectrum of the ligand showed bands at 304 nm, attributed to a π-π* transition of the –C=C– bond; 382 nm, corresponding to an n-π* transition; and 497 nm, assigned to an n-π* transition of the azomethine chromophore (–C=N–).

Characterization of N-benzenesulfonyl-2-(1H-benzo[d]imidazol-2-yl)-6-methoxypheno1 (BIL1)

Light red solid; Yield:68.0%, Mp:230-232^{o}C; IR(KBr, Cm^{-1}): 3210 (-OH), 2923(C-H, aromatic), 2854(C-H), 1458(C=N), 1377(O=S=O); ^{1}HNMR(DMSO-d_6,400MHZ): δ_H 13.2 (s,1H,OH), 7.9(d, *J*= 8.4Hz,2H), 7.7(m, 2H), 7.6(d, *J*=7.4Hz,2H), 7.5(m,1H), 7.4(d, *J*=6.5Hz,1H), 7.3(m,2H), 7.1(d, *J*=7.65Hz,1H), 6.9(m,1H,), 3.7(s,3H, OCH_3);^{13}C-NMR (DMSO-d_6, 100MHz): δ_C 153.1, 147.6, 136.0, 133.8, 129.8, 128.3, 126.9, 126.4, 123.0, 122.7, 122.5, 115.6, 115.0, 56.4

Electronic spectra of compound BIL1

The UV/Visible spectral for BIL1 compound recorded in DMSO, the electronic absorption spectrum of the ligands showed band at 302nm attributed to –C=C-,$\pi \rightarrow \pi^*$ transition, the band around 382nm and 495nm is because of n$\rightarrow \pi^*$ transition of the(-C=N-) azomethine chromophore.

Characterization of N-benzenesulfonyl-2-(1H-benzo[d]imidazol-2-yl) phenol (BIL2)

Yellow solid; Yield:71.2 %, Mp:196-198 ^{o}C, IR(KBr, Cm^{-1}): 3232 (O-H), 2954(C-H, aromatic), 1458(C=N),1176 (C-O) strong band at1377 (O=S=O); ^{1}H-NMR(400MHz, DMSO-d_6)δ_H:13.15(s, 1H, -OH), 7.74-7.61(m, 5H, Ar-H), 7.29-7.20(m, 4H, Ar-H), 7.08-7.06 (m, 2H, Ar-H), 6.97-6.91(m, 2H, Ar-H); ^{13}C-NMR (100 MHz,DMSO-d_6) δ_C:115.3, 118.1, 119.5, 121.3, 121.52, 121.94, 122.64, 123.0, 123.33, 128.9, 131.1, 137.9, 138.9, 141.5, 155.3

Characterization of Cu(II) complexes of BIL1(CuC)

The product was obtained as a light brown solid with a 74.5% yield and a melting point of 214-216 °C. The IR spectrum (KBr, cm^{-1}) showed characteristic peaks at 3394 (O-H stretching of water), 2923-2858 (C-H), 1604 (C=N), and 1377 (S=O). The C-O stretch, observed at a higher frequency in the Cu (II)

complexes compared to the free ligands, suggests logical coordination through the deprotonated phenolic-O. This is supported by the disappearance of the weak phenolic OH band in the complex spectra. Far-infrared bands corresponding to M-O bonds, including a band at 1188 cm^{-1} assigned to the (Cu-O) bond in the complexes, further corroborate the proposed coordination mode of the Schiff base ligands.

The Uv/visible spectra recorded in DMSO, the electronic absorption spectrum of the ligands showed band at 301nmattributed to $\pi \rightarrow \pi^*$ transition of –C=C-, the band around 382nm and 502nmis due to n→ π^* transition of the (-C=N-) azomethine chromophore.

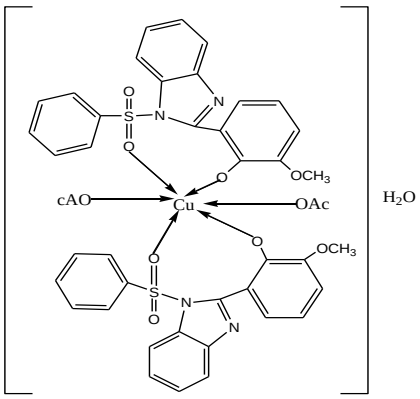

Proposed structure of Cu(II) complex of BIL1(CuC)

Characterization of Ni(II) complexes of BIL1(NiC)

Pale green solid, yield 76.9%, Mp: 220-222^oC; IR (KBr, Cm^{-1}):3240 (O-H stretching of water), 2923-2858(C-H, stretching), 1604(C=N), 1461 (C-O), 1377 (S=O). The C-O stretch of the free ligands was observed at a higher frequency in the spectra of the Ni(II) complexes, suggesting coordination of the Schiff base ligands through the deprotonated phenolic–O, This was substantiated by the disappearance of the weak phenolic OH band in the spectra of the complexes. The mode of coordination of the Schiff base ligands was further corroborated by the appearance of bands in the far-infrared spectra of the complexes due to the M-O bonds. The new bands in the low frequency region 510 and 440 are due to the formation of (M–O) and (M–N) vibrations respectively.

Electronic spectra of compound NiC

The Uv/visible spectral for compound NiC are recorded in DMSO the data are presented in the electronic absorption spectrum revealed band at 302nm attributed to $\pi \rightarrow \pi^*$transition of (–C=C) ,the band around 382nm and 499nm is due to$\pi \rightarrow \pi^*$and n→ π^* transition of the (-C=N-) azomethine chromophore.

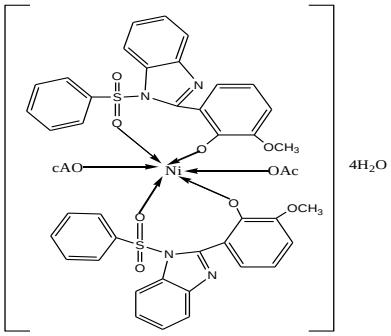

Proposed structure of Ni(II) complexof BIL1(NiC)

Characterization of Co (II) complexes of BIL1 (CoC)

Yellow solid, Yield 88.8%, Mp:210-212^oC, The IR stretching (KBr, *v* in cm^{-1}) spectral information for compound CoC, showed distinguishing medium band at 3394cm^- confirmed the presence of O-H stretching of water. Strong band at 2923-2858cm^{-1}

guaranteed the presence of C-H stretching of aromatic. A medium band at 1604cm^{-1} confirmed the availability of C=N stretching of azomethine. A medium narrow band at 1461cm^{-1}confirmed the presence of C-O stretching of aromatic. A medium narrow band at 1677cm^{-1} confirmed the presence of C=C stretching aromatic and the strong band at 1377cm^{-1} confirmed the presence of two S=O stretching of benzene sulfonyl. A higher C-O stretching frequency was observed in the infrared spectra of the Co(II) complexes compared to the free ligands, which indicates coordination of the Schiff base ligands via the deprotonated phenolic oxygen. The conclusion made based on these findings was supported by the absence of the weak phenolic O-H band in the complex spectra. Moreover, the far-infrared spectra of the complexes showed bands that can be assigned to M-O vibrations, including one at 1130 cm^{-1} corresponding to the Co-O bond.

Electronic spectra of compound CoC

The Uv/visible spectra for compound CoC were noted in DMSO, the electronic absorption spectrum of the ligands showed band at 267nm associated with –C=C- ,$\pi \rightarrow \pi^*$ transition, the band around 302nm and 319nm is because of $\pi \rightarrow \pi^*$and n$\rightarrow \pi^*$ transition of the-C=N-azomethine chromophore. No spectral bands were found below 300nm which supports octahedral geometry.

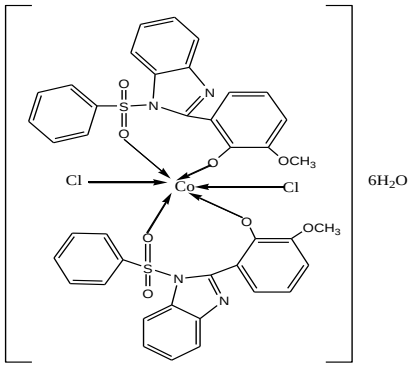

Proposed structure of Co (II) complex of BIL1(CoC)

Characterization of copper (II) complexes of BIL2 (CuC2)

The light brown solid, CuC2, was obtained with an 86.7% yield and a melting point of 160-162 °C. The IR spectrum (KBr, cm^{-1}) exhibited a medium band at 3363 cm^{-1} indicative of O-H stretching from water, strong bands at 2923-2858 cm^{-1} due to aromatic C-H stretching, a medium band at 1612 cm^{-1} consistent with C=N stretching in the azomethine, a medium narrow band at 1461 cm^{-1} corresponding to aromatic C-O stretching, a medium narrow band at 1917 cm^{-1} assigned to aromatic C=C stretching, and a strong band at 1377 cm^{-1} suggesting two S=O stretching in the benzene sulfonyl group. A shift to higher frequency in the C-O stretching band was observed for the Co(II) complexes compared to the free ligands, indicating coordination of the Schiff base ligands through deprotonated phenolic oxygen. This observation was substantiated by the absence of the characteristic phenolic OH band in the complex spectra. Additionally, the far-infrared spectra of the complexes exhibited

bands that can be attributed to M-O vibrations, including one at 1170 cm^{-1} corresponding to the Co-O bond.

Electronic spectra of compoundCuC2

The Uv/visible spectral for compound CuC2 are recorded in DMSO. The data are offered in the electronic absorption spectrum of the ligands showed band at 274nm (36496cm^{-1}) attributed to –C=C-,$\pi \rightarrow \pi^*$transition the band around 300nm and 332nm due to $\pi \rightarrow \pi^*$and n→ π^*transition of the (-C=N-) azomethine chromophore. No spectral bands were found below 10000cm^{-1} which supports octahedral geometry.

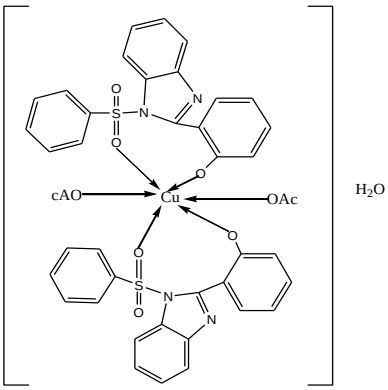

Proposed structure of Cu(II) complex of BIL2 (CuC2).

Table-1: In-vitro antibacterial activity values of the synthesized benzimidazol derivatives and their Cu(II), Ni(II) and Co(II) complexes

		Zone of inhibition (in mm)		
Entry	**Compounds**	***E. coli***	***S. aureus***	***K. pneumonia***
1	IN1	5	10	5
2	BIL 1	15	18	8
3	BIL2	5	7	5
4	CuC $[Cu(BIL1)_2(OAc)_2].H_2O$	11	18	8
5	NiC $[Ni(BIL1)_2(OAc)_2].4H_2O$	10	20	6
6	CoC $[Co(BIL1)_2(Cl)_2].6H_2O$	12	23	11
7	CuC2 $[Cu(BIL2)_2(OAc)_2].H_2O$	5	5	5
Standard	Gentamycin	14	21	5

The synthesized benzimidazol derivative and Cu(II), Ni(II) and Co(II) complexes were tested for *in-vitro* antibacterial activity against *E. coli, S. aureus* and *K. pneumonia*. Gentamicin was used as standard antibacterial drug. The zone of inhibition values clearly showed that all the compounds exhibited a varied range 5-23mm (table 1) against all the tested bacterial strains. Compounds IN, BIL2 and CuC2 had less activity against *E. coli* and *S. aureus*. Compounds NiC and CuC showed moderate antibacterial activity against *E. coli* and *S. aureus.* Compound BIL1 exhibited better activity against *E. coli* (15mm zone of

inhibition) compared to standard (14mm zone of inhibition) but moderate activity against *S. aureus*; compound CoC exhibited better activity against *S. aureus* (23mm zone of inhibition) compared to standard (21mm zone of inhibition) but moderate activity against *E. coli.*

CONCLUSION

All the synthesized compounds in this study showed better activity against *K. pneumonia* compared to standard. Comparing the two benzimidazole derivatives BIL1 and BIL2; BIL1 showed better activity against all the tested bacterial strain, structurally the two compounds are differ by the presence of methoxy substituent at 3 position of phenyl ring, it can be concluded that the dramatic increase in the activity is due to the presence of this substituent. This compound is a good starting point to develop new drug for treating pathogenic diseases. Therefore, synthesis of more analogue were recommended for further discovery of a new drug candidate.

Acknowledgement

The authors thank Addis Ababa University for running the NMR, IR, and UV-vis spectra and Hawassa University for providing research funding.

References

Ashraf A., Siddiqui W. A., Akbar J., Mustafa G., Krautscheid H., Ullah N., Mirza B., Sher F., Hanif M. and Hartinger C.G. 2016. Metal complexes of benzimidazole derived sulfonamide: Synthesis, molecular structures and antimicrobial activity. *Inorganica Chimica Acta* **443**: 179–185.

Arpi M., Ragini G. and Anshu J. 2013. Microwave-assisted, synthesis of nitrogen-containing heterocycles. *Green Chemistry Letters and Reviews* **6**:2, 151-182,

Bhagdev K. and Sarkar S. 2021. Benzothiazole Moiety and Its Derivatives as Antiviral Agents. *Med. Sci. Forum*. 7 (1): 1-9

Fatmah A.S. Alasmary, Snelling A.M., Zain M.E., Alafeefy A.M., Awaad A.S. and Karodia N. 2015. Synthesis and Evaluation of Selected Benzimidazole Derivatives as Potential Antimicrobial Agents. *Molecules* **20**(**8**): 15206–15223,

Kumaravel G. and Raman N. 2017. A treatise on benzimidazole based Schiff base metal(II) complexes accentuating their biological efficacy: Spectroscopic evaluation of DNA interactions, DNA cleavage and antimicrobial screening Ganesan Kumaravel. *Mater. Sci. Eng*. **70**: 184–194

Mariappan G., Hazarika R., Alam F., Karki R., Patangia U. and Nath S. 2015. Synthesis and biological evaluation of 2-substituted benzimidazole derivatives. *Arab. J. Chem*. **8**: 715–719

Błaszczak-Swiatkiewicz K., Olszewska P. and Mikiciuk-Olasik E. 2014. Biological approach of anticancer activity of new benzimidazole derivatives. *Pharmacol Rep*. **66**: 100–106

Kavitha A., Kallappa H. and Harisha S. 2010. In-vivo analgesic and anti-inflammatory activities of newly synthesized benzimidazole derivatives, *Eur. J. Med. Chem*. **45**: 2048–2054

Ansari K.F. and Lal C.. 2009. Synthesis, physicochemical properties and antimicrobial activity of some new benzimidazole derivatives. *Eur. J. Med. Chem*. **44**: 4028–4033

Horacio L.S., Londonõ-Lemos M. E., Raúl G.-V., Israel P.M. , Pilar G.M., Isabel G.M. and Norah N.B. 2008. Synthesis, structure and biological activities of cobalt (II) and zinc (II) coordination compounds with 2-benzimidazole derivatives. *J. Inorg. Biochem*. **102**: 1267–1276

Ting-Ting M., Xu-Bing T., Dong-Dong L., Chen H., Xiao-Yan J., Geng Y., Shi-Fa W. and Gu W. 2018. Synthesis and biological evaluation of 2-aryl-benzimidazole derivatives of dehydroabietic acid as novel tubulin polymerization inhibitors. *RSC Adv*. **8**: 17511–17526

Marinescu, M. 2021. Synthesis of Antimicrobial Benzimidazole–Pyrazole Compounds and Their Biological Activities. *Antibiotics*. **10**: 1002, 1-29

Sharma P., Reddy T.S., Kumar N.P., Senwar K.R., Bhargava S.K. and Shankaraiah N. 2017. Conventional and microwave-assisted synthesis of new 1Hbenzimidazole-thiazolidinedione derivatives: A potential anticancer scaffold. *Eur. J. Med. Chem*. **138**: 234-245

Kopel P., Wawrzak D., Langer V., Cihalova K., Chudobova D., Vesely R., Adam V. and Kizek R. 2015. Biological Activity and Molecular Structures of Bis(benzimidazole) and Trithiocyanurate Complexes. *Molecules.* **20**: 10360-10376

Zou R., Ayres K.R., Drach J.C. and Townsend L.B. 1996. Synthesis and Antiviral Evaluation of Certain Disubstituted Benzimidazole Ribonucleosides. *J. Med. Chem.* **39**: 3477–3482

Galal S.A., Hegab K.H., Hashem A.M. and Youssef N.S. 2010. Synthesis and antitumor activity of novel benzimidazole-5-carboxylic acid derivatives and their transition metal complexes as topoisomerease II inhibitors. *Eur. J. Med. Chem*. **45**: 5685-5691

Hirashima S., Suzuki T., Ishida T., Noji S., Yata S., Ando I., Komatsu M., Ikeda S. and Hashimoto H. 2006. Benzimidazole Derivatives Bearing Substituted Biphenyls as Hepatitis C Virus NS5B RNA-Dependent RNA polymerase Inhibitors: Structure−Activity Relationship Studies and Identification of a Potent and Highly Selective Inhibitor JTK-109. *J. Med. Chem.* **49**: 4721–4736

Shaharyar M., Mazumder A. and Abdullah M. 2017. Synthesis, characterization and antimicrobial activity of 1,3,4-oxadiazole bearing 1H-benzimidazole derivatives. *Arab. J. Chem.* **10**: 503–508

Özkay Y., Tunal Y., Karaca H. and Isíkdag I. 2010. Antimicrobial activity and a SAR study of some novel benzimidazole derivatives bearing hydrazone moiety. *Eur. J. Med. Chem*. **45**: 3293-3298.

.

East African Journal of Biophysical and Computational Sciences

Journal homepage : https://journals.hu.edu.et/hu-journals/index.php/eajbcs

Numerical Solutions of Advection Diffusion Equations Using Finite Element Method

Kassahun Getnet Mekonen*, Zerihun Kinfe Birhanu

Department of Mathematics, College of Natural and Computational Sciences, Hawassa University, Hawassa, Ethiopia.

KEYWORDS:

Finite Element Method; Varational Formulation; Numerical integration

Research article

ABSTRACT

In this paper, we have implemented the finite element method for the numerical solution of a boundary and initial value problems, mainly on solving the one and two dimensional advection-diffusion equation with constant parameters. In doing so, the basic idea is to first rewrite the problem as a variational equation, and then seek a solution approximation from the space of continuous piece-wise linear's. This discretization procedure results in a linear system that can be solved by using a numerical algorithm for systems of these equations. The techniques are based on the finite element approximations using Galerkin's method in space resulting system of the first order ODE's and then solving this first order ODE's using backward Euler descritization in time. For the two dimensional problems, we use the ODE solver ODE15I to descritize time. The validity of the numerical model is verified using different test examples. The computed results showed that the use of the current method is very applicable for the solution of the advection-diffusion equation.

INTRODUCTION

An advection-diffusion equation (ADE) is a mathematical model that has been used to model the concentration of pollutants. It gives the amount of pollutant concentration fields a fter i nput o f t he velocity data from the hydrodynamic model which are derived from mass balances. Formally the ADE equation is given by

$$u_t + a\nabla u = \nabla(D\nabla u) + f, \qquad (1)$$

where u is the concentration of the pollutant, a is the velocity of the considered particle, D the diffusion coefficient and f defines the sources and sinks due to different processes.

For the vast majority of geometries and problems, Eq. 1 cannot be solved with analytical methods, and an approximation of the equations can be constructed with different types of discretizations. Many numerical schemes have been implemented to approximately solve the ADE (Lima et al., 2021; Mahmud, 2012; Pochai and Deepana, 2011; Lian et al., 2016; Szymkiewicz and Gka-

* *Corresponding author:*
Email: kassahunm@hu.edu.et +251918491415 *https://dx.doi.org/10.4314/eajbcs.v4i1.5S*

siorowski, 2021). In numerical method, a discrete approximations for the solution is computed by descritizing the given domain in to different sets of sub domains. In this paper we were focus on finite element method to solve the PDE given in Eq. 1. We will implement the method for one and two dimensional PDE's. In this method, first we develop a weak formulation, from which we derive the discretization by multiplying both sides of the ADE equation by a test function and integration by parts (Green-Gauss Theorem) to reduce second order derivatives to first order terms, i.e., weak formulation. Then we represent the approximate solution by the linear combination of basis functions, by constructing a set of basis functions based on the mesh of our domain. That is, the solution u can be approximated by a function u_h using the linear combinations of the basis functions ϕ_i according to the following expressions:

$$u \approx u_h = \sum u_i \phi_i. \tag{2}$$

Here, ϕ_i denotes the basis functions and u_i denotes the coefficients of the functions that approximate u with u_h. After this we get a system of linear equations and we solve the linear system of equations to obtain the approximate solution.

The development of finite element method has favored by the progress of computer technology and numerical calculus, and originally applied for mechanical structures (Lima et al., 2021; Mahmud, 2012; Donea and Huerta, 2003) . Several procedures have been tried to interpret separately the advection and diffusion pollutant transport. The FEM can help to face more complex problems and the privilege importance of the method is that it can be adapted to complex geometry domains, but the element wise intervals can assume any form of size, and obviously there is an expense of more burdensome calculations. We had to do the descritization process of the finite element method for the $1D$ and $2D$ Poisson equations in which it is an auxiliary step in solving the advection diffusion equation with the FEM. Usually the numerical solutions of PDE' including the equation (Eq. 1) are done with the finite difference method.

MATHEMATICAL MODEL FORMULATION

To derive the advection diffusion equations for the application of pollution models, consider an elementary water body. Water quality within this body depends on the polluting substance mass present there. The water quality models describe the change in the mass of a polluting substance within the water body. The change is calculated as the difference between mass-flows (mass fluxes) entering and leaving this water body, considering also the effects of internal sources and sinks of the substance, if any. The mechanism of mass transfer into and out of this water body includes the following processes:

- Mass is transported by the flow, a, of the velocity vector. This process is termed as the advective mass transfer. The transfer of mass, that is the mass flux can be calculated as $u \times a$, where u is the concentration of the substance in the water.
- The dispersive mass transfer is usually expressed by the law of Fix which states that the transport of

the substance in the direction of a space is proportional to the concentration of this substance in that direction and the proportionality factor being the coefficient of dispersion, $D\nabla u$.

By considering a volume element of porous mediums in three dimensional cartesian coordinates the equations are derived (Bajellan, 2015). Since we are considering advection and diffusion as the two modes of transport of a fluid within the porous medium, we can represent these two transport modes in the x-direction mathematically as:

$$\text{transport by advection} = audA \ ,$$

$$\text{transport by diffusion} = D_x \frac{\partial u}{\partial x} \ ,$$

where dA is an elemental cross-sectional area of the cubic element, and D_x is the diffusion coefficient in the x-direction.

Assuming that the two components (advection and diffusion) may be superposed, the total amount of material transported parallel to any given direction is obtained by summing the advective and diffusive transports. Using the mass balance approach by equating the difference between the mass of material entering a volume element and that leaving the element (i.e., net influx of mass) to the rate of accumulation of mass inside the volume.

$$\frac{\partial}{\partial t}u(x,t) + \frac{\partial}{\partial x}\left(a(x,t)u(x,t)\right) = \frac{\partial}{\partial x}\left(d(x,t)\frac{\partial}{\partial x}u(x,t)\right) + f(t,x). \tag{3}$$

The multidimensional advection-diffusion equation is used for analyzing mixing problems in rivers. One of the practical difficulties is that the equation requires some prior information about water depths, velocities, and diffusion coefficients, which could not conveniently be gathered in field experiments. In some particular mixing problems, however, some of the terms in the multidimensional advection-diffusion equation are negligibly small, so that the problem can be simplified by reducing the model to one dimension (Lima et al., 2021; Hundsdorfer, 1996) and the one dimensional advection diffusion equation is given in Eq. 3.

The time-derivative term expresses accumulation of mass at a point in space, the advection term $a\nabla u$ transport of mass with the flow, and the diffusion term $D\nabla^2 u$ reflects transport of mass due to molecular diffusion (Langtangen, 1999). We shall consider the equation in the space interval $\Omega \subset \mathbb{R}$ with time $t \geq 0$. An initial condition $u(x,0)$ will be given and we also assume that suitable boundary conditions are provided, and for our work we consider the velocity field and the diffusion term as constants.

Both advection and diffusion move a pollutant material from one place to another, but each accomplishes this differently. The essential difference of the advection and diffusion is that advection moves the pollutants in one way (downstream) but diffusion goes in both ways (regardless of a stream direction). This is seen in the respective mathematical expressions of the advection equation $a\frac{\partial u}{\partial x}$ which has a first-order derivative, and the diffusion equation $D\frac{\partial^2 u}{\partial x^2}$ that has a second-order derivative.

Questions are arise like, can we have cases of fast advection and relatively weak diffusion and other cases of negligible advection and fast diffusion? To answer this

question, we must compare the sizes of the $a\frac{\partial u}{\partial x}$ and $D\frac{\partial^2 u}{\partial x^2}$ terms to each other, and this is accomplishes by introducing scales.

Variable	scale	choice of value
u	U	The concentration value such as initial, boundary, or average value
a	V	The maximum velocity value
x	X	Approximate length of the domain or size of release location

Using these scales, we can derive estimates of the sizes of the different terms. Since the derivative $\frac{\partial u}{\partial x}$ is expressing the difference in concentration over a distance of infinitesimal limit, we can estimate it to be approximately $\frac{U}{X}$, and the advection term scales as:

$$a\frac{\partial u}{\partial x} \sim V\frac{U}{X}.$$

Similarly, the second derivative $\frac{\partial^2 u}{\partial x^2}$ represents the difference of a gradient over a specified distance and is estimated at $\frac{(\frac{U}{X})}{X} = \frac{U}{X^2}$, and the diffusion term scales as:

$$D\frac{\partial^2 u}{\partial x^2} \sim D\frac{U}{X^2}.$$

Equipped with these estimates, we can then compare the two processes by forming the ratio of their scales:

$$\frac{\text{Advecton}}{\text{Diffusion}} = \frac{V\frac{U}{X}}{D\frac{U}{X^2}} = \frac{VX}{D}$$

This ratio is dimensionless and Traditionally, it is called the Peclet number and is denoted by Pe:

$$Pe = \frac{VX}{D}.$$

If $Pe \ll 1$ (if $Pe < 0.1$): the advection term will result significantly smaller than the diffusion term. Physically, diffusion dominates and advection is negligible. So, spreading occurs symmetrically despite of the flow of the directional bias. If we wish to simplify the problem, we may drop the $a\frac{\partial u}{\partial x}$ term, as if a were nil (no amount at all). The relative error occurred in the solution is expected to be on the order of the Peclet number, and the smaller Pe leads to the smaller error. The solutions established with diffusion only were based on such simplification and are thus valid as long as $Pe \ll 1$.

If $Pe \gg 1$ (if $Pe > 10$): the advection term is significantly bigger than the diffusion term. Physically, the diffusion term is negligible and advection dominates, and spreading is existent, with the patch (small area) of pollutant being simply moved along by the flow. If we wish to simplify the problem, we may drop the $D\frac{\partial^2 u}{\partial x^2}$ term, as if D were zero. The relative error occurred in doing the solution is expected as the order of the Peclet number inverse $(1/Pe)$, and the larger Pe will result the smaller error.

If $Pe \sim 1$ (in practice, if $0.1 < Pe < 10$): the advection and diffusion terms are not significantly different which results for the non dominance of the two in the process. The full equation must be utilized as there will no approximation to the equation will be justified.

NUMERICAL METHOD

In this paper we use the finite element method (FEM) to approximate the solution of the advection diffusion equation. The method is examined as an emerging tool for the approximate solution of differential equations describing different physical processes (Yang et al., 2020). It is based on the basic finite e lement procedures, those are: the variation form for-

mulation of the problem, the discretization of the formulation in a finite element, and the solution of the resulting finite element equations. FEM cuts a given domain into several elements (pieces of the domain) and connected in a finite number of nodal points.

The FEM is based on the integration of the terms in the equation to be solved, in form of point discretization schemes. It utilizes the method of weighted residuals and integration by parts (Green-Gauss Theorem) to reduce second order derivatives to first order terms. The solution domain is discretized into individual elements and these elements are operated upon individually and then solved globally using matrix solution techniques. Such a task could be done automatically by a computer, but it necessitates an amount of mathematical skill that to day still requires human involvement, (Brenner et al., 2008).

The theories of finite element methods provided the reasons why it worked well for the class boundary/initial value problems (Lima et al., 2021; Ahsan, 2012; Larson and Bengzon, 2010). Extension of the mathematical basis to nonlinear and non-structural problems was achieved through the method of weighted residuals (MWR), originally conceived by Galerkin in the early 20th century. The basics of the method requires multiplying of the governing differential equation by a set of predetermined weights and integrating the resulting product over a region. Most of the finite element method uses the Galerkin's method to establish the approximations of the governing equations, (Aragonés et al., 2019; Lima et al., 2021; Ahsan, 2012; Yang et al., 2020; Brenner et al., 2008). It allows us to convert a continuous form of the problem, such as the weak formulation for the partial differential equation into a discrete problem that may be solved numerically.

Finite Element Implementation of the $1D$ Governing Equation

Let us consider the one dimensional Advection-Diffusion equation given by:

$$\frac{\partial u}{\partial t} + a\frac{\partial u}{\partial x} = D\frac{\partial^2 u}{\partial x^2} + f,\ u(0) = u(1) = 0, \tag{4}$$

where u is the concentration of the pollutant, a is the velocity, f is the source term, and D is the diffusion coefficient, with all the three variables be constants.

Implementation of the $1D$ Advection Equation

Let we first consider only an advection equation, that is the diffusion term does not exist;

$$\frac{\partial u}{\partial t} + a\frac{\partial u}{\partial x} = 0.$$

The first step is constructing a variational or weak formulation, by multiplying both sides of the differential equation by a test function $v(x)$ satisfying the boundary conditions (BC) $v(0) = 0, v(1) = 0$ and $v \in H_0^1(0,1)$, where $H_0^1(0,1)$ is the Sobolev space,

$$H_0^1(0,1) = \{v \in L^2(0,1); v' \in L^2(0,1)\},$$

and it is a function space where all the functions are bounded. Let us now define a sub-space of H where we can find our solution u. We call this V and

$$V = \{v \in H(X) : v|_{\partial\Omega} = 0\},\ \text{where } \Omega \text{ is our domain,}$$

Then multiplying and integrating both sides in the domain we have that:

$$\frac{\partial u}{\partial t}.v + a\frac{\partial u}{\partial x}.v = 0,$$

$$\int_0^1 \left(\frac{\partial u}{\partial t}.v + a\frac{\partial u}{\partial x}.v\right) = 0.$$

That is;

$$\int_0^1 \frac{\partial u}{\partial t}.v + \int_0^1 a\frac{\partial u}{\partial x}.v = 0, \qquad (5)$$

which is the weak formulation of the one dimensional advection equation.

Advantages of weak form compared to strong form

Equation 5 is the final weak formulation. It is equivalent to the strong form, since we can reverse all the steps, and get back to the original equation. Firstly, if we look at the strong form, we have two separate partial derivatives of u, so the strong form requires that u be continuously differentiable until at least second partial derivative. Our new formulations has lowered this requirement to only first partial derivatives by transforming one of the partial derivatives onto the weight-function $v(x, y)$. This is the first big advantage of a weak formulation. The subspace V is not difficult to understand; it is a subspace of H because our weak form requires that the functions are in H; our strong form requires that u be 0 along the boundary, so V is the subspace of all function which are zero on the boundary.

The next step is to generate a mesh, let be a uniform Cartesian mesh $x_i = ih, i = 0, 1, ..., n$, where $h = \frac{1}{n}$, and we define the intervals as $[x_{i-1}, x_i], i = 1, 2, ..., n$.
After generating a mesh we construct a set of basis functions based on the mesh for each intervals, such as the piece wise linear functions for $i = 1, 2, ..., n-1$. The characteristic basis functions are characterized by the following property, (Quarteroni and Quarteroni, 2009)

$$\phi_i(x_j) = \delta_{ij},\ i, j = 1, ..., n-1, \qquad (6)$$

where δ_{ij} being the Kronecker delta. The function ϕ_i is therefore piece wise linear and are fix with one node (vertex) and associate the value one to this node and zero at the remaining nodes of the partition (see Fig. 1, (Larson and Bengzon, 2010)).

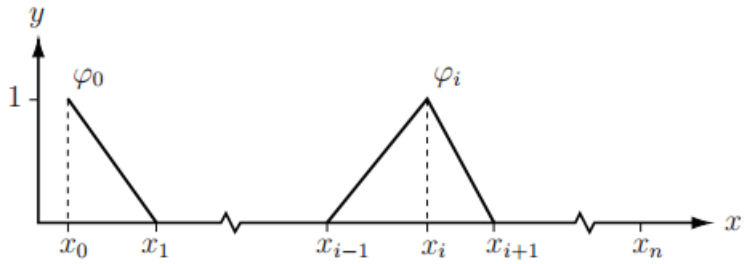

Figure 1: The basis (hat) function ϕ_i associated to node x_j, in this figure φ_i on a mesh. Also shown is the half hat ϕ_0.

Its expression is given by

$$\phi_i(x) = \begin{cases} \frac{x-x_{i-1}}{x_i-x_{i-1}}, & \text{if } x_{i-1} \le x \le x_i \\ \frac{x_{i+1}-x}{x_{i+1}-x_i}, & \text{if } x_i \le x \le x_{i+1} \\ 0, & \text{other wise} \end{cases}, \text{ for } i = 1, 2, \ldots, n-1. \qquad (7)$$

That is,

$$\phi_i(x_j) = \delta_{ij} = \begin{cases} 1, & \text{if } i = j \\ 0, & \text{if } i \neq j \end{cases}. \qquad (8)$$

We use this hat (basis) functions through out the $1D$ space of this research using equal spaced step size ($x_{i+1}-x_i = h$, for all i). We say that the functions are basis for the following reasons. If we want to approximate our continuous function u with a piece wise continuous linear function u', these functions are what we need. These functions are linearly independent of each other; it is not possible to make one out of a combination of others. For example, only one of these functions, ϕ_i, is non-zero (equal to 1) at node i. The next step in approximating a PDE with FEM is represent the approximate (FE) solution by the linear combination of such basis functions, (Quarteroni and Quarteroni, 2009) as

$$u_h(x) = \sum_{j=1}^{n-1} c_j \phi_i(x), \tag{9}$$

where the coefficients c_j are the unknowns to be determined. since the hat (basis) functions are piece wise linear, $u_h(x)$ is also a piece wise linear function, although this is not usually the case for the true solution u(x), and here we have,

$$u_h(x_j) = \sum_{i=1}^{n-1} c_j \phi_i(x_j) = c_j.$$

We then derive a linear system of equations for the coefficients by substituting the approximate solution $u_h(x)$ for the exact solution $u(x)$ in the weak form:

Then let the approximate solution for u be given by a linear combination of basis functions $\phi_i = \delta_{ij}$, as given in Eq. 10, and also for v as in Eq. 11. Now we find a finite element solution of the discrete problem by using the hat functions $\phi_i(x)$ defined in Eq. 7. For the given basis function the approximation of u and v can be written as :

$$u(t,x) = \sum_{i=1}^{N-1} u_i \phi_i(x), \tag{10}$$

$$v(t,x) = \sum_{j=1}^{N-1} v_j \phi_j(x). \tag{11}$$

Now substituting Eq.10 and Eq.11 in the weak formulation of the equation Eq.5, we have:

$$\int_0^1 \frac{\partial}{\partial t} \sum_{i=1}^{N-1} u_i \phi_i . \sum_{j=1}^{N-1} v_j \phi_j + \int_0^1 a \frac{\partial}{\partial x} \left(\sum_{i=1}^{N-1} u_i \phi_i \right) . \sum_{j=1}^{N-1} v_j \phi_j = 0.$$

which then implies,

$$\sum_{j=1}^{N-1} v_j \left(\frac{\partial}{\partial t} \sum_{i=1}^{N-1} u_i \int_0^1 \phi_i . \phi_j + a \sum_{i=1}^{N-1} u_i \int_0^1 \phi_i' . \phi_j \right) = 0.$$

That is

$$\frac{\partial}{\partial t} \sum_{i=1}^{N-1} u_i \int_0^1 \phi_i . \phi_j + a \sum_{i=1}^{N-1} u_i \int_0^1 \phi_i' . \phi_j = 0.$$

In a matrix form it can be written as:

$$M\dot{U} + aBU = 0, \tag{12}$$

where,

- M is the mass matrix with entries:

$$M_{i,j} = \int_0^1 \phi_i(x)\phi_j(x)dx.$$

- B is a matrix with entries:

$$B_{ij} = \int_0^1 \phi_i'(x)\phi_j(x)dx = \begin{cases} 0, & \text{if } i = j \\ \frac{-1}{2}, & \text{if } i - j = 1 \\ \frac{1}{2}, & \text{if } j - i = 1 \\ 0, & \text{other wise} \end{cases} . \tag{13}$$

Here M and A are tridiagonal matrices and Eq.12 is a simple system of ODE.

The next step is to descritize the sys-tem Eq.12 in time. Here we were consider finite difference approximations specially the implicit Euler (Back ward Euler) method. By using the back ward Euler scheme, the system Eq.12 results the following system of algebraic equations:

$$M\left(\frac{U^{n+1} - U^n}{\Delta t}\right) + aBU^{n+1} = 0.$$

Here U^n denotes U at time $t = t^n = \Delta tn$, and Δt is the time step. Rearranging the terms we obtain the system:

$$\left(\frac{M}{\Delta t} + aB\right) U^{n+1} = \frac{1}{\Delta t} MU^n,\ n = 0, 1, 2, \ldots,$$

to be solved for U^{n+1} by using initial condition for $U^0 = U(x, t = 0)$.

Euler Back ward represents an implicit scheme which is stable for all choices of Δt (?). Since the scheme is implicit, we have to solve a system of algebraic equations at each time step.

Assembly of the mass matrix M in $1D$

Let us now go through the details of how to assemble the mass matrix M. We begin by calculating the entries $M_{i,j}$ of the mass matrix, which involve products of hat functions given in Eq. 7. Since each hat is a linear polynomial, the product of two hats is a quadratic polynomials. Thus, Simpson's formula (Eq. 18) can be used to integrate $M_{i,j} = \int_\Omega \phi_i\phi_j dx$ exactly. Moreover, since the hats ϕ_i and ϕ_j lack common support for $|i - j| > 1$ only $M_{i,i}$, $M_{i,i+1}$, and $M_{i+1,i}$ need to be calculated. All other matrix entries are zero by default. This is clearly seen from Figure 2, (Larson and Bengzon, 2010) showing two neighboring hat functions and their support. As a consequence, the mass matrix M is tridiagonal.

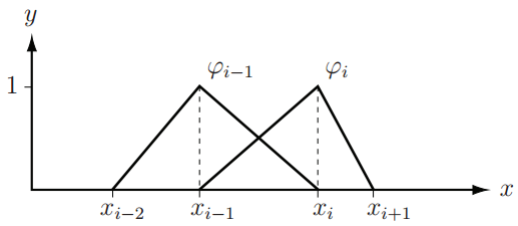

Figure 2: Illustration of the hat functions ϕ_{i-1} and ϕ_i, in this figure φ, and their support.

On the interval $I = (a, b)$, Simpson's formula is of the form, (Larson and Bengzon, 2010)

$$\int_a^b f(x)dx = \frac{f(a) + 4f(\frac{a+b}{2}) + f(b)}{6}(b-a). \tag{14}$$

Let we start on the diagonal entries of M, $M_{i,i}$ using Simpson's formula:

$$\begin{aligned} M_{i,i} &= \int_\Omega \phi_i^2 dx, \\ &= \int_{x_{i-1}}^{x_i} \phi_i^2 dx + \int_{x_i}^{x_{i+1}} \phi_i^2 dx, \\ &= \frac{0 + 4(\frac{1}{2})^2 + 1}{6} h_i + \frac{1 + 4(\frac{1}{2})^2 + 0}{6} h_{i+1}, \\ &= \frac{h_i}{3} + \frac{h_{i+1}}{3}, \text{ for } i = 1, 2, \ldots, n-1, \end{aligned}$$

where $h_{i+1} = x_{i+1} - x_i$ and $h_i = x_i - x_{i-1}$, but in our case we use a uniform mesh length $h = x_{i+1} - x_i = x_i - x_{i-1}$ and $M_{ii} = \frac{2h}{3}$. The first and last diagonal entry are $M_{00} = \frac{h_1}{3}$ and $M_{nn} = \frac{h_n}{3}$, respectively, since the hat functions ϕ_0 and ϕ_n are only half.

We know continue with the sub diagonal entries $M_{i+1,i}$ still using Simpson's formula we have

$$\begin{aligned} M_{i+1,i} &= \int_\Omega \phi_{i+1}\phi_i dx, \\ &= \int_{x_i}^{x_{i+1}} \phi_{i+1}\phi_i dx, \\ &= \frac{1.0 + 4(\frac{1}{2})^2 + 0.1}{6} h_{i+1} \\ &= \frac{h_{i+1}}{6}, \text{ for } i = 0, 1, 2, \ldots, n-1. \end{aligned}$$

By using a similar calculation the super diagonal entries $M_{i,i+1}$ have the values

$$M_{i,i+1} = \frac{h_{i+1}}{6}, \text{ for } i = 0, 1, 2, \ldots, n-1.$$

Hence, the mass matrix m takes the form

$$M = \begin{bmatrix} \frac{h_1}{3} & \frac{h_1}{6} & & & & & & \\ \frac{h_1}{6} & \frac{h_1}{3} + \frac{h_2}{3} & \frac{h_2}{6} & & & & & \\ & \frac{h_2}{6} & \frac{h_2}{3} + \frac{h_3}{3} & \frac{h_3}{6} & & & & \\ & & \ddots & \ddots & \ddots & & & \\ & & & \frac{h_{n-1}}{6} & \frac{h_{n-1}}{3} + \frac{h_n}{3} & \frac{h_n}{6} & \\ & & & & \frac{h_n}{6} & \frac{h_n}{3} \end{bmatrix}. \tag{15}$$

The global mass matrix M can be written as a sum of n simpler elemental matrices as:

$$M = \begin{bmatrix} \frac{h_1}{3} & \frac{h_1}{6} & & \\ \frac{h_1}{6} & \frac{h_1}{3} & & \\ & & & \\ & & & \end{bmatrix} + \begin{bmatrix} & & & \\ & \frac{h_2}{3} & \frac{h_2}{6} & \\ & \frac{h_2}{6} & \frac{h_2}{3} & \\ & & & \end{bmatrix} + \ldots + \begin{bmatrix} & & & \\ & & & \\ & & \frac{h_n}{3} & \frac{h_n}{6} \\ & & \frac{h_n}{6} & \frac{h_n}{3} \end{bmatrix}.$$

i.e., $M = M^{\Omega_1} + M^{\Omega_2} + \ldots + M^{\Omega_n}$.

Each matrix $M^{\Omega^e}, i = 1, 2, \ldots, n$, is obtained by restricting the integration to one sub interval or element Ω_e and is therefore called an element mass matrix. From the sum we see that on each element e this small block takes the form: $M^e = \frac{h}{6}\begin{bmatrix} 2 & 1 \\ 1 & 2 \end{bmatrix}$, where h is the length of e. We refer to M^e as the local element mass matrix. The summation of the element mass matrices into the global mass matrix is called assembling.

Now the system of equation, that is Eq.12 is a simple system of ordinary differential equations. To solve this system of ode's, we have to use a back ward Euler method and a Matlab soft ware to solve the system at each time steps using an initial condition.

Implementation of the $1D$ Diffusion Equation

Let we now consider the diffusion equation

$$\frac{\partial u}{\partial t} = D\frac{\partial^2 u}{\partial x^2}.$$

We multiply the equation by a test function $v(x)$, which satisfies the boundary conditions $v(0) = v(1) = 0$ and then integrating by parts we have that:

$$\frac{\partial u}{\partial t}.v = D\frac{\partial^2 u}{\partial x^2}.v$$

$$\int_0^1 \left(\frac{\partial u}{\partial t}.v\right) = \int_0^1 \left(D\frac{\partial^2 u}{\partial x^2}.v\right)$$

Hence by using integration by parts, we obtain

$$\int_0^1 \frac{\partial u}{\partial t}.v = -D\int_0^1 \frac{\partial u}{\partial x}.\frac{\partial v}{\partial x}, \qquad (16)$$

which is the weak formulation of the one dimensional Diffusion equation.

Now substituting Eq.10 and Eq.11 in the weak formulation of the equation Eq.16, we have:

$$\int_0^1 \frac{\partial}{\partial t}\sum_{i=1}^{N-1} u_i\phi_i.\sum_{j=1}^{N-1} v_j\phi_j = -D\int_0^1 \frac{\partial}{\partial x}\sum_{i=1}^{N-1} u_i\phi_i.\frac{\partial}{\partial x}\sum_{j=1}^{N-1} v_j\phi_j.$$

which then implies,

$$\sum_{j=1}^{N-1} v_j\left(\frac{\partial}{\partial t}\sum_{i=1}^{N-1} u_i\int_0^1 \phi_i.\phi_j\right) = \sum_{j=1}^{N-1} v_j\left(-D\sum_{i=1}^{N-1} u_i\int_0^1 \phi_i'.\phi_j'\right).$$

That is

$$\frac{\partial}{\partial t}\sum_{i=1}^{N-1} u_i\int_0^1 \phi_i.\phi_j = -D\sum_{i=1}^{N-1} u_i\int_0^1 \phi_i'.\phi_j'.$$

In a matrix form it can be written as:

$$M\dot{U} + DAU = 0, \qquad (17)$$

where M is the mass matrix with entries given in Eq. 15 and A is the stiffness matrix with entries given in Eq. 19.

Here the matrix A is often referred to as the stiffness matrix, a name coming from corresponding matrices in the context of structural problems.

Assembly of the stiffness matrix in $1D$

The stiffness matrix A is symmetric for this simple problem, which makes the computation of the matrix faster since we don't have to compute all of the elements, symmetric matrices are also much faster to invert. Here ϕ_i's are the hat functions given in Eq. 7, the entries of each element of the stiffness matrix A is given by

$$\begin{aligned} A_{i,j} &= \int_0^1 \phi_i' \phi_j' dx, \\ &= \sum_{e=1}^{N-1} \int_{\Omega_e} \phi_i' \phi_j' dx, \\ &= \sum_{e=1}^{N-1} A_{ij}^e. \end{aligned}$$

similarly the load vector

$$F_i = \int_0^1 f\phi_i dx = \sum_{e=1}^{N-1} \int_{\Omega_e} f\phi_i dx = \sum_{e=1}^{N-1} F_i^e.$$

On the interval $I = (a, b)$ Simpson's formula is of the form, (Larson and Bengzon, 2010)

$$\int_a^b f(x)dx = \frac{f(a) + 4f(\frac{a+b}{2}) + f(b)}{6}(b-a). \tag{18}$$

Then we can be illustrate by the hat functions and Simpsons formula as follows:

$$\phi_i(x) = \begin{cases} \frac{x-x_{i-1}}{h_i}, & \text{if } x_{i-1} \le x \le x_i \\ \frac{x_{i+1}-x}{h_{i+1}}, & \text{if } x_i \le x \le x_{i+1} \\ 0, & \text{other wise} \end{cases}, \quad \phi_{i-1}(x) = \begin{cases} \frac{x-x_{i-2}}{h_{i-1}}, & \text{if } x_{i-2} \le x \le x_{i-1} \\ \frac{x_i-x}{h_i}, & \text{if } x_{i-1} \le x \le x_i \\ 0, & \text{other wise} \end{cases},$$

and $\phi_{i+1}(x) = \begin{cases} \frac{x-x_i}{h_{i+1}}, & \text{if } x_i \le x \le x_{i+1} \\ \frac{x_{i+2}-x}{h_{i+2}}, & \text{if } x_{i+1} \le x \le x_{i+2} \\ 0, & \text{other wise} \end{cases}$.

Now

$$\begin{aligned} A_{i,i} = a(\phi_i, \phi_i)^e &= \int_{\Omega_e} \phi_i' \phi_i' dx, \\ &= \int_{x_{i-1}}^{x_i} \phi_i' \phi_i' dx + \int_{x_i}^{x_{i+1}} \phi_i' \phi_i' dx, \\ &= \int_{x_{i-1}}^{x_i} \frac{1}{h_i}\frac{1}{h_i} dx + \int_{x_i}^{x_{i+1}} \frac{-1}{h_{i+1}}\frac{-1}{h_{i+1}} dx, \\ &= \frac{h_i}{6}\left(\frac{1}{h_i^2} + \frac{4}{h_i^2} + \frac{1}{h_i^2}\right) + \frac{h_{i+1}}{6}\left(\frac{1}{h_{i+1}^2} + \frac{4}{h_{i+1}^2} + \frac{1}{h_{i+1}^2}\right), \\ &= \frac{1}{h_i} + \frac{1}{h_{i+1}}. \end{aligned}$$

,

$$\begin{aligned} A_{i-1,i} = a(\phi_{i-1}, \phi_i)^e &= \int_{\Omega_e} \phi_{i-1}' \phi_i' dx, \\ &= \int_{x_{i-1}}^{x_i} \phi_{i-1}' \phi_i' dx + \int_{x_i}^{x_{i+1}} \phi_{i-1}' \phi_i' dx, \\ &= \int_{x_{i-1}}^{x_i} \frac{-1}{h_i}\frac{1}{h_i} dx, \\ &= \frac{h_i}{6}\left(\frac{-1}{h_i^2} + \frac{-4}{h_i^2} + \frac{-1}{h_i^2}\right) = \frac{-1}{h_i}. \end{aligned}$$

and

$$\begin{aligned} A_{i,i+1} = a(\phi_{i+1}, \phi_i)^e &= \int_{\Omega_e} \phi'_{i+1}\phi'_i dx, \\ &= \int_{x_{i-1}}^{x_i} \phi'_{i+1}\phi'_i dx + \int_{x_i}^{x_{i+1}} \phi'_{i+1}\phi'_i dx, \\ &= \int_{x_i}^{x_{i+1}} \frac{-1}{h_{i+1}}\frac{1}{h_{i+1}} dx, \\ &= \frac{h_{i+1}}{6}\left(\frac{-1}{h_{i+1}^2} + \frac{-4}{h_{i+1}^2} + \frac{-1}{h_{i+1}^2}\right) = \frac{-1}{h_{i+1}}. \end{aligned}$$

Each generic interior element contributes to the stiffness matrix of a 2×2 sub matrix.

$$A = \int_0^1 \phi'_i\phi'_j dx = \sum_{e=1}^{N-1} A^e = \begin{bmatrix} \frac{1}{h_1} & \frac{-1}{h_1} & & & & & \\ \frac{-1}{h_1} & \frac{1}{h_1}+\frac{1}{h_2} & \frac{-1}{h_2} & & & & \\ & -\frac{-1}{h_2} & \frac{1}{h_2}+\frac{1}{h_3} & \frac{-1}{h_3} & & & \\ & & \ddots & \ddots & \ddots & & \\ & & & \frac{-1}{h_{n-1}} & \frac{1}{h_{n-1}}+\frac{1}{h_n} & \frac{-1}{h_n} & \\ & & & & \frac{-1}{h_n} & \frac{1}{h_n} & \end{bmatrix}. \tag{19}$$

The global stiffness matrix A can be written as a sum of n simpler elemental matrices as:

$$A = \frac{1}{h_1}\begin{bmatrix} 1 & -1 & \\ -1 & 1 & \\ & & \end{bmatrix} + \frac{1}{h_2}\begin{bmatrix} & & \\ & 1 & -1 \\ & -1 & 1 \end{bmatrix} + \ldots + \frac{1}{h_n}\begin{bmatrix} & & \\ & 1 & -1 \\ & -1 & 1 \end{bmatrix}.$$

i.e., $A = A^{\Omega_1} + A^{\Omega_2} + \ldots + A^{\Omega_n}$.
Each matrix $A^{\Omega_e}, e = 1, 2, \ldots, n$, is obtained by restricting the integration to one sub interval or element Ω_e and is therefore called an element stiffness matrix. From the sum we see that on each element e this small block takes the form: $A^e = \frac{1}{h}\begin{bmatrix} 1 & -1 \\ -1 & 1 \end{bmatrix}$, where h is the length of e. We refer to A^e as the local element stiffness matrix.

Now the system of equation, that is Eq.17 also is a simple system of ordinary differential equations and we can solve this system of Ode's to get the solution of the original PDE.

Implementation of One Dimensional Advection Diffusion equation

Let us now solve the $1D$ governing (advection diffusion) equation

$$\frac{\partial u}{\partial t} + a\frac{\partial u}{\partial x} = D\frac{\partial^2 u}{\partial x^2} + f,\ u(0) = u(1) = 0,$$

by using FEM. Let we find the weak formulation of the equation by multiplying the equation with a test function $v(x)$, which satisfies the boundary conditions $v(0) = v(1) = 0$ and then integrating by parts as the same procedure above. we have that:

$$\frac{\partial u}{\partial t}.v + a\frac{\partial u}{\partial x}.v = D\frac{\partial^2 u}{\partial x^2}.v + f.v,$$

$$\int_0^1 \left(\frac{\partial u}{\partial t}.v + a\frac{\partial u}{\partial x}.v\right) = \int_0^1 \left(D\frac{\partial^2 u}{\partial x^2}.v + f.v\right).$$

Using integration by parts, we have then

$$\int_0^1 \frac{\partial u}{\partial t}.v + \int_0^1 a\frac{\partial u}{\partial x}.v = -D\int_0^1 \frac{\partial u}{\partial x}.\frac{\partial v}{\partial x} + \int_0^1 f.v, \tag{20}$$

which is the weak formulation of the one dimensional advection-Diffusion equation. Substituting Eq.10 and Eq.11 in the weak formulation of the equation Eq.20, we have:

$$\begin{aligned}\int_0^1 \frac{\partial}{\partial t}\sum_{i=1}^{N-1} u_i\phi_i.\sum_{j=1}^{N-1} v_j\phi_j + \int_0^1 a\frac{\partial}{\partial x}\left(\sum_{i=1}^{N-1} u_i\phi_i\right).\sum_{j=1}^{N-1} v_j\phi_j \\ = -D\int_0^1 \frac{\partial}{\partial x}\sum_{i=1}^{N-1} u_i\phi_i.\frac{\partial}{\partial x}\sum_{j=1}^{N-1} v_j\phi_j + \int_0^1 f.\sum_{j=1}^{N-1} v_j\phi_j.\end{aligned}$$

which then implies,

$$\sum_{j=1}^{N-1} v_j\left(\frac{\partial}{\partial t}\sum_{i=1}^{N-1} u_i\int_0^1 \phi_i.\phi_j + a\sum_{i=1}^{N-1} u_i\int_0^1 \phi_i'.\phi_j\right) = \sum_{j=1}^{N-1} v_j\left(-D\sum_{i=1}^{N-1} u_i\int_0^1 \phi_i'.\phi_j' + \int_0^1 f.\phi_j\right). \tag{21}$$

That is

$$\frac{\partial}{\partial t}\sum_{i=1}^{N-1} u_i\int_0^1 \phi_i.\phi_j + a\sum_{i=1}^{N-1} u_i\int_0^1 \phi_i'.\phi_j = -D\sum_{i=1}^{N-1} u_i\int_0^1 \phi_i'.\phi_j' + \int_0^1 f.\phi_j.$$

In a matrix form it can be written as:

$$M\dot{U} + aBU + DAU = F, \tag{22}$$

where M is the mass matrix with entries given in Eq. 15, B is a matrix with entries given in Eq. 13, A is the stiffness matrix given in Eq. 19 and F is a load vector given in Eq. 25.

Assembly of the Load Vector in $1D$

The right-hand-side, load vector of Eq. 20 contains an integral over a function $f(x)$. In general, exactly computing this integral is very difficult, so another numerical approximation is required. We can use a well known integration rule composite simpson rule to approximate these integration whose formula (for more information you can see, (**?**)) is given in Eq. 23, by selecting a set of distinct N nodes in the interval $[a, b]$ with $h = \frac{b-a}{N}$, $x_i = a+ih$ for each $i = 0, 1, \ldots, N$:

$$\int_a^b f(x)dx = \frac{h}{3}\left(f(x_0) + 2\sum_{j=1}^{\frac{N}{2}-1} f(x_{2j}) + 4\sum_{j=1}^{\frac{N}{2}} f(x_{2j-1}) + f(x_N)\right),\ j = 1, 2, ..., (\frac{N}{2}) - 1. \tag{23}$$

Using the another quadrature rule for simplicity, for instance, using the Trapezoidal rule, (Larson and Bengzon, 2010)

$$\int_a^b f(x)dx = \frac{f(a)+f(b)}{2}(b-a), \tag{24}$$

we have

$$\begin{aligned} f_i &= \int_I f\phi_i dx, \\ &= \int_{x_{i-1}}^{x_{i+1}} f\phi_i dx, \\ &= \int_{x_{i-1}}^{x_i} f\phi_i dx + \int_{x_i}^{x_{i+1}} f\phi_i dx, \\ &\approx \frac{f(x_{i-1})\phi_i(x_{i-1}) + f(x_i)\phi_i(x_i)}{2} h_i + \frac{f(x_{i+1})\phi_i(x_{i+1}) + f(x_i)\phi_i(x_i)}{2} h_{i+1}, \\ &= \frac{0 + f(x_i)}{2} h_i + \frac{f(x_i) + 0}{2} h_{i+1}, \\ &= f(x_i)\left(\frac{h_i}{2} + \frac{h_{i+1}}{2}\right). \end{aligned}$$

Now using this trapezoidal method, the approximate load vector takes the form

$$F = \begin{pmatrix} f(x_0)\frac{h_1}{2} \\ f(x_1)\left(\frac{h_1+h_2}{2}\right) \\ f(x_2)\left(\frac{h_2+h_3}{2}\right) \\ \vdots \\ f(x_{n-1})\left(\frac{h_{n-1}+h_n}{2}\right) \\ f(x_n)\frac{h_n}{2} \end{pmatrix}. \tag{25}$$

Splitting F into a sum over the elements yields the n global element load vectors F^{Ω_e}:

$$F = \begin{pmatrix} f(x_0) \\ f(x_1) \\ \\ \\ \\ \end{pmatrix} \frac{h_1}{2} + \begin{pmatrix} \\ f(x_1) \\ f(x_2) \\ \\ \end{pmatrix} \frac{h_2}{2} + \begin{pmatrix} \\ \\ f(x_2) \\ f(x_3) \\ \end{pmatrix} \frac{h_3}{2} + \ldots + \begin{pmatrix} \\ \\ \\ f(x_{n-1}) \\ f(x_n) \end{pmatrix} \frac{h_n}{2}$$

i.e., $F = F^{\Omega_1} + F^{\Omega_2} + \ldots + F^{\Omega_n}$. Each vector $F^{\Omega_e}, e = 1, 2, \ldots, n$, is formally derived by restricting the integration to element Ω_e.

Now the system of equation, that is Eq.22 can be written in the form:

$$M\dot{U} + (aB + DA)\,U = F, \tag{26}$$

which is a simple system of ordinary differential equations. For solving this system of Ode's, we have to use a Matlab soft ware in which it has a number of tools for numerically solving ordinary differential equations. We would focus on the back ward Euler method to descritize time.

FEM implementation of the Two Dimensional AD equation

The $2D$ advection diffusion equation with the same and constant velocity and diffusion term is given by

$u_t + a(u_x + u_y) = D(u_{xx} + u_{yy}) + f,$
$(x, y) \in \Omega = [0, 1],$

with homogeneous boundary conditions. That is

$$u_t + a\nabla u = D\nabla^2 u + f.$$

Now to find a weak formulation for this $2D$ equation, we multiply both sides of the equation with a test function $v = v(x, y) \in V$ which satisfies the boundary conditions.

$$u_t.v + a\nabla u.v = D\nabla^2 u.v + fv.$$

Here integrating this over the domain Ω yields the following:

$$\int_\Omega (u_t.v + a\nabla u.v) = \int_\Omega \big(D\nabla^2 u.v + fv\big).$$

We see from the 2D FEM of Poisson equation (using Gauss theorem and the transformation of a surface integral to a line integral) that $\int_\Omega v\nabla^2 u = -\int_\Omega \nabla v\nabla u$, and hence we get:

$$\int_\Omega (u_t.v + a\nabla u.v) = -D\int_\Omega (\nabla v\nabla u) + \int_\Omega fv.$$

$$\int_\Omega u_t.v = -\int_\Omega (D\nabla v\nabla u + a\nabla u.v) + \int_\Omega fv. \tag{27}$$

Here Eq. 27 is the weak formulation and it can be simplified as

$$(u_t, v) = l(u, v) + (f, v)\ \forall v \in V, \tag{28}$$

where $(u_t, v) = \int_\Omega u_t.v$ and $l(u, v) = -\int_\Omega (D\nabla v\nabla u + a\nabla u.v)$.

Given a FE space V, with $\phi_i(x, y),\ i = 1, 2, \ldots, N$ denoting a set of basis functions for V, we seek the FE solution of form

$$u_h(x, y, t) = \sum_{j=1}^{N} u_j(t)\phi_j(x, y). \tag{29}$$

And taking the test function $v(x, y)$ as a linear combination of basis functions

$$v(x, y) = \sum_{j=1}^{N} v_j\phi_j, \text{ with } v_j \text{ are constants.} \tag{30}$$

Substituting this expression (29 and 30) into eq.28, we obtain

$$\left(\sum_{j=1}^{N} u_j'(t)\phi_j(x, y), \sum_{j=1}^{N} v_j\phi_j\right) = l\left(\sum_{j=1}^{N} u_j(t)\phi_j(x, y), \sum_{j=1}^{N} v_j\phi_j\right) + (f, \sum_{j=1}^{N} v_j\phi_j). \tag{31}$$

Then we get the linear system of ordinary differential equations in the $u_j(t)$ as:

$$\left(u_1'(t)\phi_1(x, y) + \sum_{j=2}^{N} u_j'(t)\phi_j(x, y), \sum_{j=1}^{N} v_j\phi_j\right) = l\left(u_1(t)\phi_1(x, y) + \sum_{j=1}^{N} u_j(t)\phi_j(x, y), \sum_{j=1}^{N} v_j\phi_j(x, y)\right) +$$

$$(f, \sum_{j=1}^{N} v_j\phi_j(x, y)),$$

$$\left(u_1'(t)\phi_1, \sum_{j=1}^{N} v_j\phi_j\right) + \left(\sum_{j=2}^{N} u_j'(t)\phi_j, \sum_{j=1}^{N} v_j\phi_j\right) = l\left(u_1(t)\phi_1, \sum_{j=1}^{N} v_j\phi_j\right) +$$

$$l\left(\sum_{j=1}^{N} u_j(t)\phi_j, \sum_{j=1}^{N} v_j\phi_j\right) + (f, \sum_{j=1}^{N} v_j\phi_j),$$

$$\sum_{j=1}^{N}\left(u_j'(t)\phi_j, \sum_{j=1}^{N} v_j\phi_j\right) = \sum_{j=1}^{N} l\left(u_j(t)\phi_j, \sum_{j=1}^{N} v_j\phi_j\right) + (f, \sum_{j=1}^{N} v_j\phi_j),$$

$$\sum_{j=1}^{N}\sum_{j=1}^{N}\left(u_j'(t)\phi_j, v_j\phi_j\right) = \sum_{j=1}^{N}\sum_{j=1}^{N} l\left(u_j(t)\phi_j, v_j\phi_j\right) + \sum_{j=1}^{N}(f, v_j\phi_j).$$

Since v_j's are constants we have also that:

$$\sum_{j=1}^{N} v_j \sum_{j=1}^{N} \left(\phi_j, \phi_j\right) u_j'(t) = \sum_{j=1}^{N} v_j \sum_{j=1}^{N} l\left(\phi_j, \phi_j\right) u_j(t) + \sum_{j=1}^{N} v_j(f, \phi_j).$$

The corresponding problem can therefore be expressed as

$$V^T M\dot{U} = V^T AU + V^T F.$$

That is

$$M\dot{U} = AU + F. \tag{32}$$

$$\text{Where, } M = \begin{pmatrix} (\phi_1,\phi_1) & (\phi_1,\phi_2) & \dots & (\phi_1,\phi_N) \\ (\phi_2,\phi_1) & (\phi_2,\phi_2) & \dots & (\phi_2,\phi_N) \\ \vdots & \vdots & \vdots & \\ (\phi_N,\phi_1) & (\phi_N,\phi_2) & \dots & (\phi_N,\phi_N) \end{pmatrix},$$

$$A = \begin{pmatrix} l(\phi_1,\phi_1) & l(\phi_1,\phi_2) & \dots & l(\phi_1,\phi_N) \\ l(\phi_2,\phi_1) & l(\phi_2,\phi_2) & \dots & l(\phi_2,\phi_N) \\ \vdots & \vdots & \vdots & \\ l(\phi_N,\phi_1) & l(\phi_N,\phi_2) & \dots & l(\phi_N,\phi_N) \end{pmatrix}, \text{ and } F = \begin{pmatrix} (f,\phi_1) \\ (f,\phi_2) \\ \vdots \\ (f,\phi_N) \end{pmatrix}.$$

There are many methods to solve the above problem involving the system of first order ODE. We can use FD methods that will descritize in time by using Explicit Euler method, Implicit Euler method or the Crank-Nicolson method, by considering an appropriate initial condition, (Johnson, 2012). But for this paper in the two dimensional case, we can use the ODE Suite in Matlab which is the Matlab build in system of ODE solver, ODE15I.

RESULTS AND DISCUSSION

In this section, we are compared for the advection-diffusion equations with an exact solution for the given finite element methods and then we solve the equation with out knowing the exact solution. The comparison is carried out by means of computed solutions for a wide range

of characteristic parameters. Linear elements are employed at the discretization in case of one-dimensional problem and bilinear elements in case of two-dimensional problems. Dirichlet and general boundary conditions are considered with different initial conditions and different size of computational domain.

First, consider the advection equation $u_t + au_x = f$ with sources and sinks function, $f(x,t) = \cos(\pi x) - at\pi \sin(\pi x)(x - x^2) + t\cos(\pi x)(1 - 2x)$ and the velocity parameter $a = 3$, with homogeneous boundary conditions. The FM solution using Matlab with a back ward Euler descritization in time is given in Fig. 3(a), with $N = 100$ nodes. To saw our error the exact solution for this equation is $u(x,t) = t\cos(\pi x)(x - x^2)$ and its graph is Fig. 3(b). The error of this equation is an order of 10^{-4}. If we increase the number of nodes from $N = 100$ to $N = 1000$, then our numerical solution becomes more accurate and we saw that the error is an order of 10^{-7} by modifying $h = 0.001$ from the algorithm.

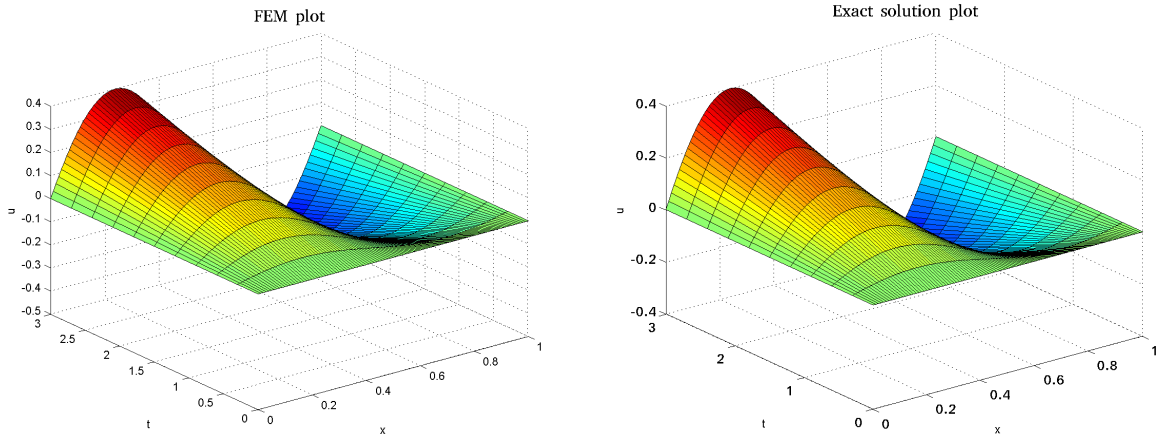

(a) FEM solution

(b) Exact solution

Figure 3: The Matlab implementation of the advection dominated equation with $f(x,t) = \cos(\pi x) - at\pi \sin(\pi x)(x - x^2) + t\cos(\pi x)(1 - 2x)$.

In (Bergara, 2011), there is a diffusion ($u_t = Du_{xx}$) example solved with finite difference methods, and let we solve that equation with the finite element method. He solves the diffusion (heat) equation by using initial condition $u(x,0) = \sin(\pi x)$ and with homogeneous Dirichlet boundary conditions in the interval $0 \leq x \leq 1$. If we consider different values for final time and diffusion coefficient we get the following simulations (Fig. 4 to Fig. 6) with a similar descritization of space (x) in to 50 nodes.

When we saw the results of those figures (Fig. 4 to Fig. 6) we can observe the following. If we use a small amount of diffusion coefficient, then it has a mall diffusion process and if we consider relatively large diffusion coefficient, the diffusion process is faster. Hence our finite element method is reasonable and accurate.

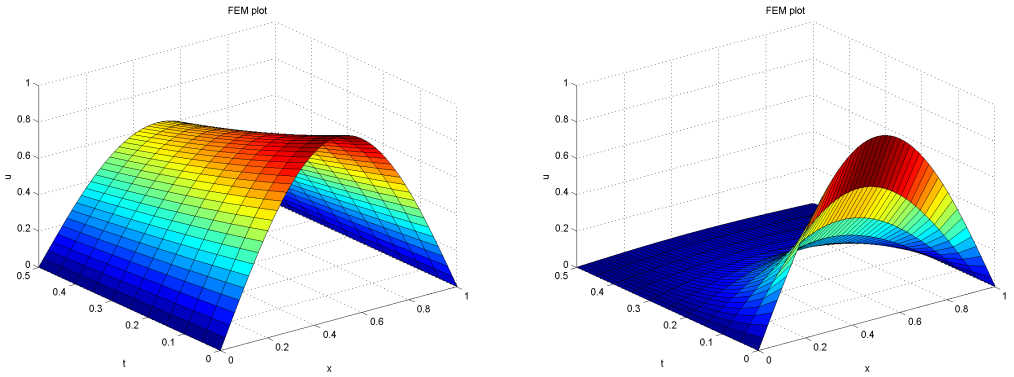

(a) FEM sol. with $D = 0.1$ and $t_f = 0.5$ (b) FEM sol. with $D = 1$ and $t_f = 0.5$

Figure 4: Solution of the diffusion equation using $D = 0.1$ and $D = 1$ for a constant final time of $t_f = 0.5$.

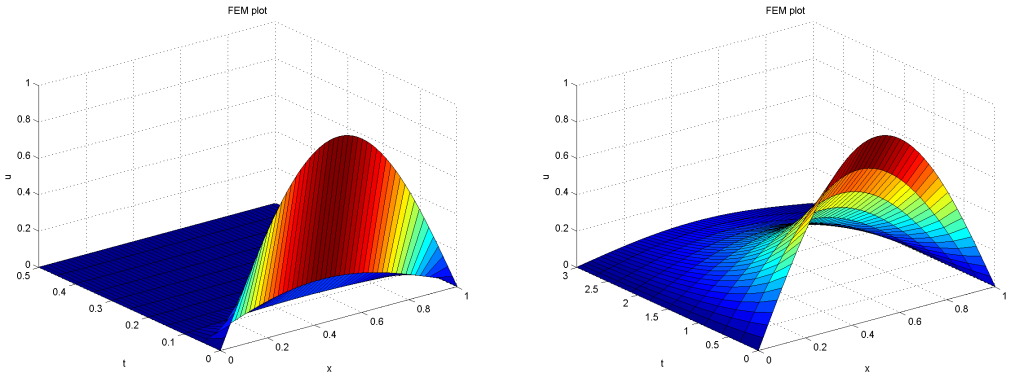

(a) FEM sol. with $D = 10$ and $t_f = 0.5$ (b) FEM sol. with $D = 0.1$ and $t_f = 3$

Figure 5: Solution of the diffusion equation using $D = 10$ with $t_f = 0.5$ and $D = 0.1$ for final time of $t_f = 3$.

Let we know consider the ADE $u_t + au_x - Du_{xx} = f$ with $f(x,t) = \sin(\pi x)\,(1 + D\pi^2 t) + a\pi t \cos(\pi x)$, $u(x,0) = 0$, $u(0,t) = u(1,t) = 0$. By using the forward Euler descritization in time the Matlab implementation with $a = 0.03$ and $D = 10$ for this problem is given in Fig. 7. The peclet's number $Pe = \frac{al}{D} = 0.003 \ll 1$ which is diffusion dominated for this choice of a and D.

Since we implements zero flux concentrations of the pollutants in the boundaries, the total mass of the pollution should remain constant. These boundaries physically correspond to a system where the species is enclosed inside a mesh that it cannot penetrate, however, the mesh allows the fluids to diffuse through the flow field. We see that all masses eventually concentrate along the domain as we have seen in Fig. 7. This steady state corresponds to diffusive and advective fluxes balancing each other. The flow carries additional mass towards the domain, but the density gradient limits how much more mass can be deposited.

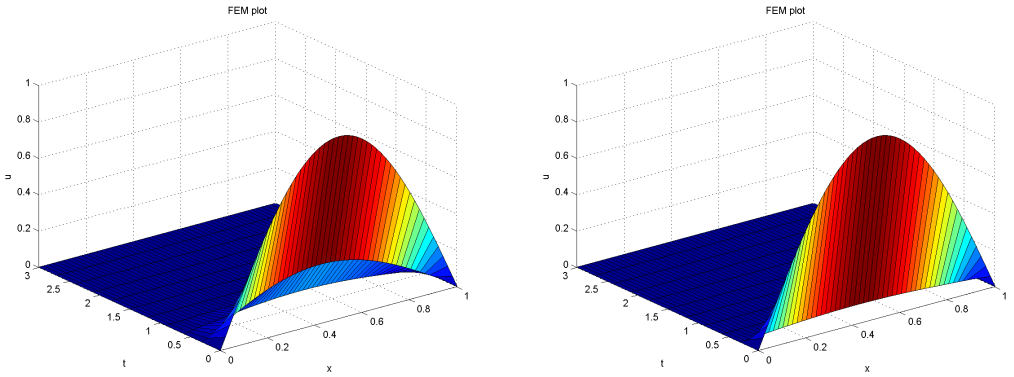

(a) FEM sol. with $D = 1$ and $t_f = 3$ (b) FEM sol. with $D = 10$ and $t_f = 3$

Figure 6: Solution of the diffusion equation using $D = 1$ and $D = 10$ for a constant final time of $t_f = 0.5$.

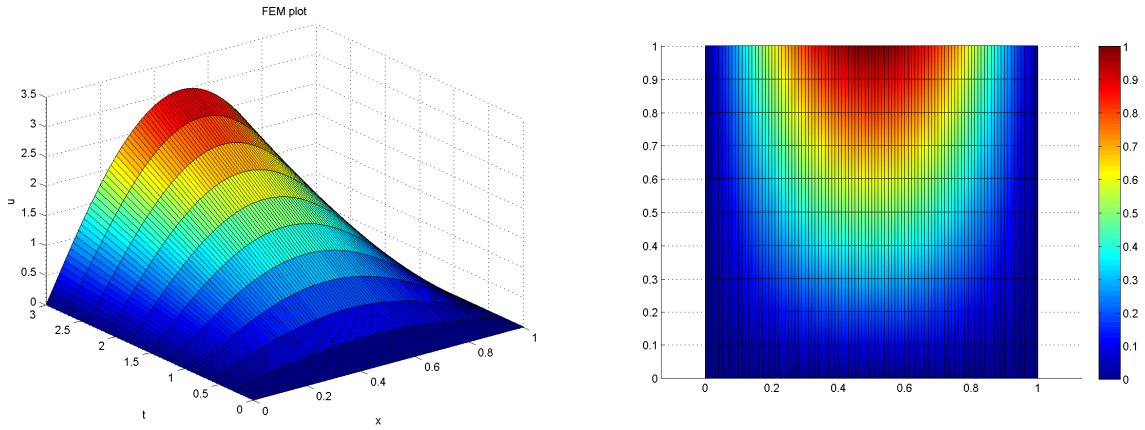

(a) FEM solution (b) Bar plot of the solution

Figure 7: Implementation of $1D$ AD equation with the source function $f(x,t) = sin(\pi x)\,(1 + D\pi^2 t) + a\pi t\cos(\pi x)$ and homogeneous Dirichlet boundary conditions and $a = 0.03,\ D = 10$, in which the peclet's number $Pe = \frac{al}{D} = 0.003 \ll 1$ which is diffusion dominated.

We see know on an arbitrary input concentration by using Neumann and Robin boundary conditions. Here, the problem is undetermined because of an unknown input concentration and hence unknown exit concentration and depends on the parameters. Authors of previous works on problems of this type have done on a known exit concentration by assuming a continuous and constant concentration at the flow boundary of Dirichlet type. This yields we to consider a problem by forcing the flow boundaries using Neumann and Robin boundary conditions. This conditions yields the flow of the concentration to move freely. Here the velocity term and the diffusion coefficient highly affects the flow of the concentration. We saw it by giving a source function $f(x,t) = a(2x+1) - 2D - 1,\ 0 \leq x \leq 1,\ 0 \leq t \leq t_f$ with a robin boundary condition $Du_x(0,t) = k_0(u(0,t) + g_0$ and $-Du_x(1,t) = k_1(u(1,t) + g_1$ and by considering different robin boundary pa-

rameters.

Let we change the velocity term and the diffusion coefficient for the given source term using $D = 0.02$ and $a = 1$, $(g_0, g_1) = (0.02, 0.06)$. The solution for this conditions is given in Fig. 8(a) using a total time of $t_f = 1$ and 8(b) using a total time of $t_f = 3$. This is an advection dominated example in which the movement of the concentration is faster in advection terms relative to diffusion.

2

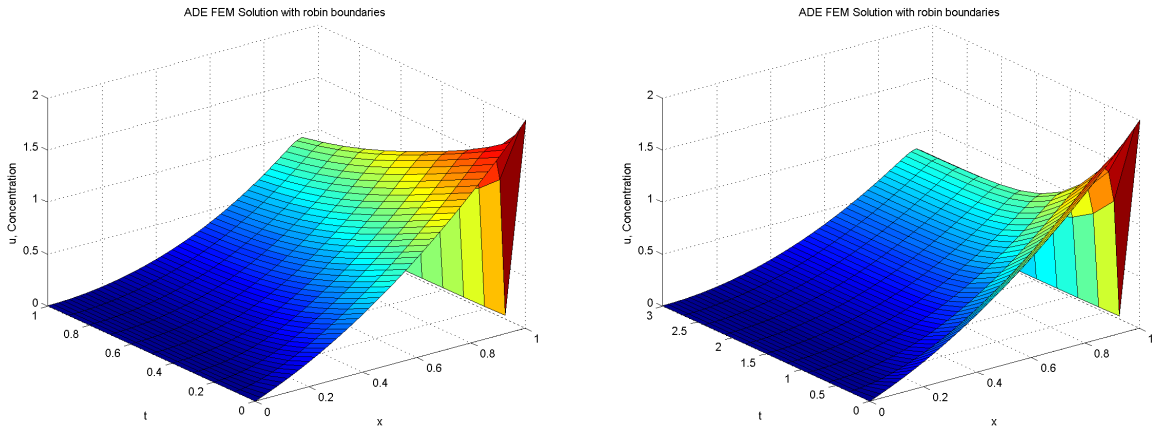

(a) FEM solution with $t_f = 1$

(b) FEM solution with $t_f = 3$

Figure 8: Numerical solution using FEM for the advection diffusion equation with $f(x,t) = a(2x+1) - 2D - 1$ and robin boundary conditions, with a diffusion coefficient $D = 0.02$ and velocity term $a = 1$ with time $t_f = 1$ for (a) and $t_f = 3$ for (b).

Let we consider the $2D$ steady diffusion equation with a source function given as $f(x,y) = D\pi^2(\sin(\pi x)+\sin(\pi y))$ to implement the $2D$ problem. The FEM numerical simulation of the PDE is given in Fig. 9.

In order to consider the finite element method of the time dependent two dimensional equations, we use the unsteady $2D$ diffusion equation. Let we test it with a known exact function and use the source terms and boundary conditions from that function. Let $u(t,x,y) = e^{-t}\sin(\pi x)\sin(\pi y)$ be the given exact solution for the diffusion equation $u_t - D\Delta u = f$, then our source function f becomes $f(t,x,y) = (2D\pi^2 - 1)e^{-t}\sin(\pi x)\sin(\pi y)$. Now by using the ODE15I, ODE solver to integrate for time in the final finite element method descritization the solutions for the equation is given in Fig. 10. The surface plots of those figures are the exact solutions, the finite element method solutions and the color bar of the finite element solution to view its properties.

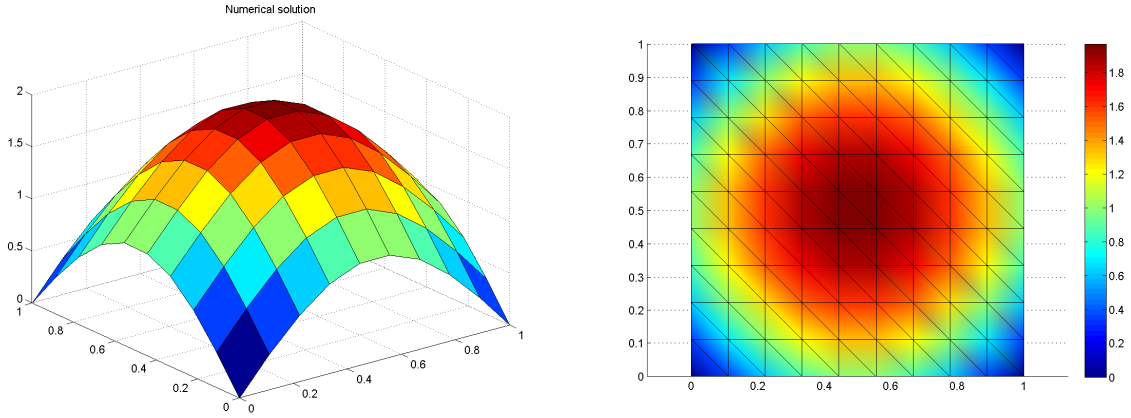

(a) FEM solution

(b) Bar plot of the solution

Figure 9: The numerical simulation using FEM for the steady $2D$ diffusion equation with $f(x, y) = D\pi^2(\sin(\pi x) + \sin(\pi y))$, with a diffusion coefficient $D = 0.5$.

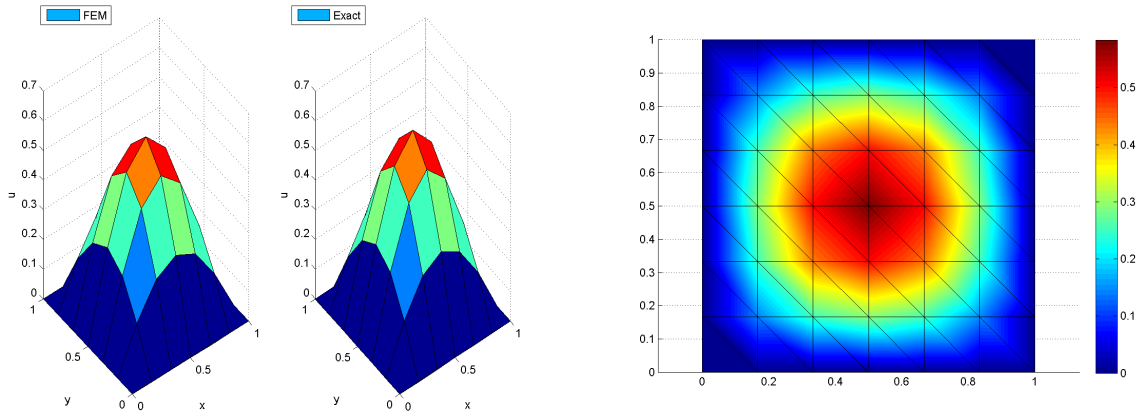

(a) FEM & exact sol

(b) Colour bar of the FEM solution

Figure 10: The surface of time dependent two dimensional diffusion equation with $D = 100$ with its color bar plot for its source term f, $f(t, x, y) = (2D\pi^2 - 1)e^{-t}\sin(\pi x)\sin(\pi y)$.

If we consider another linear test example with exact solution $u(x, y, t) = x + y + t$, then its source function becomes $f(x, y, t) = 1$. The finite element solution for this $2D$ unsteady diffusion equation with its exact solution and color bar is given in Fig. 11 by ODE solver ODE15I.

The numerical results in all the above mentioned discussions using the finite element method are almost closed to the analytical solution in the case of the test examples. This shows us that the finite element method is one of the best numerical method to solve any differential equations numerically in any type of geometries.

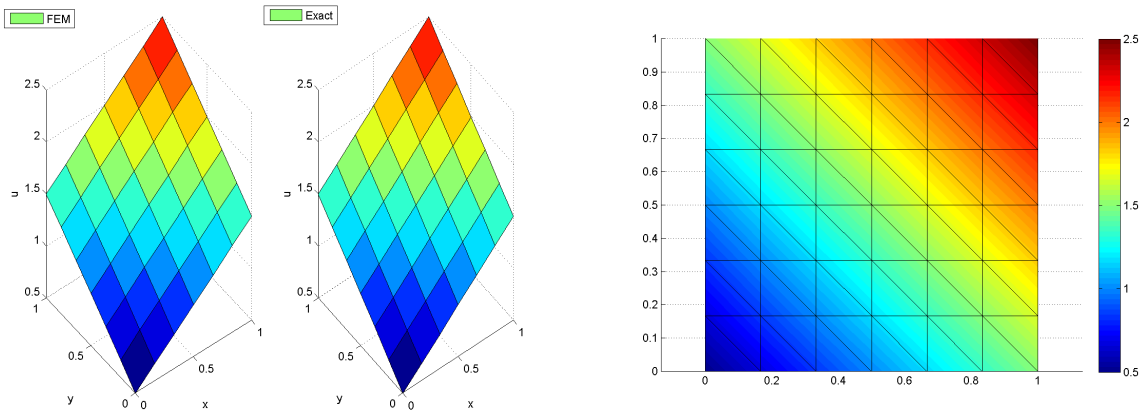

(a) FEM & exact sol

(b) Colour bar of the FEM solution

Figure 11: The surface of time dependent two dimensional diffusion equation with $D = 1$ with its color bar plot for its source term f, $f(t, x, y) = 1$.

CONCLUSIONS

In this paper, we study the finite element solution of the advection-diffusion equation. In the finite e lement analysis, we approximate a function defined in a domain, Ω, with a set of orthogonal basis functions with coefficients corresponding to the functional values at some node points. We deal with the numerical simulation of the advection-diffusion equation using the finite e lement method scheme in space and the backward Euler method in time. The main focus of the paper has been on the variational formulation techniques for the solution of the discrete Galerkin method and the other hand on computational analysis of different one and two dimensional PDE's. We have done numerical simulations for the above mentioned equations by considering the technique and using different test examples. The solution for the values at the nodes for the partial differential equations can be obtained by solving a linear system of equations involving the inversion of the sparse matrices.

We have solved the advection-diffusion e quation f or b oth o ne dimensional and two dimensional cases with the weighted residual (Galerkin) method of finite elements with constant velocity term and diffusion coefficient. These statements are supported by our test numerical investigations for the one and two dimensional Poisson equation, the advection equation, diffusion equation and the advection-diffusion equation. We have also seen the simulations of the equations by using the language of technical computing called Matlab and for time dependent equation using backward (implicit) Euler finite difference method for one dimensional problem and the built-in function ode15i to solve the system of ode's for two dimensional equations.

The generalization of the proposed Galerkin method to the three-dimensional advection diffusion is obtained within the current framework and an interested body will be done on this approach by including the reaction term. To obtain the solutions to this problems, the method can be extended to the least square finite element method, and another interested body will also be done on this approach. One can also extend this method using variable velocities and diffusion coefficients which

vary with the time and space of the given dimension. The finite element method descretizes only in space and the time descritization is based on the finite difference methods. Hence the finite element method needs human power still now for the descritization process of time. So this is a very interesting area to do researches in the future to include the time descritization in the method.

Acknowledgments

The core of this work was completed during the master study at Hawassa University and presented to former School of Mathematics and Statistical Science (currently Department of Mathematics) in partial fulfillment of the requirement for the Degree of Master. The authers would like to thank the Department of Mathematics at the University of Hawassa University. This work of has been partially supported by Hawassa University.

References

Ahsan M. 2012. Numerical solution of the advection-diffusion equation using Laplace transform finite analytical method. *Int. J. River Basin Manag.* **10**(**2**): 177- 188.

Aragonés L., Pagán J.I., López I., Navarro- González F.J. and Villacampa Y. 2019. Galerkin's formulation of the finite elements method to obtain the depth of closure. *Sci. Total Environ.* **660**: 1256-1263.

Bajellan A.A.F. 2015. Computation of the convection diffusion equation by the fourth order compact finite difference method. Doctoral dissertation, Izmir Institute of Technology, Turkey.

Bergara A. 2011. Finite Difference Numerical Methods of Partial Differential Equations in Finance with MATLAB. *Master and Banca*. New York, Springer.

Brenner S.C., Scott L.R., & Scott L.R. 2008. *The mathematical theory of finite element methods. Vol , pp* 263-291. Springer, New York.

Donea J. and Huerta A. 2003. *Finite element methods for flow problems*. John Wiley & Sons.

Hundsdorfer W.1996. Numerical solution of advection-diffusion-reaction equations: lecture notes for Ph. D. course, 1996, Thomas Stieltjes Institute. *Department of Numerical Mathematics [NM]*, (9603).

Johnson C. 2012. *Numerical solution of partial differential equations by the finite element method*. Courier Corporation.

Langtangen H.P. 2003. *Computational partial differential equations: numerical methods and diffpack programming* (Vol. 2). Berlin: Springer.

Larson M.G. and Bengzon F. 2010. The finite element method: theory, implementation, and practice. *Texts in Computational Science and Engineering, 10*, 23-44.

Lian Y., Ying Y., Tang S., Lin S., Wagner G.J. and Liu W.K. 2016. A Petrov–Galerkin finite element method for the fractional advection– diffusion equation. *Comput. Methods Appl. Mech. Eng.*, **309**: 388-410.

Lima S.A., Kamrujjaman M. and Islam M.S. 2021. Numerical solution of convection–diffusion–reaction equations by a finite element method with error correlation. *AIP Advances* **11**(**8**): 085225.

Pochai N. and Deepana R. 2011. A numerical computation of water quality measurement in a uniform channel using a finite difference method. *Procedia Eng.* **8**: 85-88.

Quarteroni A. and Quarteroni S. 2009. *Numerical models for differential problems* (Vol. 2). Milan: Springer.

Szymkiewicz R. and Gąsiorowski D. 2021. Adaptive method for the solution of 1D and 2D advection–diffusion equations used in environmental engineering. *J. Hydroinformatics* **23**(**6**): 1290-1311.

Yang W.Y., Cao W., Chung T.S. and Morris J. 2005. Applied Numerical Methods Using MATLAB. A John Wiley & Sons. *Hoboken, NJ*.

Author's guideline of the Journal

- **Information for Authors**

The East African Journal of Biophysical and Computational Sciences (EAJBCS) will provide sufficient information for all authors, including those invited to submit articles for publication (Appendix I). The information, as summarized hereunder, will cover the authorship policy, publication ethics and general requirement during the preparation of the manuscript.

All articles as well as the Editorials published in the East African Journal of Biophysical and Computational Sciences (EAJBCS) represent the opinion of the author(s) and do not necessarily reflect the official view of the Hawassa University and/or College of Natural and Computation Science, the Editorial Board or the institution within which the author(s) is/are affiliated unless this is clearly stated. Furthermore, the author(s) is/are fully responsible for the contents of the manuscript and for any claim or disclaim therein.

- **Plagiarism policy**

Before submitting any manuscript, the authors should ensure that they have prepared entirely original works (i.e. not plagiarized from others or from their previous published works). If the work of others is used in any form (such as words, phrases, paragraphs or pictures), the original work should be acknowledged and appropriately cited or quoted. In general, the journal strongly condemn the act of plagiarism and apply different *Plagiarism Checking softwares* to reduce such fraud. If the plagiarism is detected at any stage of the publication process by our esteemed peer reviewers or editorial board members, the manuscript could be automatically rejected.

- **Authorship Policy**

To qualify as an author on a research publication, an individual /the person included as a co-author must have made *substantial contributions* to at least one of the following categories:

- **Conceived of or designed the study**: *This includes conceiving the research question(s), developing the overall research plan, or designing the specific methodology. Just suggesting a general topic area does not qualify*
- **Performed research:** *This includes actively participating in the collection of data, conducting experiments, or implementing the research plan. This involves hands-on work beyond basic assistance. Routine data collection or performing technical tasks under direct supervision are not sufficient for authorship*
- **Analyzed data and interpretation:** *This refers to playing a crucial role in analyzing the collected data, interpreting results, and drawing meaningful conclusions. This includes applying statistical methods, creating visualizations, and explaining patterns*
- **Contributed new methods or models**: *This includes any significant contribution to the development or refinement of novel methods, models, or theoretical frameworks used in the research. It involves innovative contributions that go beyond standard techniques.*

- **Wrote the paper/ Manuscript drafting and revision:** *This includes making a substantial contribution to the writing process, including drafting significant sections of the manuscript, critically revising the content for intellectual input, and responding to reviewer feedback. Proofreading or minor editing (e.g. language) does not warrant authorship.*

It is the responsibility of the corresponding authors that the names, addresses, and affiliations of all authors are correct and in the right order, that institutional approvals have been obtained and that all authors have seen and agreed to a submission. This includes single authorship papers where appropriate. If at all in doubt, please double-check with e.g., Supervisors, line managers, department heads etc.

• Publication ethics

The Journal requires an author or authors of a manuscript to sign a form of submission prepared for this purpose (Appendix II). The submission to the Journal means that the author(s) agree(s) to all of the contents of the form. The corresponding author for a co-authored manuscript is solely responsible for ensuring the agreement and managing all communications between the Journal and the co-author(s) before and after publication. Before submission, the corresponding author should ensure that the names of all authors of the manuscript are included on the author list, the order of the names of the authors should appear as agreed by all authors, and that all authors are aware that the paper was submitted. Any changes to the author's list after submissions, such as a change in the order of the author, or the deletion or addition of authors, needs to be approved by a signed letter from every author.

After acceptance, the proof is sent to the corresponding author to circulate it to all co-authors and deal with the Journal on their behalf. The Journal shall not necessarily correct errors after publication. The corresponding author is responsible for the accuracy of all contents in the proof, particularly including the correct spelling of the names of co-authors and their current addresses and affiliations.

After publication, the Journal regards the corresponding author as the point of contact for queries about the published manuscript and that it is his/her full responsibility to inform all co-authors about matters arising from the publication processes and that such matter is dealt with promptly. The corresponding author’s role is to ensure that inquiries are answered promptly on behalf of all the co-authors. The names and email addresses of the author will be published in the paper. With prior permission of the Editorial Board, authors have the right to retract submitted manuscripts in case they decide to do so. Authors of a published material have the responsibility to inform the Journal promptly if they become aware of any part of their manuscript that requires correcting. The corrected part of the article will be mentioned in the next issue. In fact, any published correction requires the consent of all co-authors, so time is saved if requests for corrections are accompanied by a signed agreement by all authors (in the form of a scanned attachment to an email).

- **General requirements**

Upon submission of a manuscript, the author(s) is required to state that the paper has not been submitted for publication by any other journal or will not be submitted to any other journal by signing the manuscript submission and copyright transfer form (Appendix II).

Manuscripts should be written in English, with spelling according to recent editions of the Advanced Learner's Dictionary of Current English, Oxford University Press. The manuscript should include the following: **title**, **author's name(s)**, **Affiliation** (company or institute), **abstract** and **keywords**. The main parts of the manuscript should consist of **Introduction**, clear objective(s), **Materials and Methods**, **Results**, **Discussion** (or results and discussion merged), **Conclusion**, **Acknowledgement**, **References**, **Figures,** and **Tables** with captions and descriptions, in which detailed quantity, formatting, and unit are given under the following sub-heading.

General text formatting

Manuscripts should be submitted as Microsoft Word documents (docx, doc, rtf) and /or Latex. The manuscript's font size for the text is 12-point, Times New Roman, 1.5 point line spacing with a minimum of 2.5 cm margins on all sides. All pages in the manuscript should be numbered by using the automatic page numbering function.

Permitted length of articles

Original research articles and review articles should not exceed 6000 words in length, starting from the title page to the reference section. Generally, 3-4 tables and 5-6 figures are permitted. Short communications contain news of interest to researchers, including progress reports on ongoing research of unique nature, records of observations, short comments, corrections, and reinterpretation of articles previously published in EAJBCS *etc*. The maximum permissible length is 1500words, including title, abstract, and references; they may contain no more than two figures and/or two tables. Book reviews with critical evaluation of recently published books in areas of Natural and Computational Sciences will be published under this column. The maximum permissible length of a book review is 1500 words, including any references.

Title Page

The title page should include the title, author(s)' name and affiliation, email address of the corresponding author and a suggested running head (Maximum 50 characters).

Abstract

An informative abstract shorter than 300 words is included. Informative abstracts include the purpose of the research, the main methods used, the most important results, and the most significant conclusions. The abstract should be in one paragraph and without any abbreviations.

Keywords

Supply 3 to 7 keywords that describe the main content of the article, each separated with semicolon. Select words different than those in the title and list them alphabetically.

Text

The text should be precise, clear, and concise. Avoid verbiage, excessive citations of the literature (especially to support well-known statements), discussions marginally relevant to the paper, and other information that adds length but little substance to the paper. All tables and figures should be relevant and necessary; do not present the same data in tables and figures, and do not use short tables for information that can be easily presented using text.

Introduction

The introduction should give the pertinent background to the study and should explain why the work was done. The author(s) should clearly show the research gap, state the objectives of the work and avoid a detailed literature survey or a summary of the results.

Materials and Methods

To ensure reproducibility, the methodology section should be detailed and transparent. The following information must be included: use precise and recognized scientific nomenclature for all materials and indicate their source; specify all equipment used, including the manufacturer's name, model number, and relevant technical specifications in parentheses (e.g., "centrifuge (Eppendorf, Model 5424)"); describe your procedures step-by-step, ensuring all experimental parameters are specified; provide a comprehensive description for any novel method, including rationale and limitations; reference the original source for established methods, clearly stating and justifying any deviations; and explicitly confirm that procedures involving human subjects or animals were conducted in adherence to ethical standards set by relevant national governing bodies, including providing approval details and measures taken to minimize harm.

The statistical analysis done and statistical significance of the findings, when appropriate, should be mentioned. Unless absolutely necessary for a clear understanding of the article, a detailed description of statistical treatment/analysis may be avoided. Articles based heavily on statistical considerations, however, need to give details particularly when new or uncommon methods are employed. Standard and routine statistical methods employed need to give only authentic references.

Results

The purpose of your data presentation (i.e. the result section) is to support your discussion and conclusions. Therefore, only include data that is crucial to understand your key findings. Structure the data in a unified and logical sequence, allowing the reader to follow the remaining sections easily. Avoid unnecessary repetition: if data is presented in a table or figure, do not repeat it in the text. Instead, use the text to emphasize or summarize noteworthy findings. Choose either tables or figures to present the same data – avoid presenting it both ways. Critically

analyze and interpret the implications of your data within the discussion section, providing a thoughtful and comprehensive interpretation.

Discussion

The discussion section should provide an insightful analysis or interpretation of your results, moving beyond a mere restatement of your findings. Interpret your results and explain their relevance to the wider scientific community, drawing clear connections to established knowledge and identifying new insights. Avoid directly repeating the results and rather analyze them with logical deductions and scientific justification. Acknowledge and discuss any study limitations or potential biases. The conclusions should answer your research questions, but avoid unsupported statements and refrain from claiming priority on ongoing work. Make sure hypotheses are clearly identified, and include recommendations only when they directly address your findings and are of critical importance.

Acknowledgment

The acknowledgment section should be brief and reserved for recognizing specific and substantial scientific, technical, or financial contributions to the research. Avoid acknowledging routine departmental facilities, general encouragement, or assistance with manuscript preparation, such as typing or secretarial support. Focus only on acknowledging individuals and institutions that directly contributed to the intellectual or material aspects of the research.

Tables

Tables should be prepared in MS Word's Table Editor, using (as far as possible) "Simple1" as the model:

(Table … Insert … Table … Auto format …Simple 1). Tables taken directly from Microsoft Excel are not generally acceptable for publication.

Use Arabic (1, 2, 3 …), not Roman (I, II, III …), numerals for tables. Footnotes in tables should be indicated by superscript letters beginning with "a" in each table. Descriptive material not designated as a footnote maybe placed under a table as a Note.

Illustrations

Preparation: Similar figures should be arranged into plates whenever possible; leave very little space between adjoining illustrations or separate them with a thin white line. Line art should be scanned at 900 dpi, photographs (halftone or color) at 300 dpi, and figures with line art and halftones at 600 dpi. Crop the illustrations to remove non-printing borders. Make lines thick enough and text large enough to compensate for the reduction. Dimensions of the original artwork should not exceed 28 cm x 21.5 cm; the printed area of the journal page measures 20.3 x 14 cm. Submission: TIFF or JPG files of figures should be of high quality and readable in Adobe Photoshop. Do not embed figures in the manuscript document.

The figures will be evaluated during the Editorial reading of the article, and if necessary, instructions will be provided for the submission of adequate illustrations.

Insert … Symbol … Special characters

All data should be given in the metric system, using SI units of measurement.

Use "." (point) as the decimal symbol. Thousands are shown spaced, thus: 1 000 000. Use a leading zero with all numbers <1, including probability values (*e.g.* $p < 0.001$).

Numbers from one to nine should be written out in the text, except when used with units or in percentages (*e.g.* two occasions, 10 samples, Five seconds, 3.5%). At the beginning of a sentence, always spell out numbers (*e.g.* "Twenty-one trees were sampled... ").

Use the 24-hour time format, with a colon ":" as separator (*e.g.* 12:15 h). Use day/month/year as the full date format (*e.g.* 12 August 2001, or 12/08/01 for brevity in tables or figures). Give years in full (*e.g.* "1994–2001", never "94–01"). Use the form "1990s", not "1990"s" or "1990ies".

Use the en-dash – for ranges, as in "1994–2001" (Insert … Symbol … Special characters En dash).

In stating temperatures, use the degree symbol " º ", thus " ºC ", not a super script zero " 0 ". (Insert … Symbol … Normal text),

Define all symbols, abbreviations and acronyms the first time they are used, *e.g.* diameter at breast height (DBH), meters above sea-level (masl). In the text, use negative exponents, *e.g.* $g\ m^{-2}$, $g\ m^{-2}\ sec^{-1}$, $m^3\ ha^{-1}$ as appropriate. Use "h" for hours; do not abbreviate "day".

If possible, format mathematical expressions in their final version (*e.g.* by means of Equation Editor in MS Word or its equivalent in Word Perfect or Open Office); otherwise, make them understandable enough to be formatted during typesetting (*e.g.* use underlining for fractions and type the numerator and denominator on different lines).

MS word equations can be used for all mathematical equations and formulae (Insert….Equations).

References

All literatures referred to in the text should be cited as exemplified below.

Please inspect the examples below carefully, and adhere to the styles and punctuation shown.

Capitalize only proper names ("Miocene", "Afar", "The Netherlands") and the initial letter of the title of papers and books, *e.g.* write "Principles and procedures of statistics", not "Principles and Procedures of Statistics".

Do not italicize Latin abbreviations: write “et al.”, not “*et al.*”

References in the text should use the ‘author-year’ (Harvard) format:

(Darwin and Morgan, 1993) or, if more than two authors, (Anderson et al., 1993). Arrange multiple citations chronologically (Hartman and Kester, 1975; Anderson et al., 1993; Darwin and Morgan, 1994).

References in the list should be in alphabetical order, in the following formats:

Journal article

Kalb J.E. 1978. Miocene to Pleistocene deposits in the Afar depression, Ethiopia. SINET: *Ethiop. J. Sci.* 1: 87-98.

Books

Whitmore T.C. 1996. An introduction to tropical rain forests. Clarendon Press, Oxford, 226 pp.

Steel R.G.D. and Torrie J.H. 1980.Principles and procedures of statistics.2nd ed. McGraw-Hill Book Co., New York.633 pp.

Book chapter

Dubin H.J. and Grinkel M. 1991.The status of wheat disease and disease research in warmer areas. In: Lange L.O., Nose1 P.S. and Zeigler H. (Eds.) Encyclopedia of plant physiology. Vol. 2 A Physiological plant ecology. Springer-Verlag, Berlin. pp. 57-107.

Conference /workshop/seminar proceedings

Demel Teketay. 2001. Ecological effects of eucalyptus: ground for making wise and informed decision. Proceedings of a national workshop on the Eucalyptus dilemma, 15November 2000, Part II: 1-45, Addis Ababa.

Daniel L.E. and Stubbs R.W. 1992.Virulenceof yellow rust races and types of resistance in wheat cultivars in Kenya. In: Tanner D.G. and Mwangi W. (eds.). Seventh regional wheat workshop for eastern, central and southern Africa. September 16-19, 1991. Nakuru, Kenya: CIMMYT. pp. 165-175.

Publications of organizations

WHO (World Health Organization) 2005. Make every mother and child count: The 2005World Health Report. WHO, Geneva, Switzerland.

CSA (Central Statistical Authority) 1991.Agricultural Statistics. 1991. Addis Ababa, CTA Publications. 250 pp.

Dissertation or Thesis

Roumen E.C.1991. Partial resistance to blast and how to select for it. Ph.D. Thesis. Agricultural University, Wageningen. The Netherlands.108 pp.

Gatluak Gatkuoth 2008. Agroforestry potentials of under-exploited multipurpose trees and shrubs (MPTS) in Lare district of Gambella region. MSc. Thesis, College of Agriculture, Hawassa University, Hawassa.92 pp.

Publications from websites (URLs)

FAO 2000.Crop and Food Supply Assessment Mission to Ethiopia. FAOIWFP. Rome. (http://www. fao. or~/GIE WS). (Accessed on 21 July 2000).

Scope and indexing

East African Journal of Biophysical and Computational Sciences (EAJBCS)is a **double-blind peer-reviewed open-access journal** published by Hawassa University, College of Natural & Computational Sciences. This Journal is a multi and interdisciplinary journal that is devoted to attracting high-quality, latest, and valuable advancements in the fields of natural sciences. The Journal invites publications from different geographical contexts and disciplines to advance the depths of knowledge related to **physics, chemistry, geology, biology, & veterinary medicine**. The manuscript originated from other sciences such as **biotechnology, sport science, statistics**, and **mathematics** can also be accepted based on their adjunct nature. The Journal encourages publications of both scholarly and industrial papers on various themes with the aim of giving innovative solutions to natural sciences. It encourages the publishing of **open access academic journals** on a regular basis (presumably **biannual**). The Journal publishes original research articles, critical reviews, mini-reviews, short communications, case reports related to the specific theme & a variety of special issues **in English**. The Journal, published under the Creative Commons open access license (CC BY-NC-ND),**doesn't charge fees for publishing** an article and hence offers an opportunity to all social classes regardless of their economic statuses. This helps to promote academic research published by resource-poor researchers as a mechanism to give back to society.

East Afr. J. Biophys. Comput. Sci. is officially available online on the following sites

- ✓ https://journals.hu.edu.et/hu-journals/index.php/eajbcs
- ✓ https://doaj.org/toc/2789-3618
- ✓ https://www.ajol.info/index.php/eajbcs
- ✓ https://www.cabidigitallibrary.org (in short: https://surl.li/yjffzm)

ISSN (Online): 2789-3618 ISSN (Print): 2789-360X